Analysis of in-service PCC pavement responses from Denver International Airport

Dulce Rufino

ERES Consultants, A Division of ARA, Inc.

Presented at ISU Spring Transportation Seminar

February 20, 2004

Overview

- DIA project background
- Prediction of pavement parameters
  - Aircraft loading and wander
  - Pavement layer properties
  - Pavement temperature
  - Concrete joint characteristics
- Analysis of temperature curling
- Analysis of interface condition
- Conclusions

The Denver International Airport Instrumentation Project

Runway instrumentation

- Installed in the takeoff area of runway 34R–16L during construction
- Static and dynamic sensors collecting data under climatic and aircraft loading

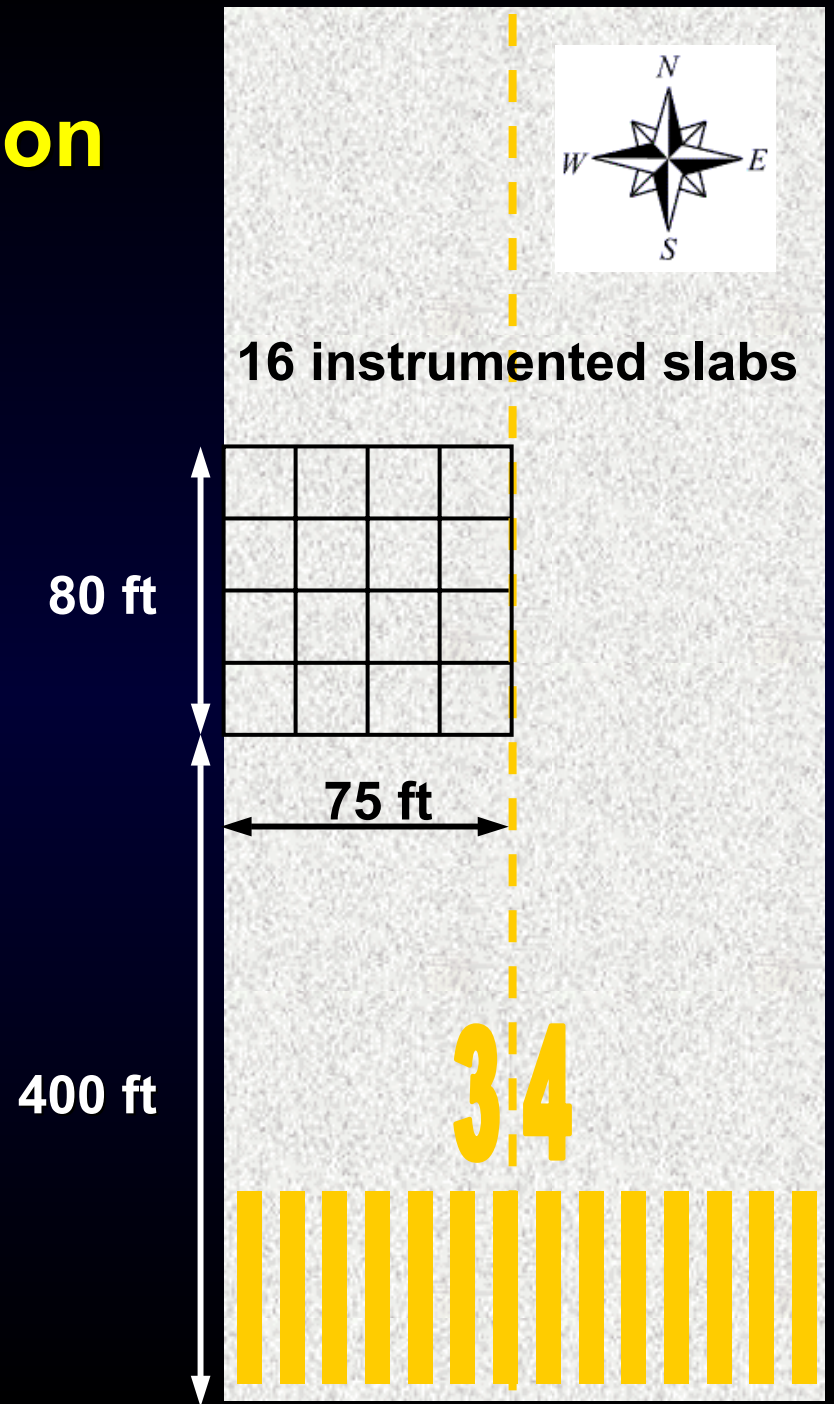

Pavement structure

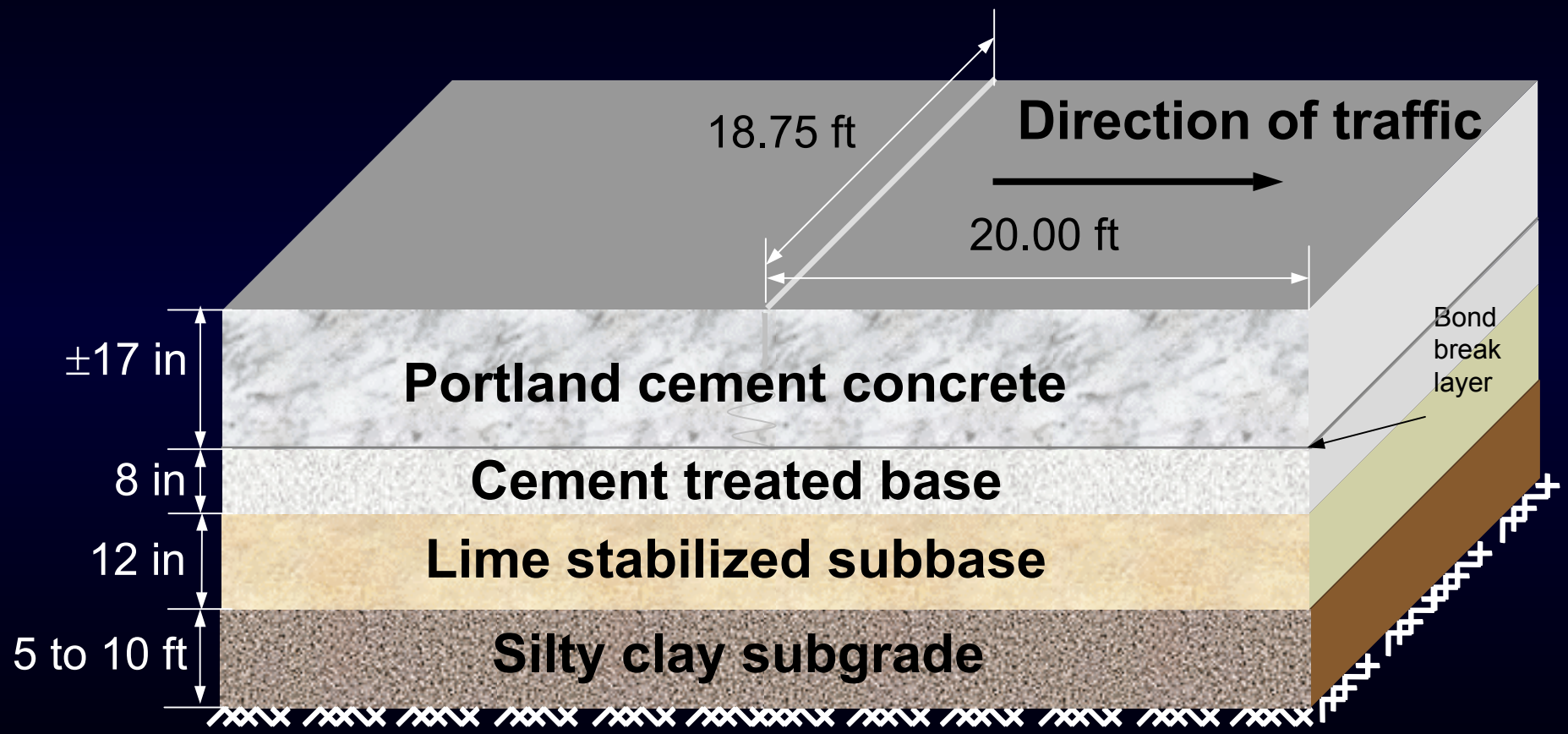

Joint design

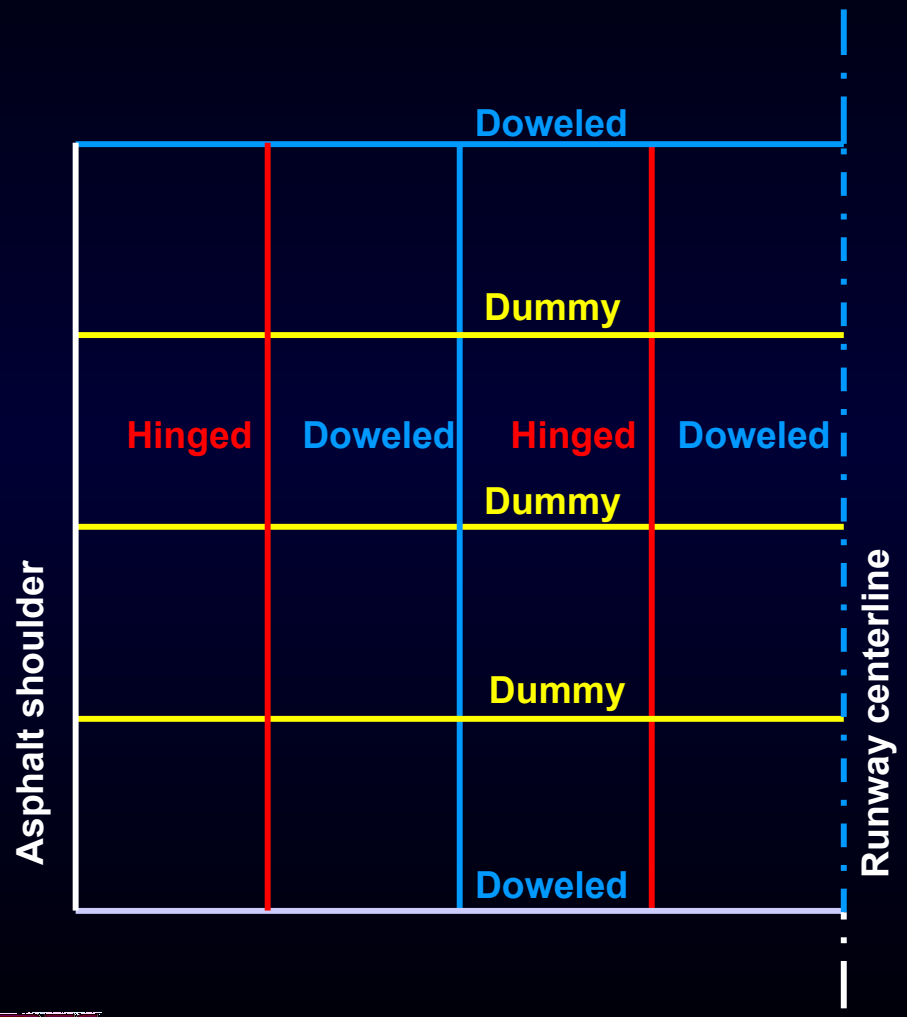

Doweled joint

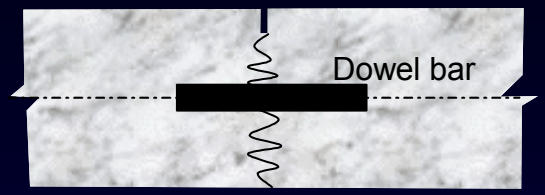

Hinged joint

Dummy joint

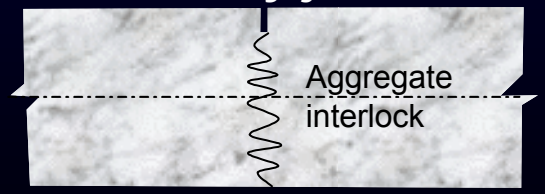

Position sensors

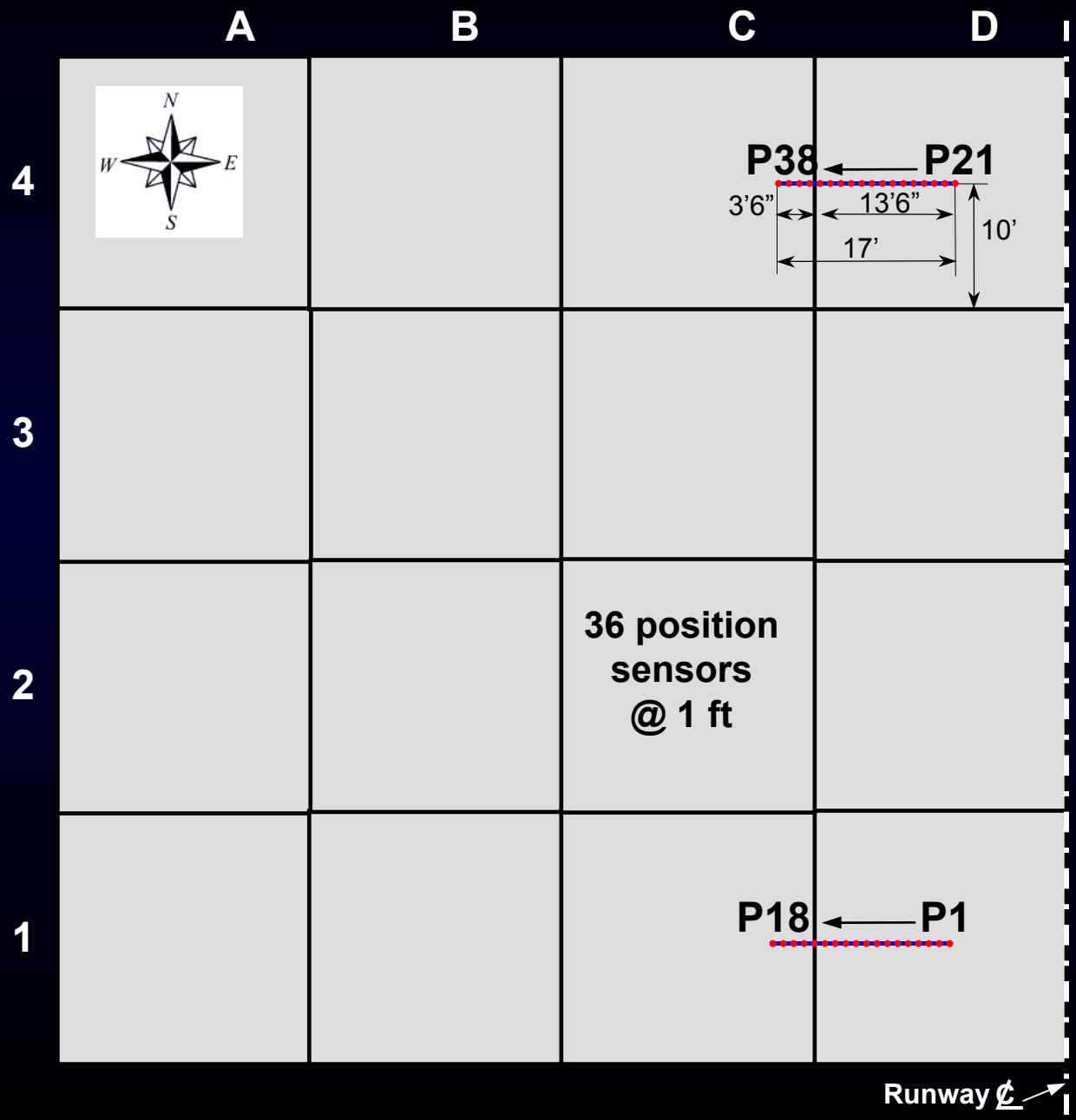

H-bar sensors

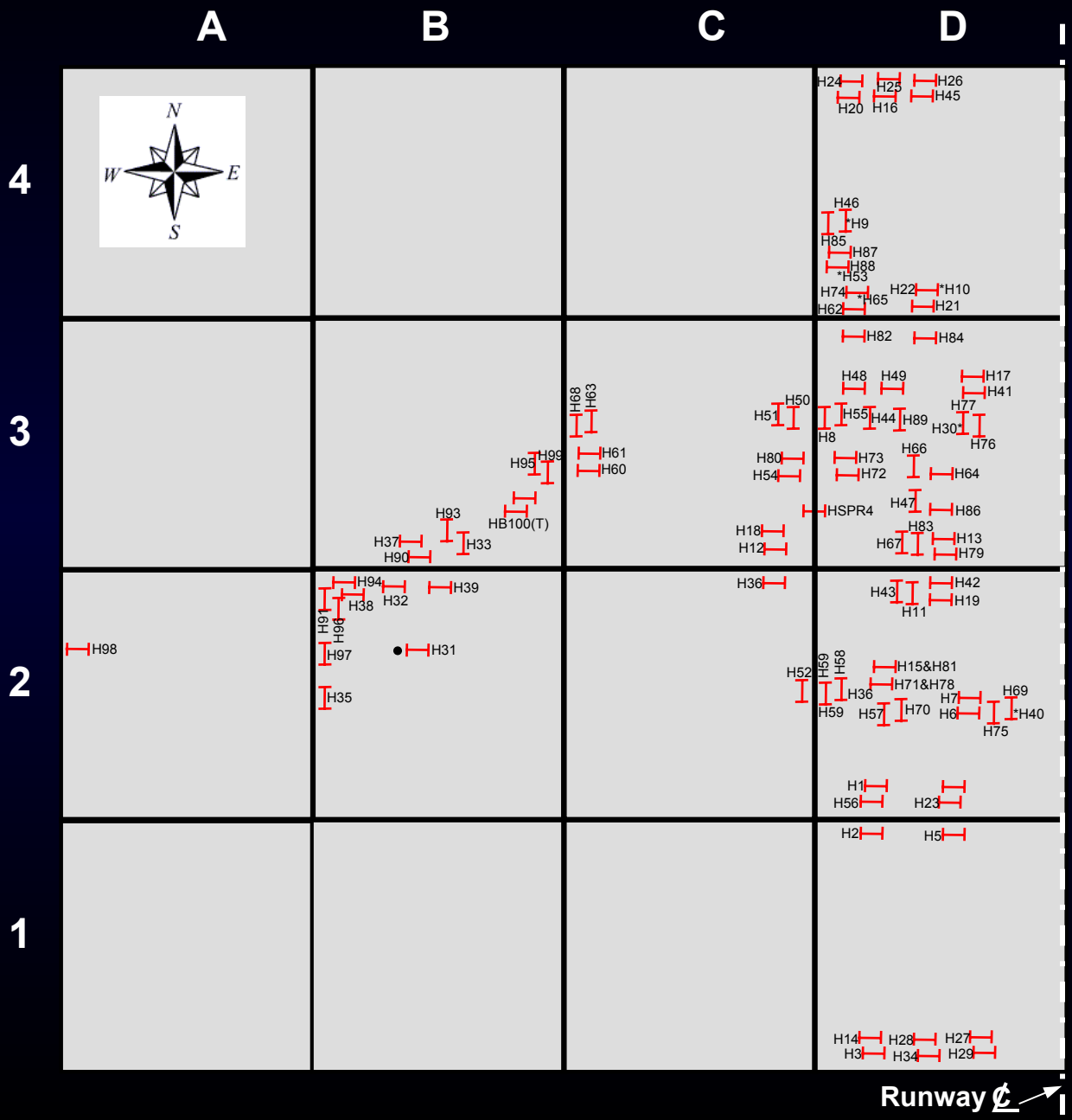

LVDT sensors

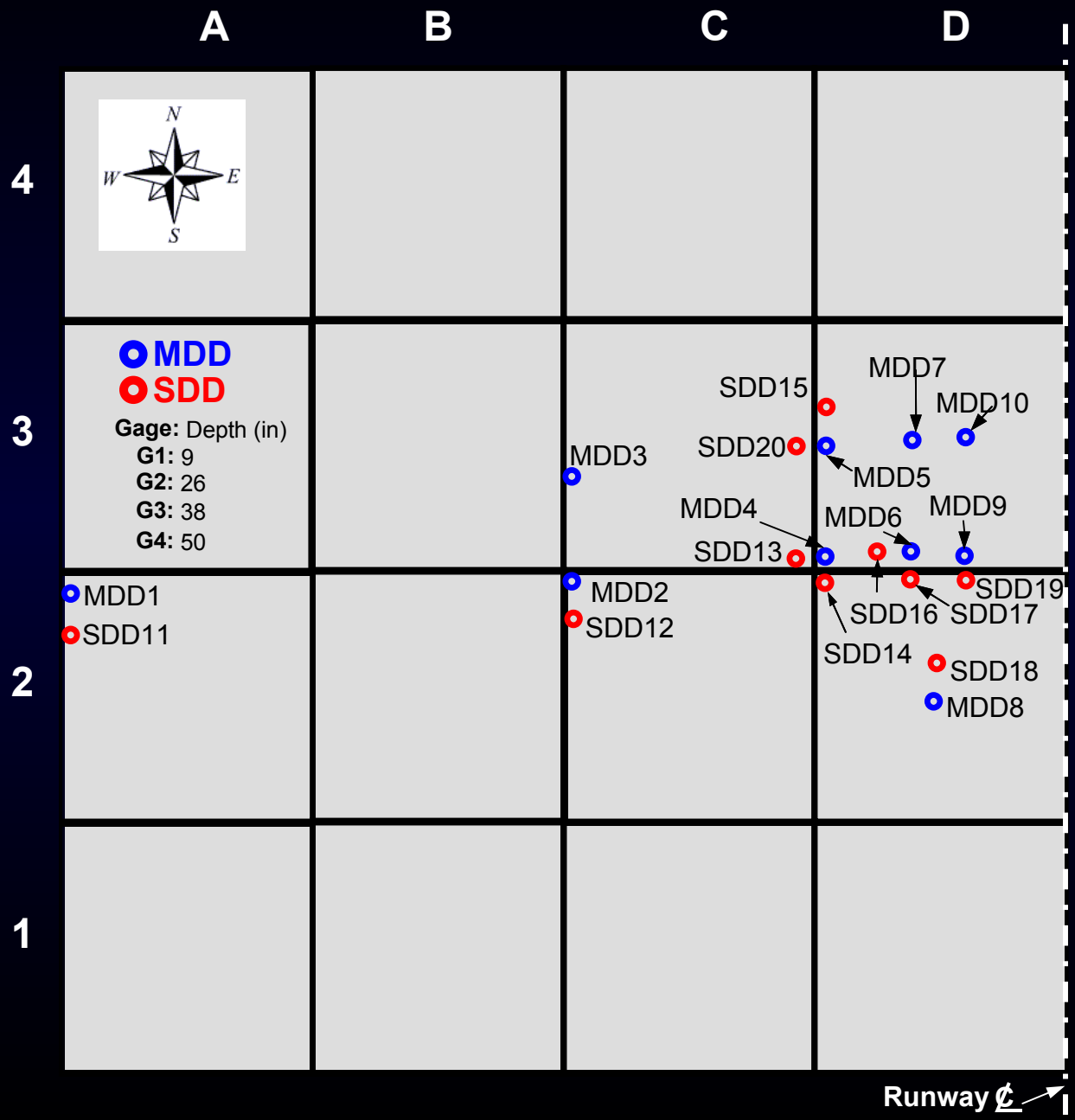

Thermocouples

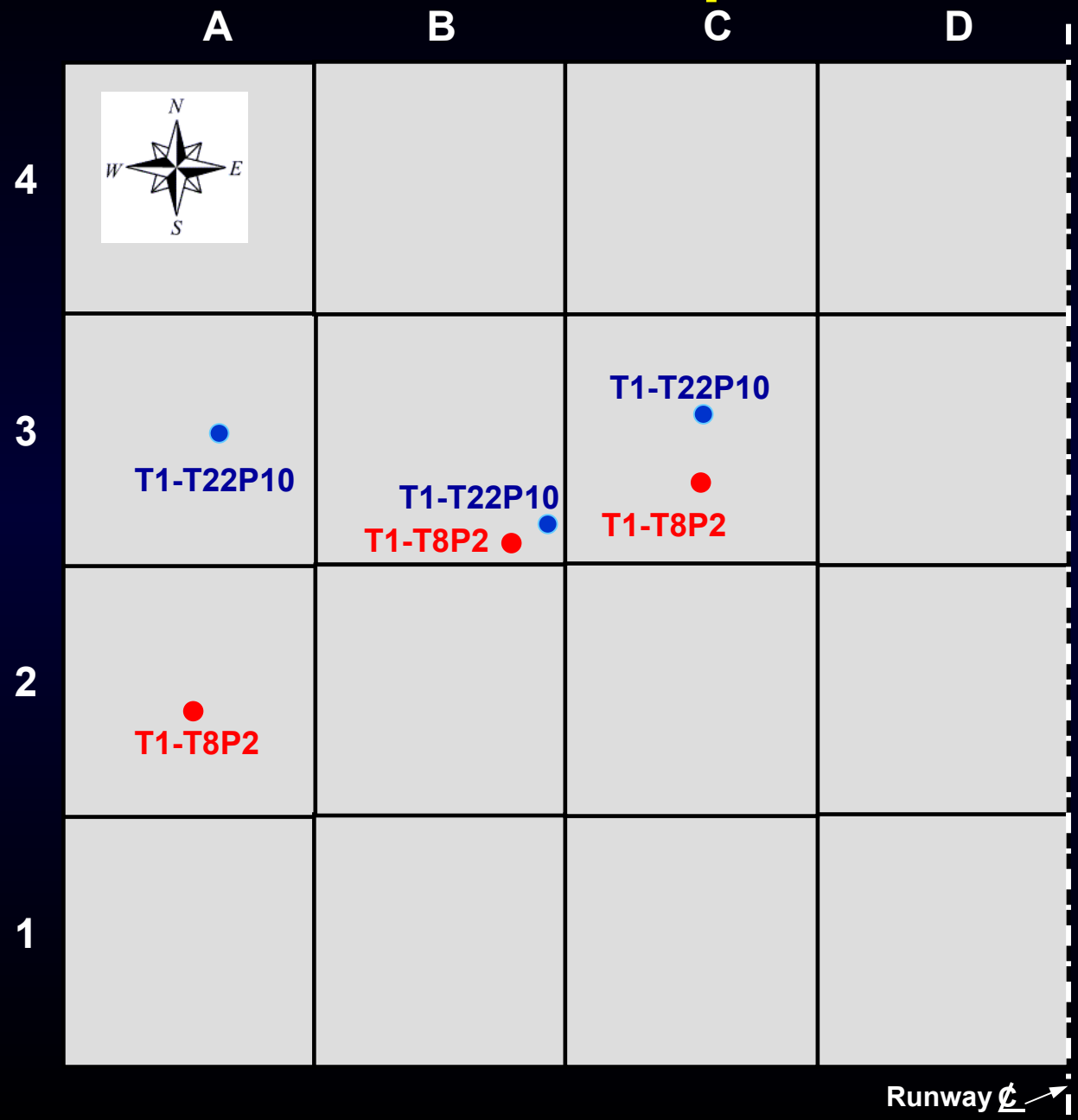

Depth of thermocouples

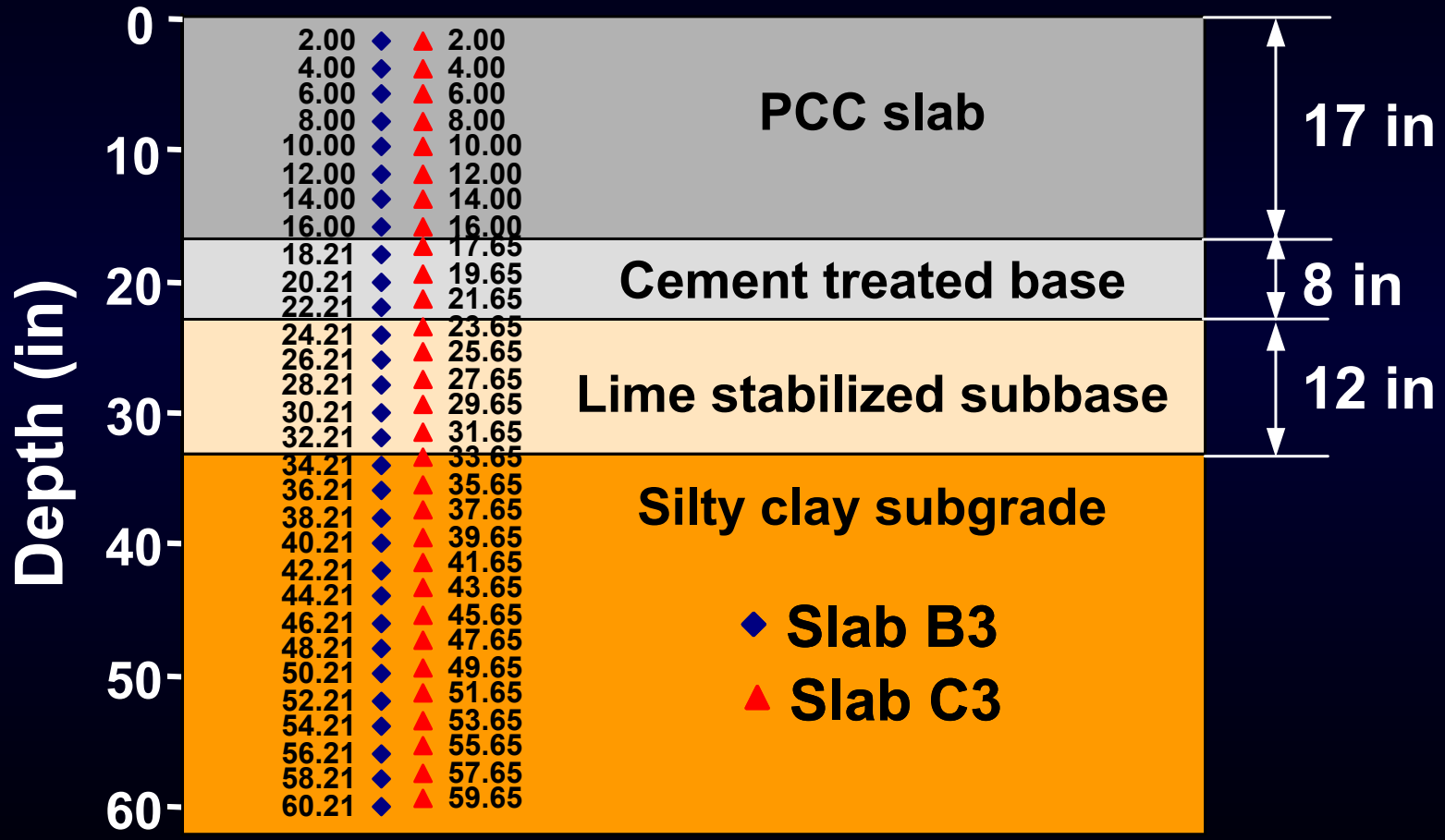

DIA Database

DIA data is accessible through the Internet at
http://www.airtech.tc.faa.gov/DENVER/

Aircraft data: **event number, triggered sensor, complete record (793.4MB)**

Aircraft	Number	Size (MB)
B-727	2937	165.0
B-737	8168	426.0
B-747	144	7.6
B-757	1843	103.0
B-767	320	18.5
B-777	172	9.8
DC-10	389	23.0
MD-80	735	40.5

Temperature data: **date, time, and temperature profile (14.5 MB)**

Displacement and strain data: **event number, number of peaks, interval time, start and end time, offset right and left, peak value and time**

- **Displacement:** **50 LVDT's (77.1 MB)**
  10 SDD's and 40 MDD's
- **Strain:** **23 Carlson (45.2 MB)**
  92 H-Bars (91.7 MB)

Total: ≈ 1 GB

Aircraft Location and Wander Analysis

Position sensors

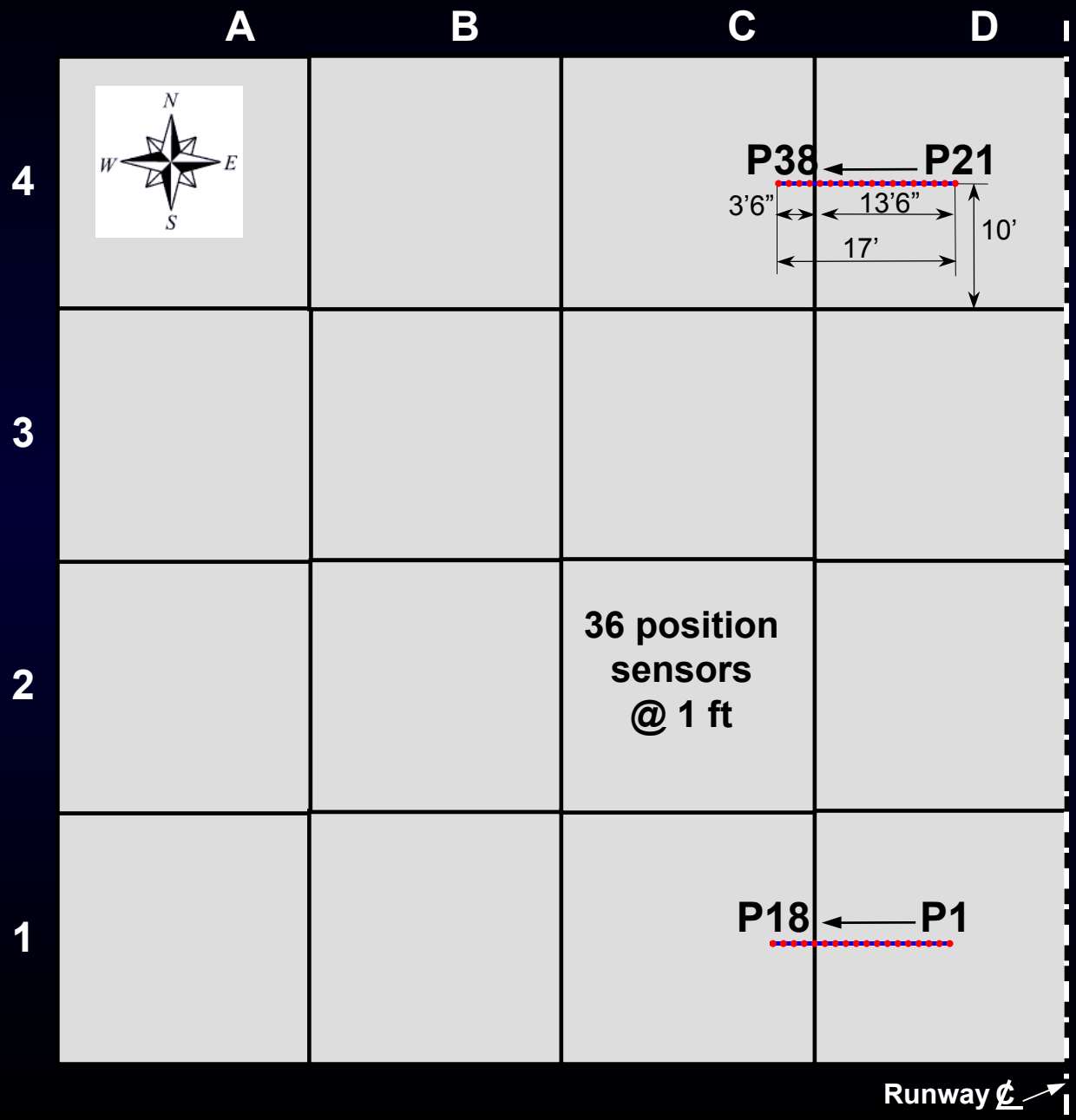

Methodology

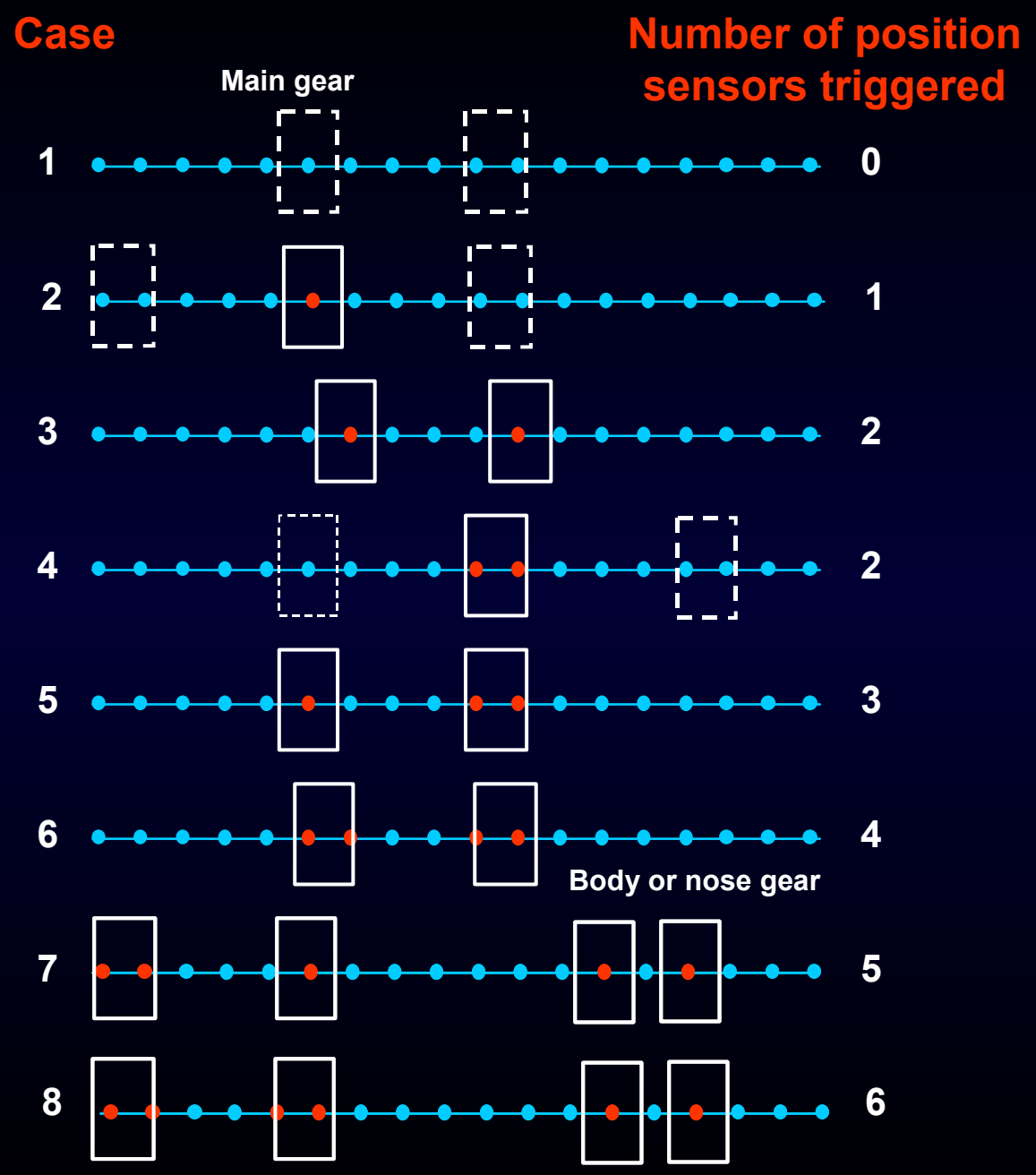

Triggered position sensor

Non-triggered position sensor

Undefined wheel position

Defined wheel position

Methodology (cont.)

$$y = a \cdot x + b$$

$$a = \frac{y_2 - y_1}{x_2 - x_1}$$

$$b = y_1 - \left(\frac{y_2 - y_1}{x_2 - x_1} \right) \cdot x_1$$

$$x = \frac{\left[y - y_1 + \left(\frac{y_2 - y_1}{x_2 - x_1} \right) \cdot x_1 \right] \cdot (x_2 - x_1)}{y_2 - y_1}$$

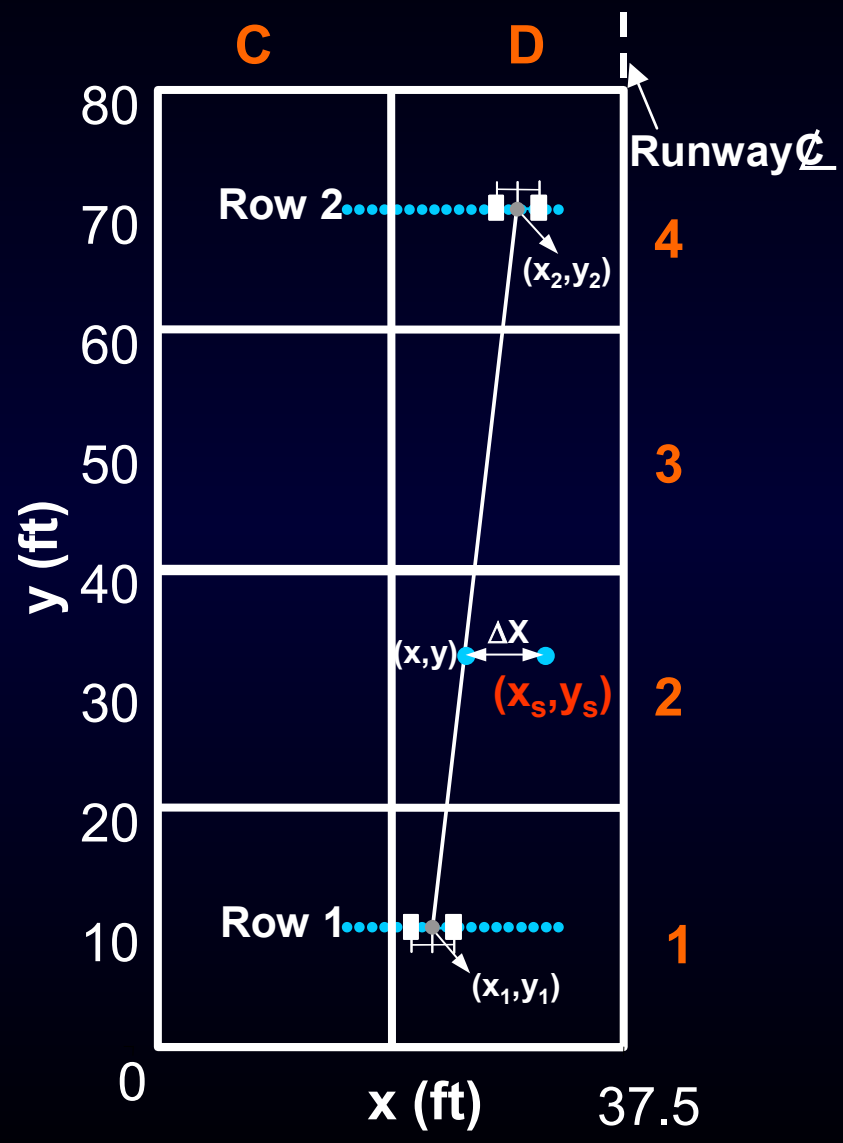

Number of passes

Aircraft	Before filtering location		After filtering location	
	All	W/ weight	All	W/ weight
B-727	2937	1266	1241	523
B-737	8168	2234	1647	382
B-747	144	4	34	1
B-757	1843	585	522	132
B-767	320	18	45	5
B-777	172	23	57	10
DC-10	389	114	218	54
MD-80	735	–	57	–

B-727 events

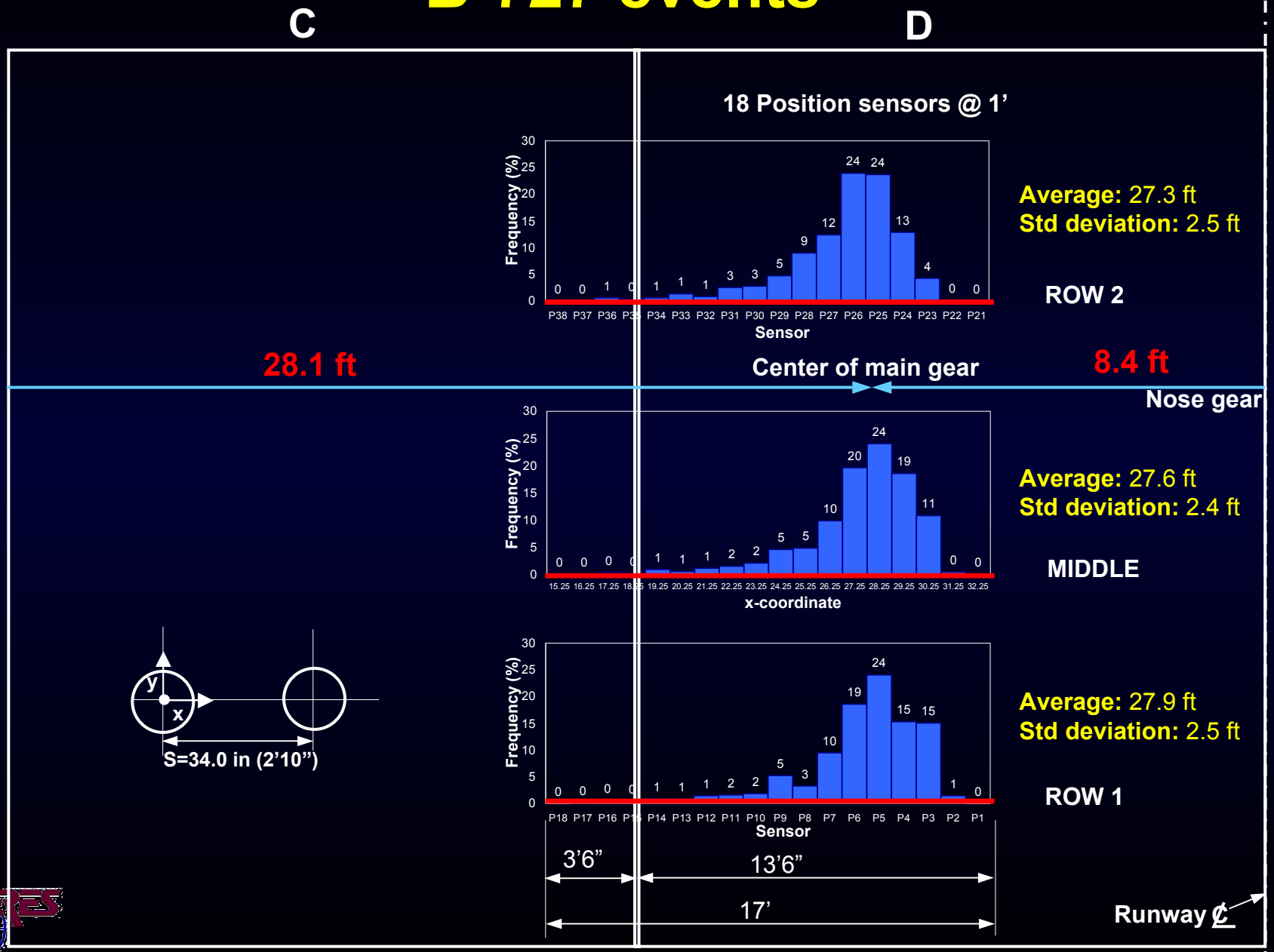
C
D
18 Position sensors @ 1'
Frequency (%)
Sensor
P38 P37 P36 P35 P34 P33 P32 P31 P30 P29 P28 P27 P26 P25 P24 P23 P22 P21
0 0 1 0 1 1 1 3 3 5 9 12 24 24 13 4 0 0
Average: 27.3 ft
Std deviation: 2.5 ft
ROW 2
28.1 ft
Center of main gear
8.4 ft
Nose gear
x-coordinate
15.25 16.25 17.25 18.25 19.25 20.25 21.25 22.25 23.25 24.25 25.25 26.25 27.25 28.25 29.25 30.25 31.25 32.25
0 0 0 0 1 1 1 2 2 5 5 10 20 24 19 11 0 0
Average: 27.6 ft
Std deviation: 2.4 ft
MIDDLE
y
x
S=34.0 in (2'10")
P18 P17 P16 P15 P14 P13 P12 P11 P10 P9 P8 P7 P6 P5 P4 P3 P2 P1
0 0 0 0 1 1 1 2 2 5 3 10 19 24 15 15 1 0
Average: 27.9 ft
Std deviation: 2.5 ft
ROW 1
3'6"
13'6"
17'
Runway ℄

Runway offset

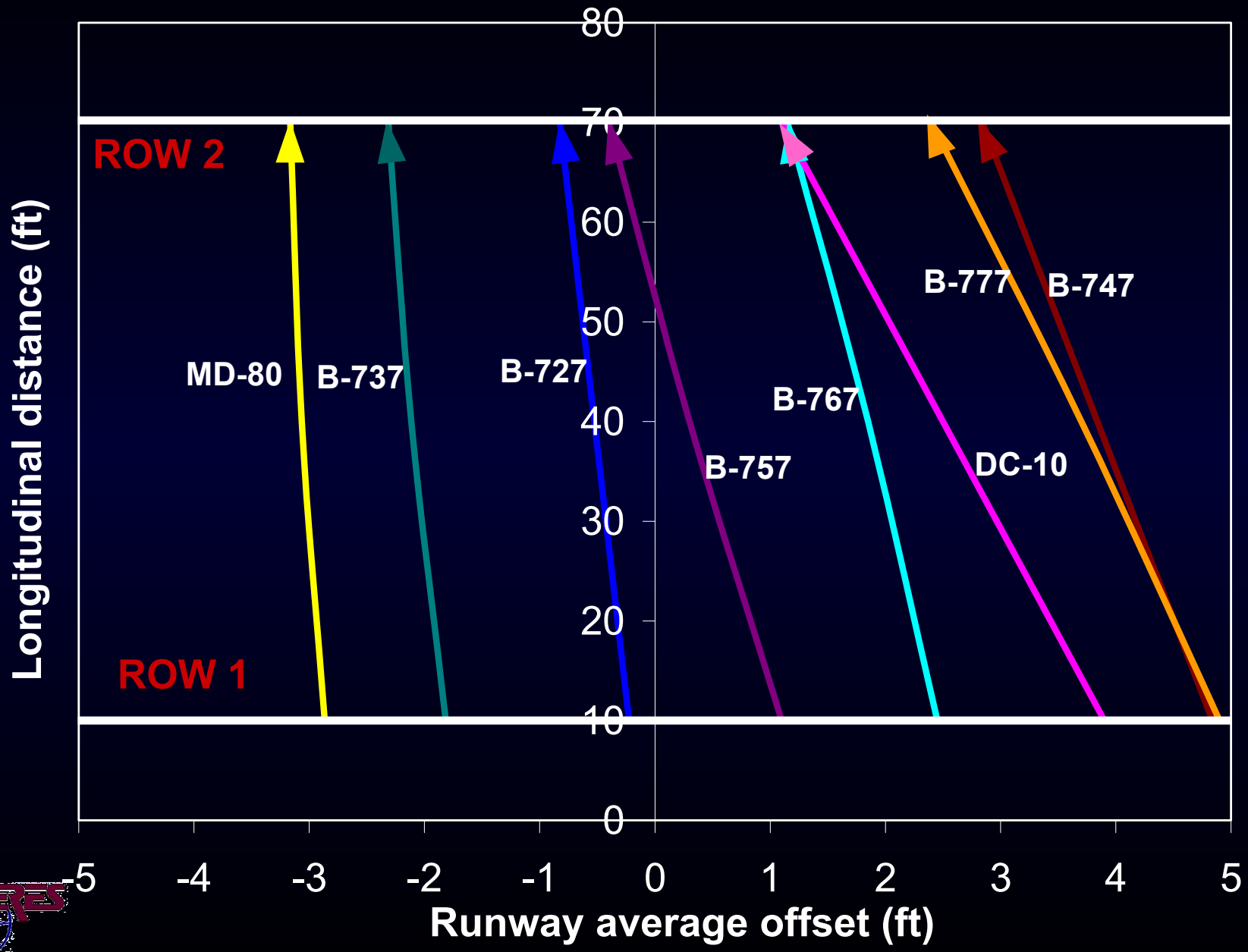

Wander and Pavement Design

- Aircraft path distribution

$$f(x) = \frac{1}{\sigma\sqrt{2\pi}} e^{-0.5\left[\frac{x-\mu}{\sigma}\right]^2}$$

- Load location relative to the joints

Single axle

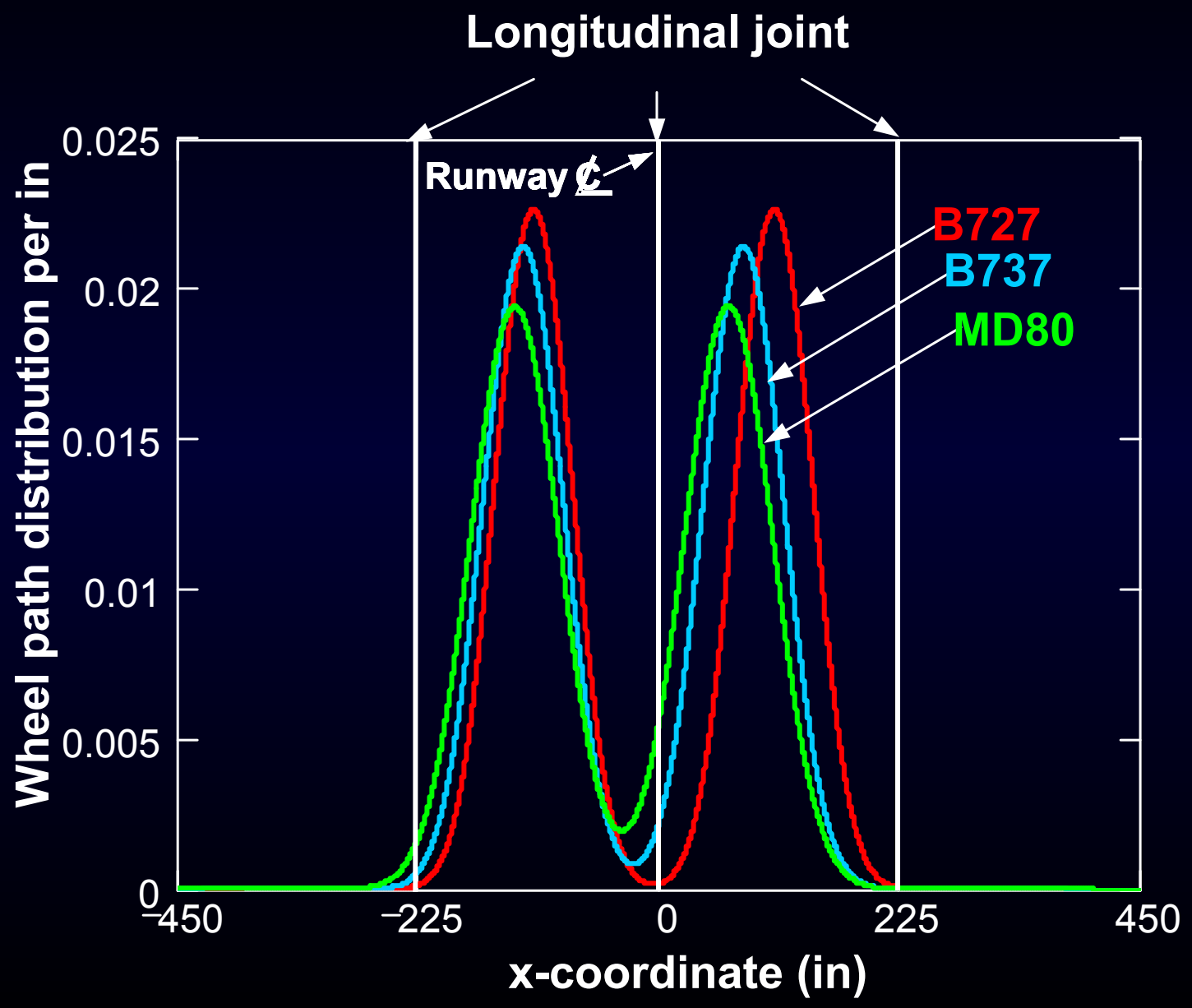
Longitudinal joint
Runway ℄
B727
B737
MD80
Wheel path distribution per in
0.025
0.02
0.015
0.01
0.005
0
−450
−225
0
225
450
x-coordinate (in)

Tandem axle

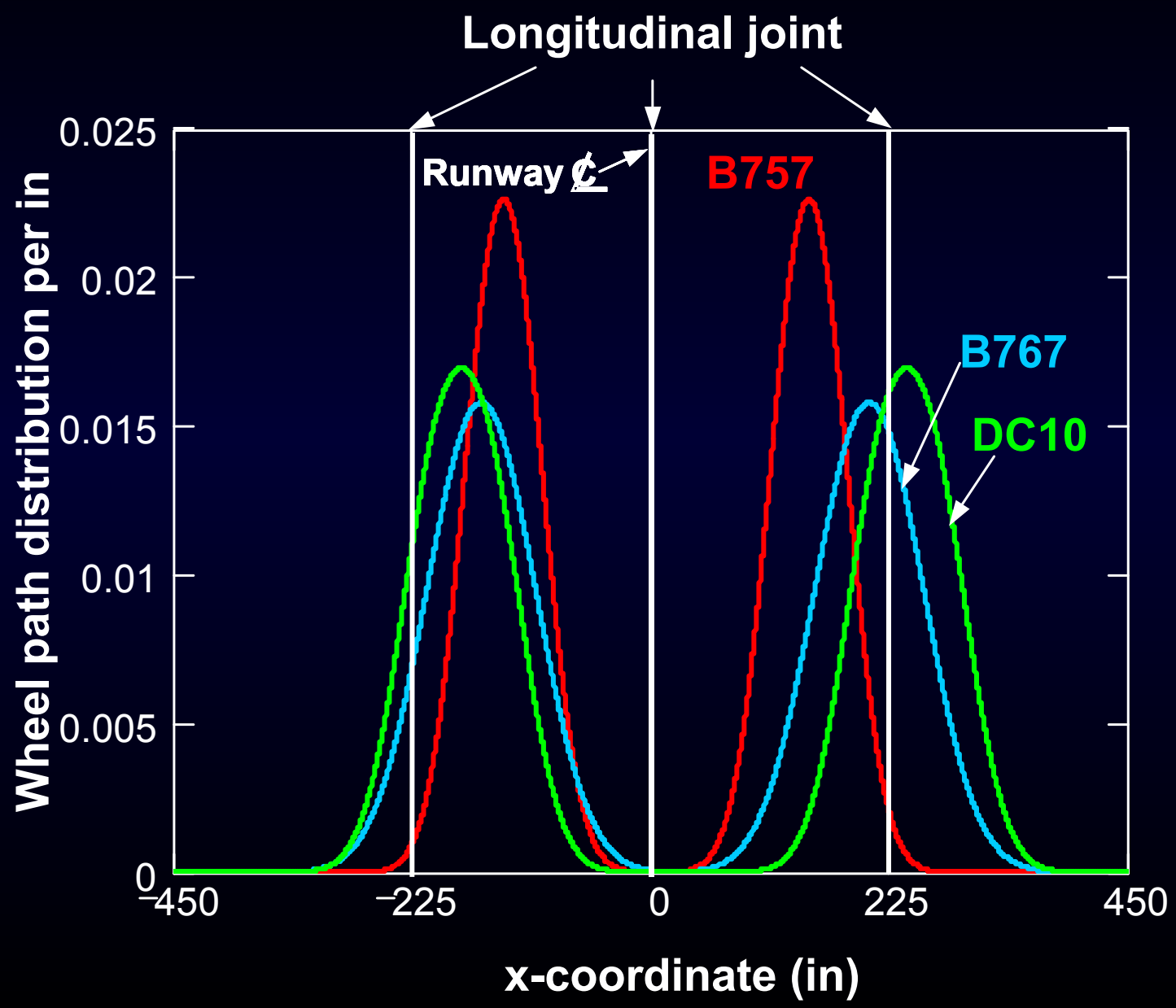
Longitudinal joint
Runway ℄
B757
B767
DC10
Wheel path distribution per in
0.025
0.02
0.015
0.01
0.005
0
−450
−225
0
225
450
x-coordinate (in)

B747 and B777

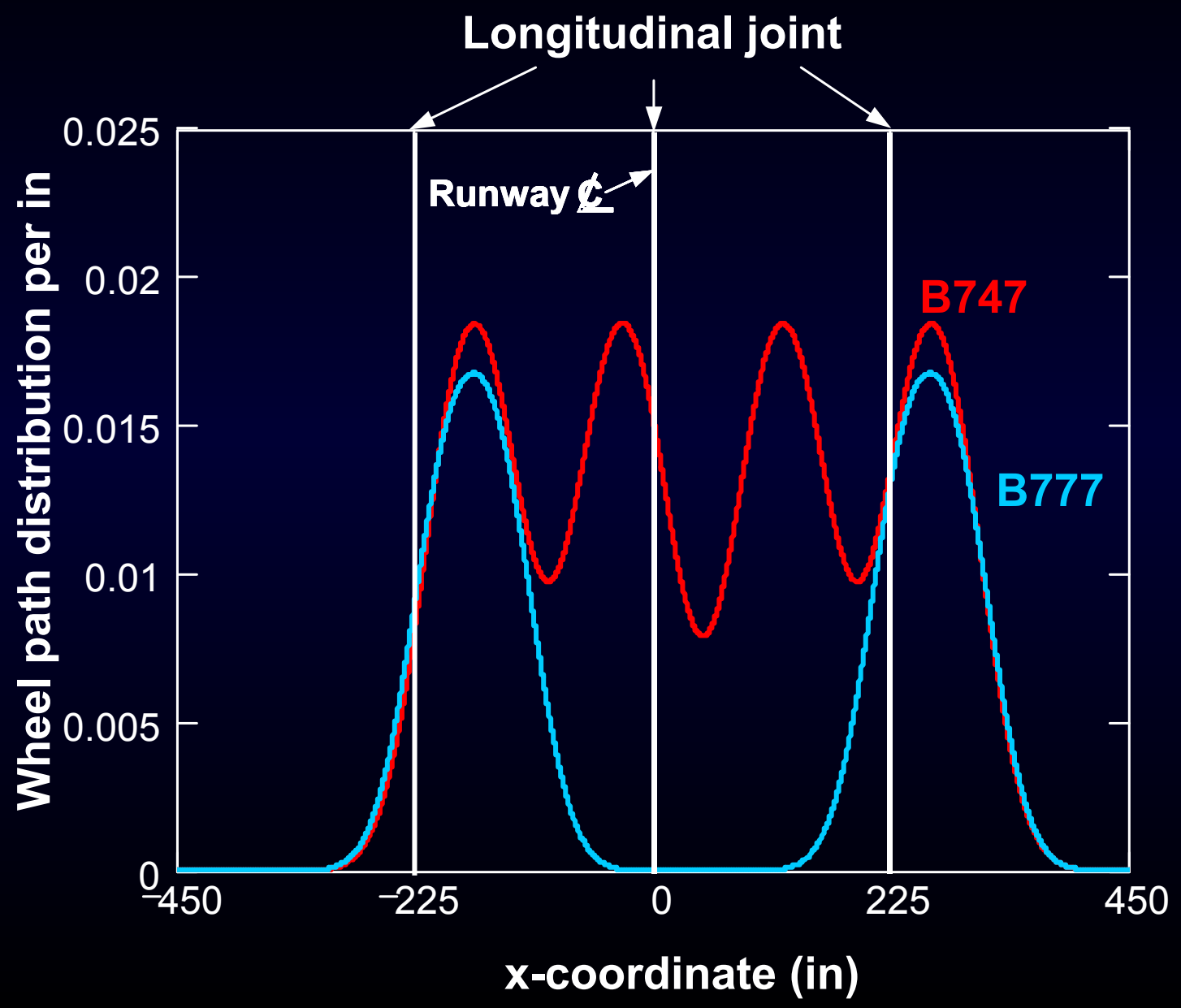

Backcalculation of Pavement Layer Properties

Pavement evaluation at DIA

Date:
05/03/95
09/15/95
03/02/96
04/08/97
07/31/97
06/06/00

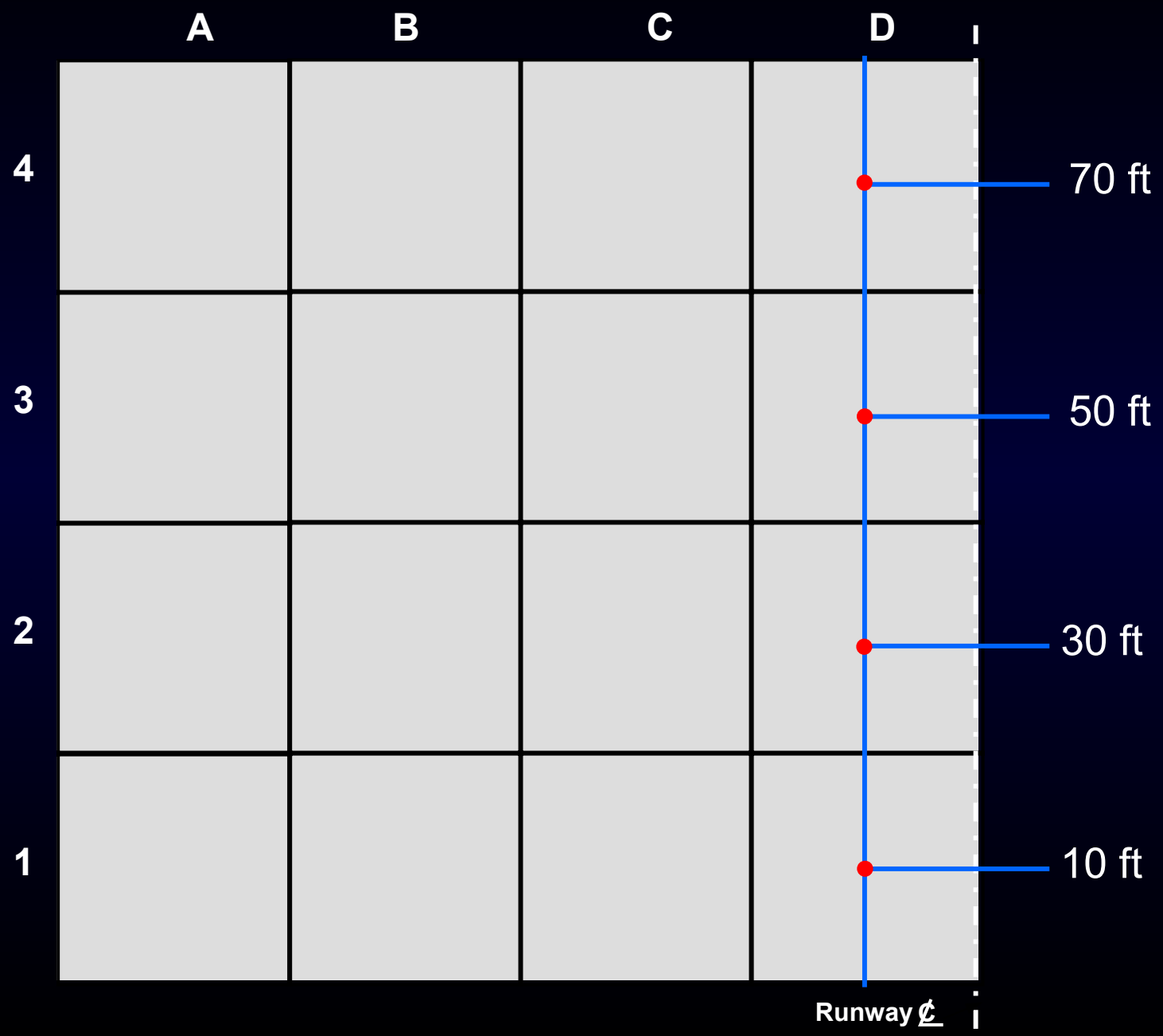

Backcalculation

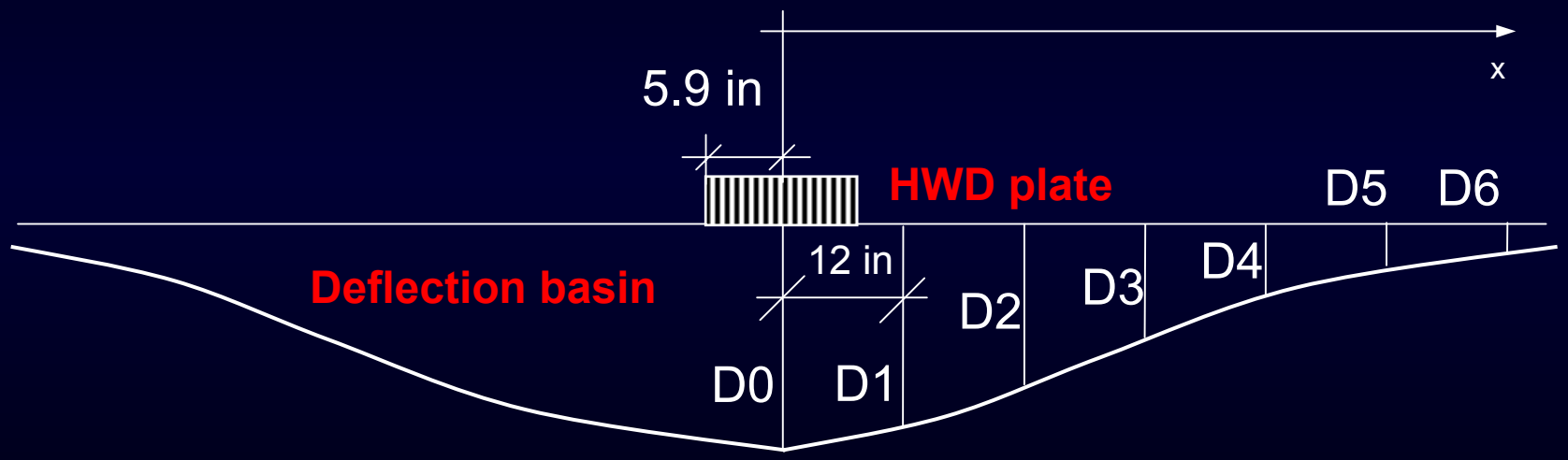

Comparison between different models

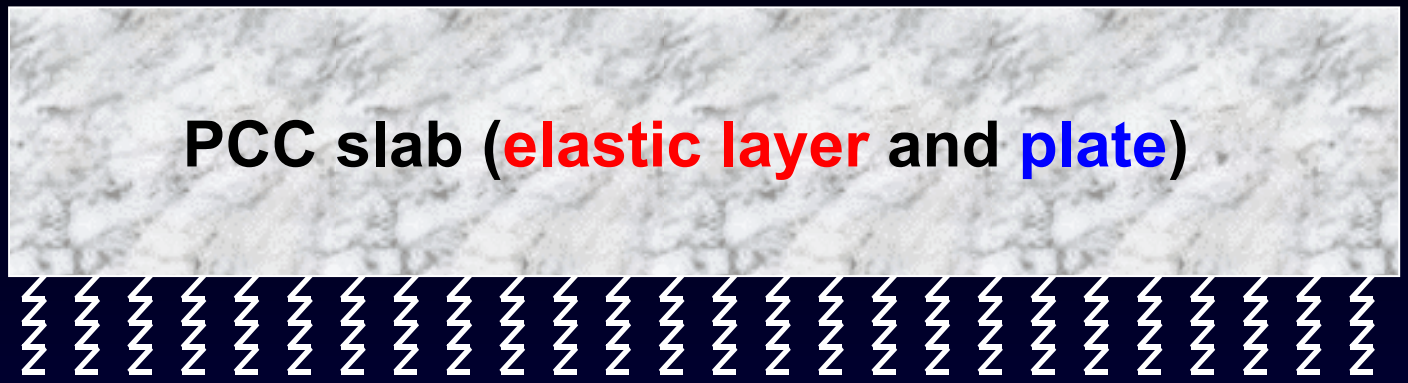

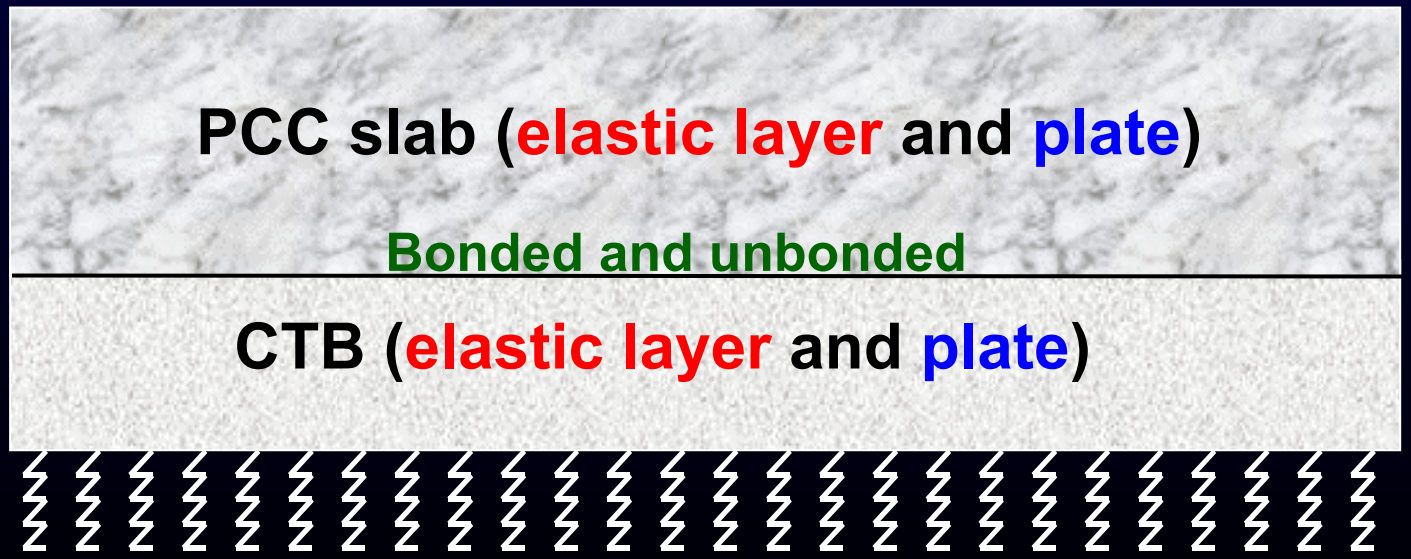

Factorial run performed with DIPLOMAT

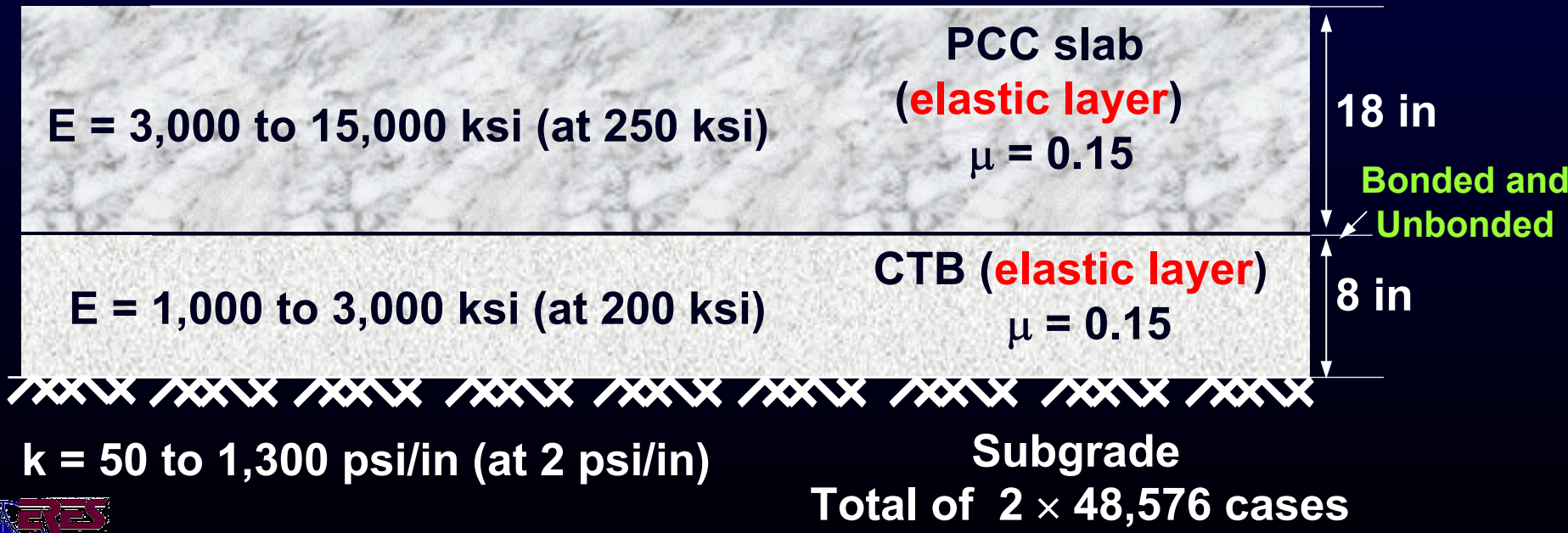

Slab modulus of elasticity for different models based on DIA

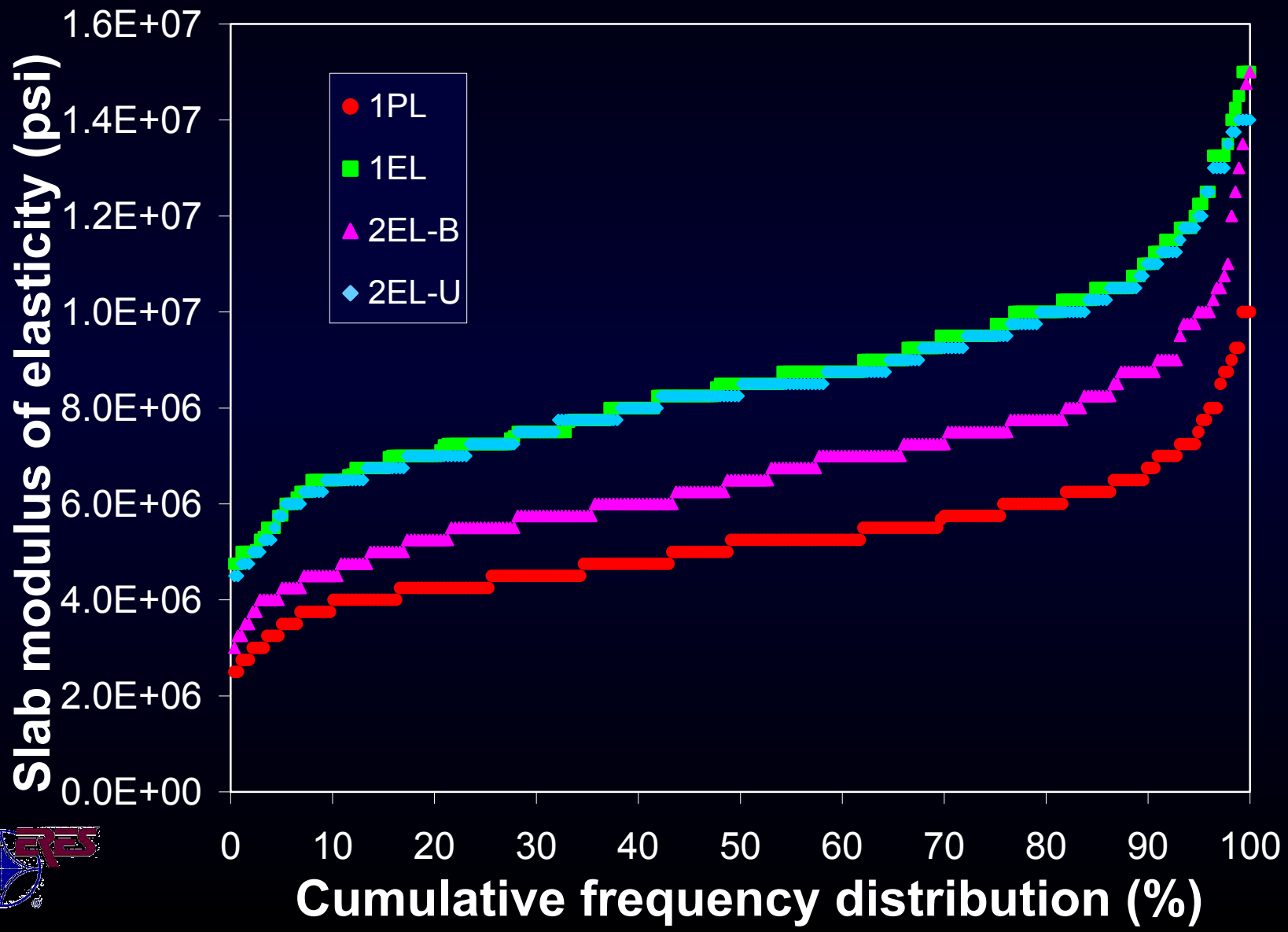

Modulus of subgrade reaction for different models based on DIA

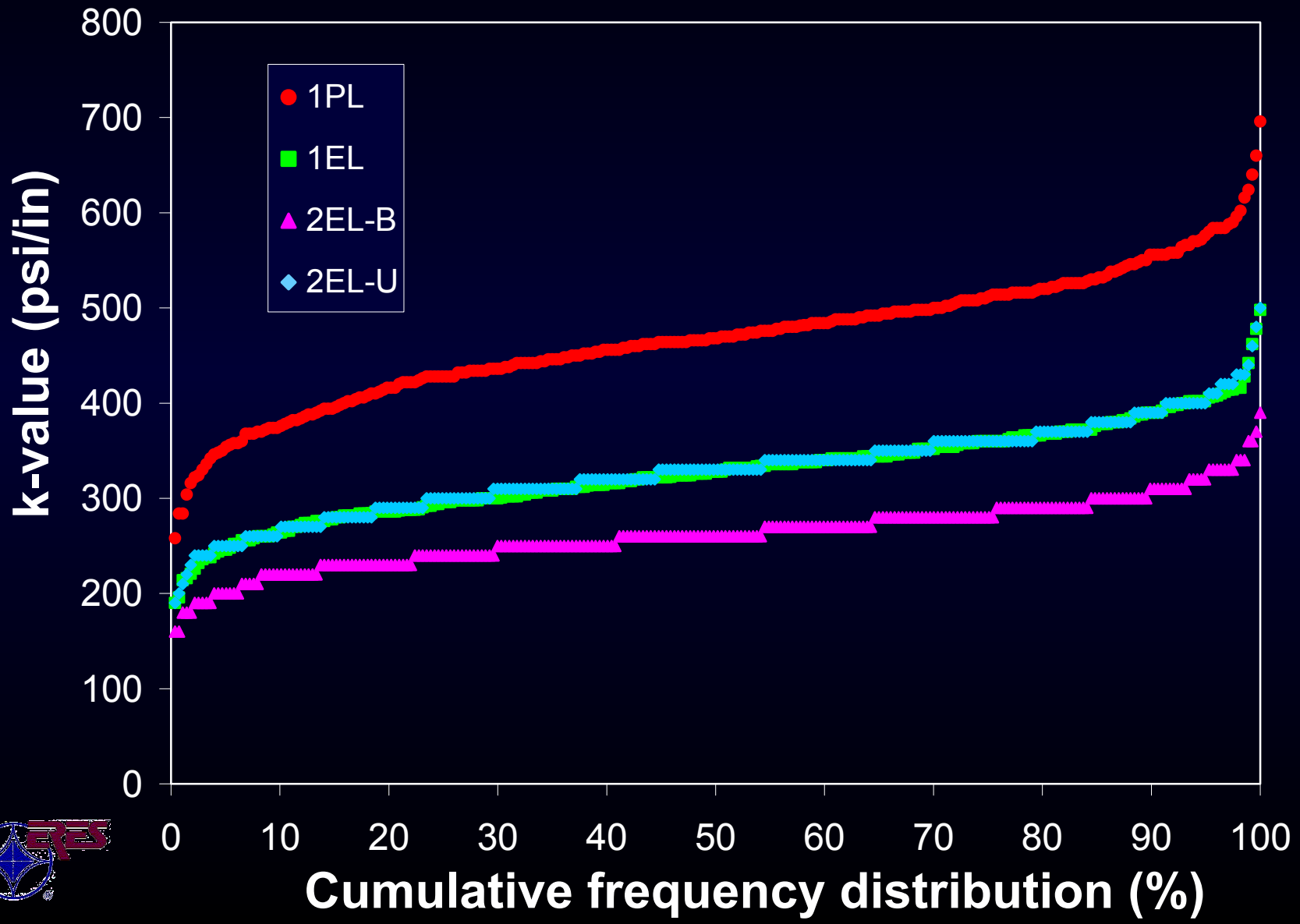

Prediction of Pavement Temperature and Its Effect on Joint Behavior

Thermocouples

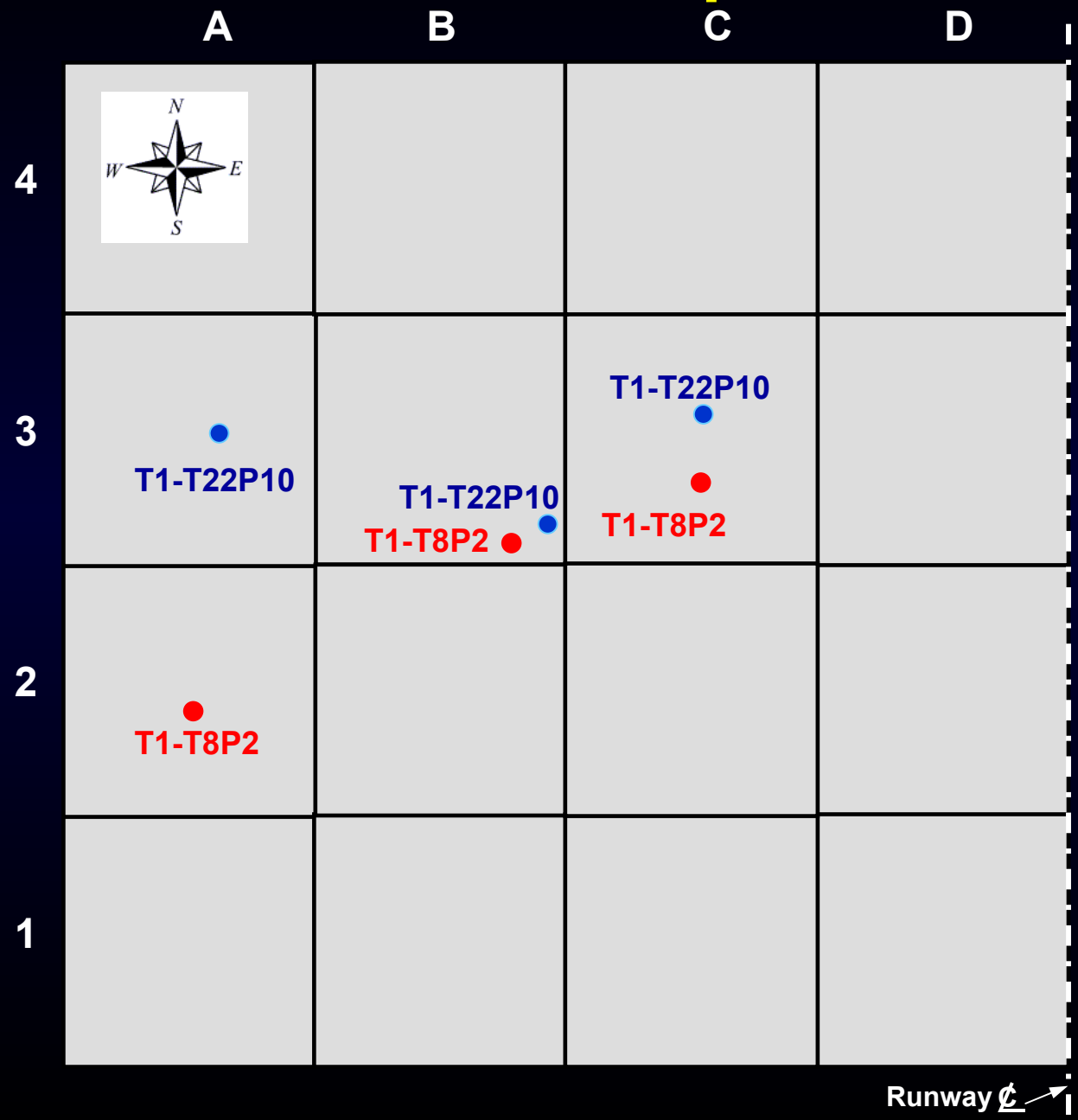

Data collection

Sensor	Slab	1995	1996	1997	1998	1999
T1-T8P2	B3	2016	2200	842	2690	1086
	C3	2016	2409	376	2690	1086
T1-T22P10	B3	2016	2200	842	2690	1086
	C3	2016	2409	376	2690	1086

Collected combined data: **9,057**

Annual data: **8,760**

Total data: **43,800**

Prediction of pavement temperature using Integrated-Climatic Model (ICM)

Material properties

- Thermal conductivity
- Heat capacity
- Emissivity factor
- Surface short-wave absorptivity

Climatic data

Obtained from National Oceanic and Atmospheric Association (NOAA)

- Air temperature
- Precipitation
- Percent sunshine
- Wind speed
- Radiation

Depth of thermocouples and ICM nodes

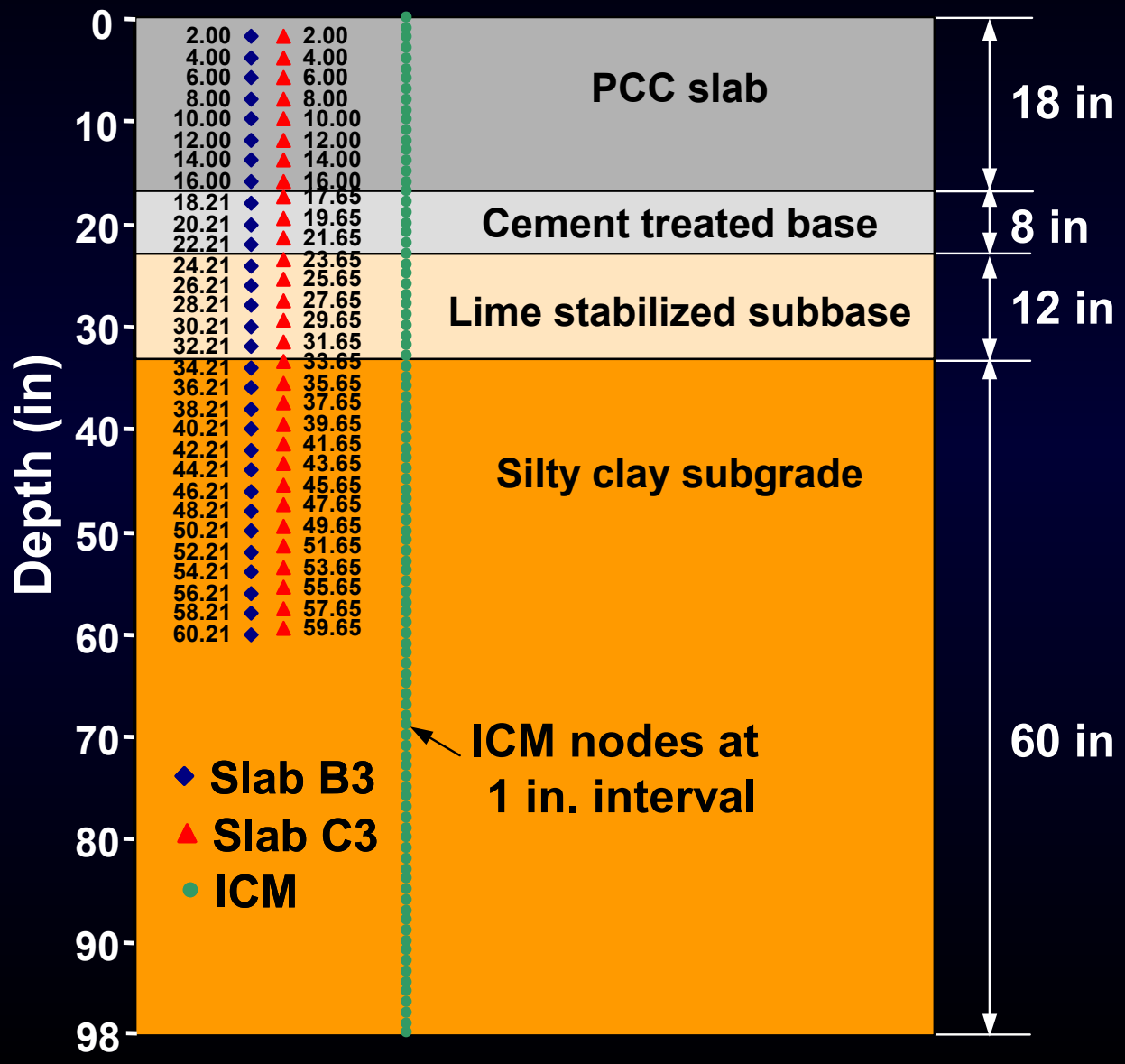

Measured versus predicted temperature differential

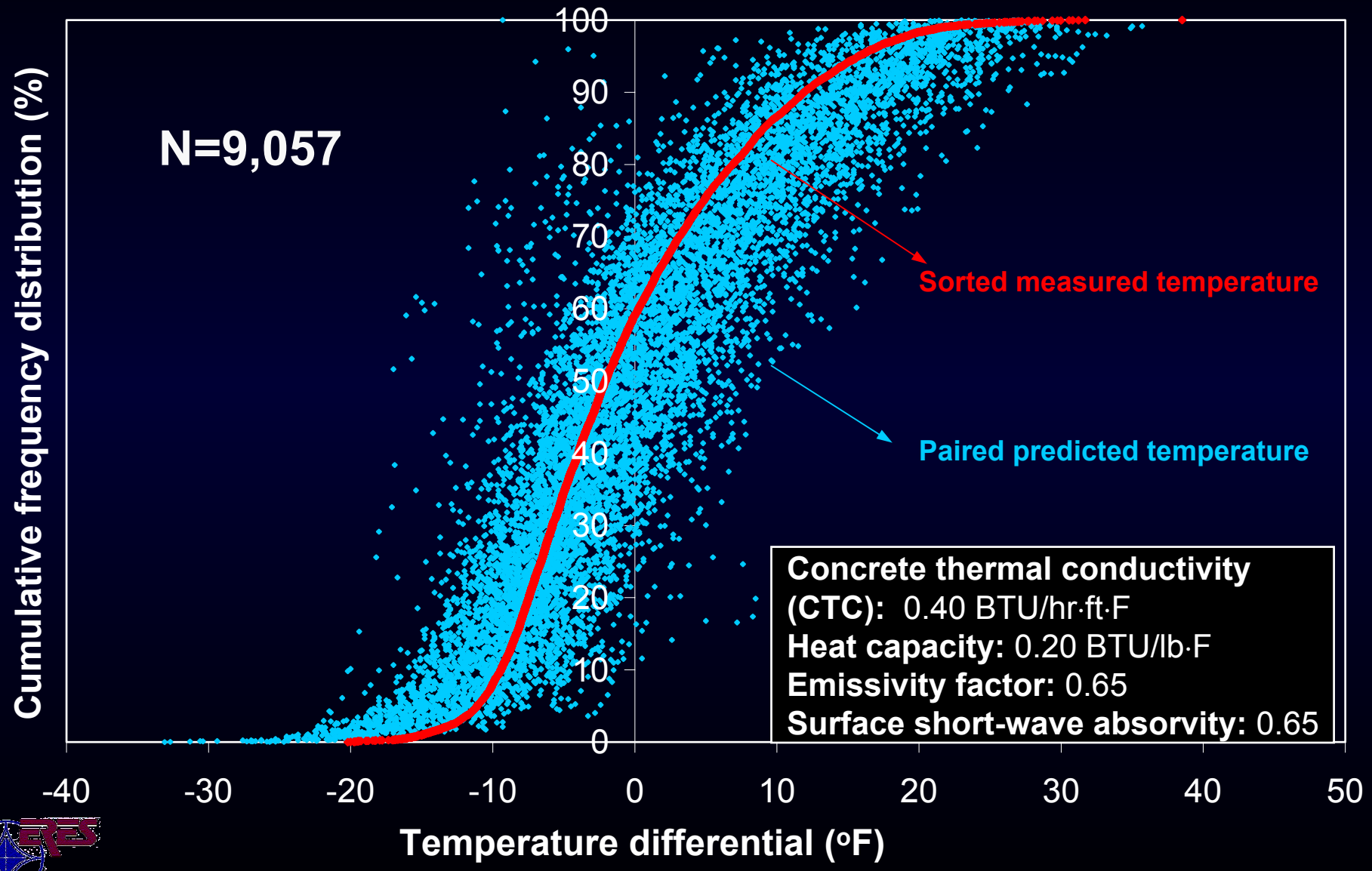

Differential pavement temperature distribution

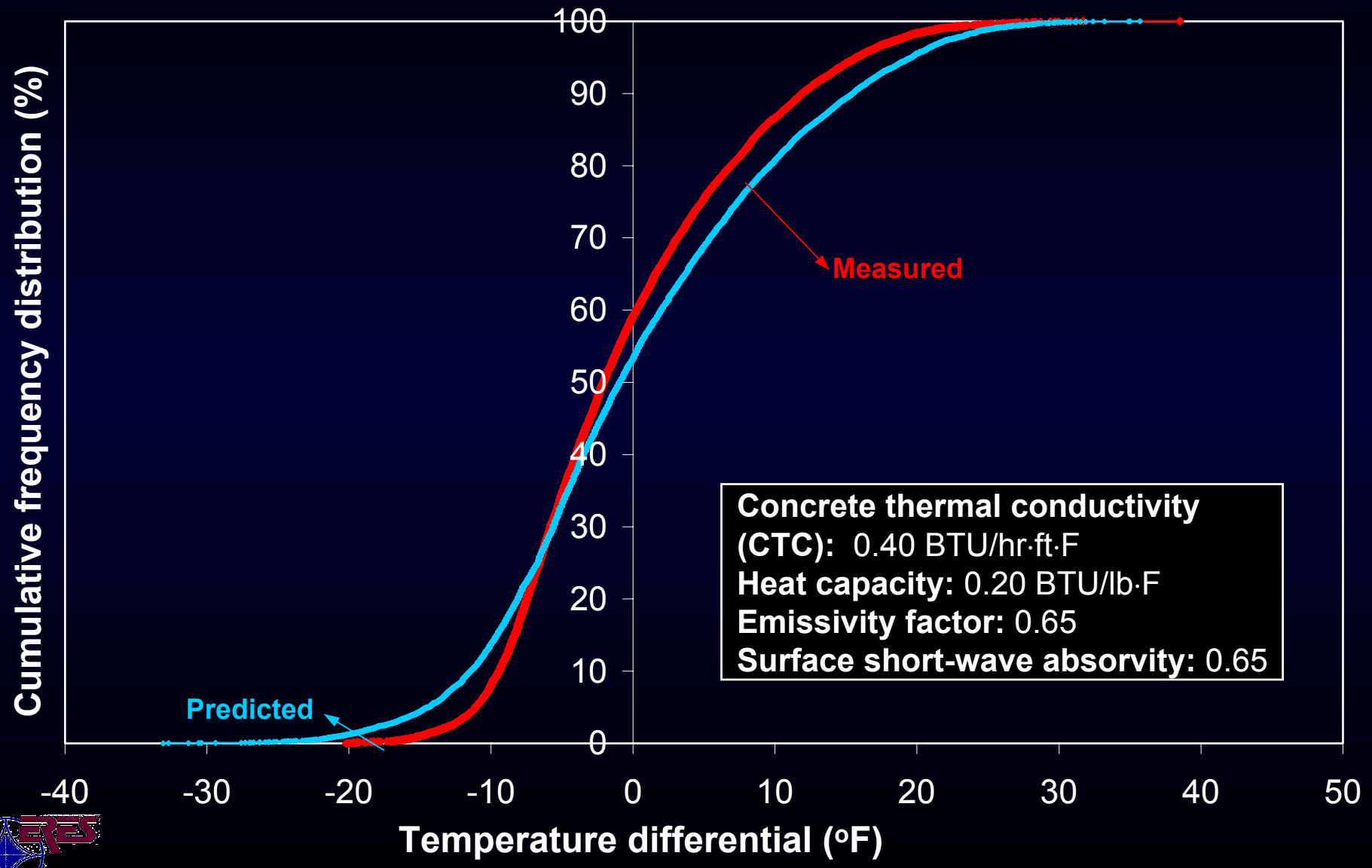

Measured versus predicted average pavement temperature

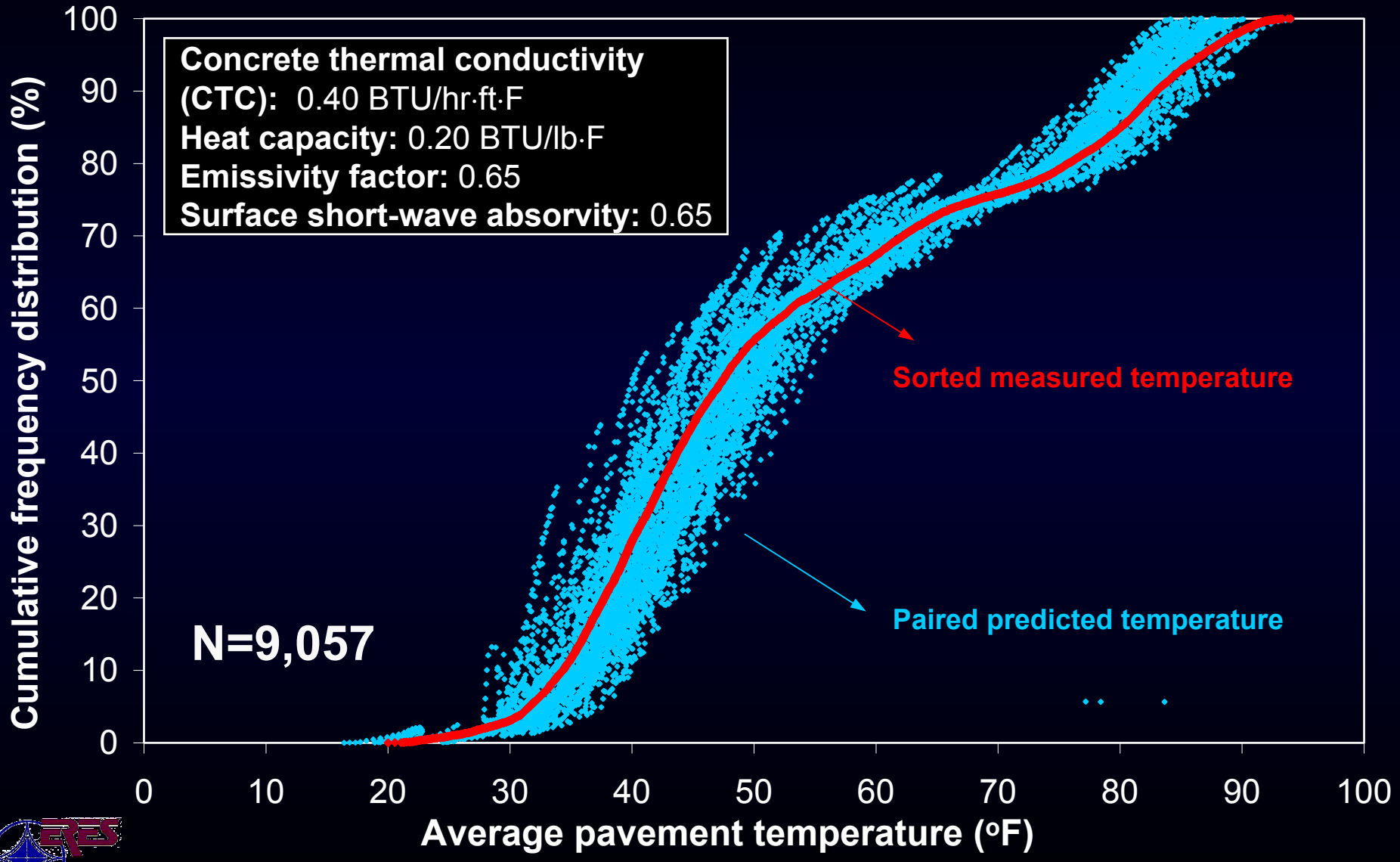

Average pavement temperature distribution

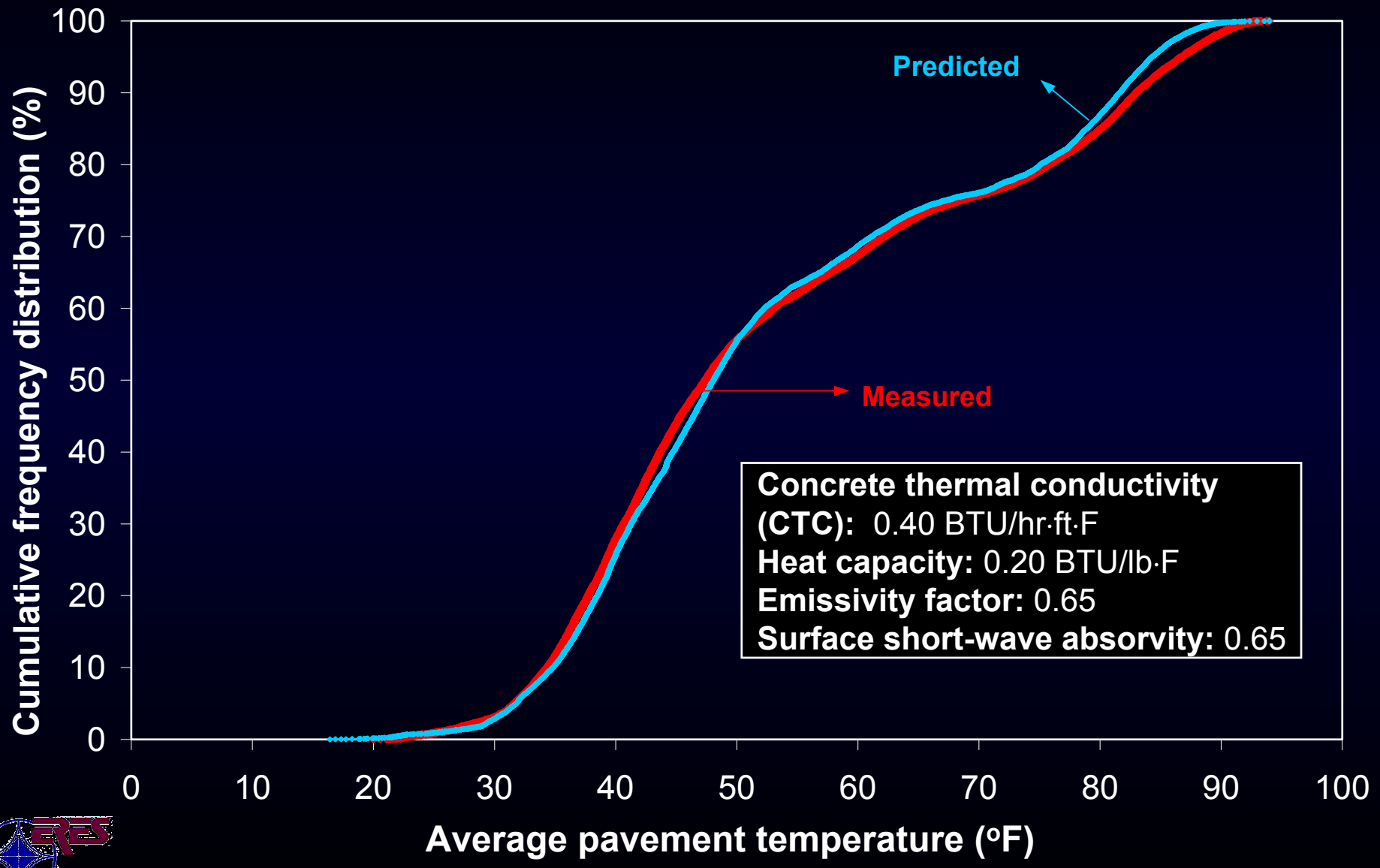

Joint gages

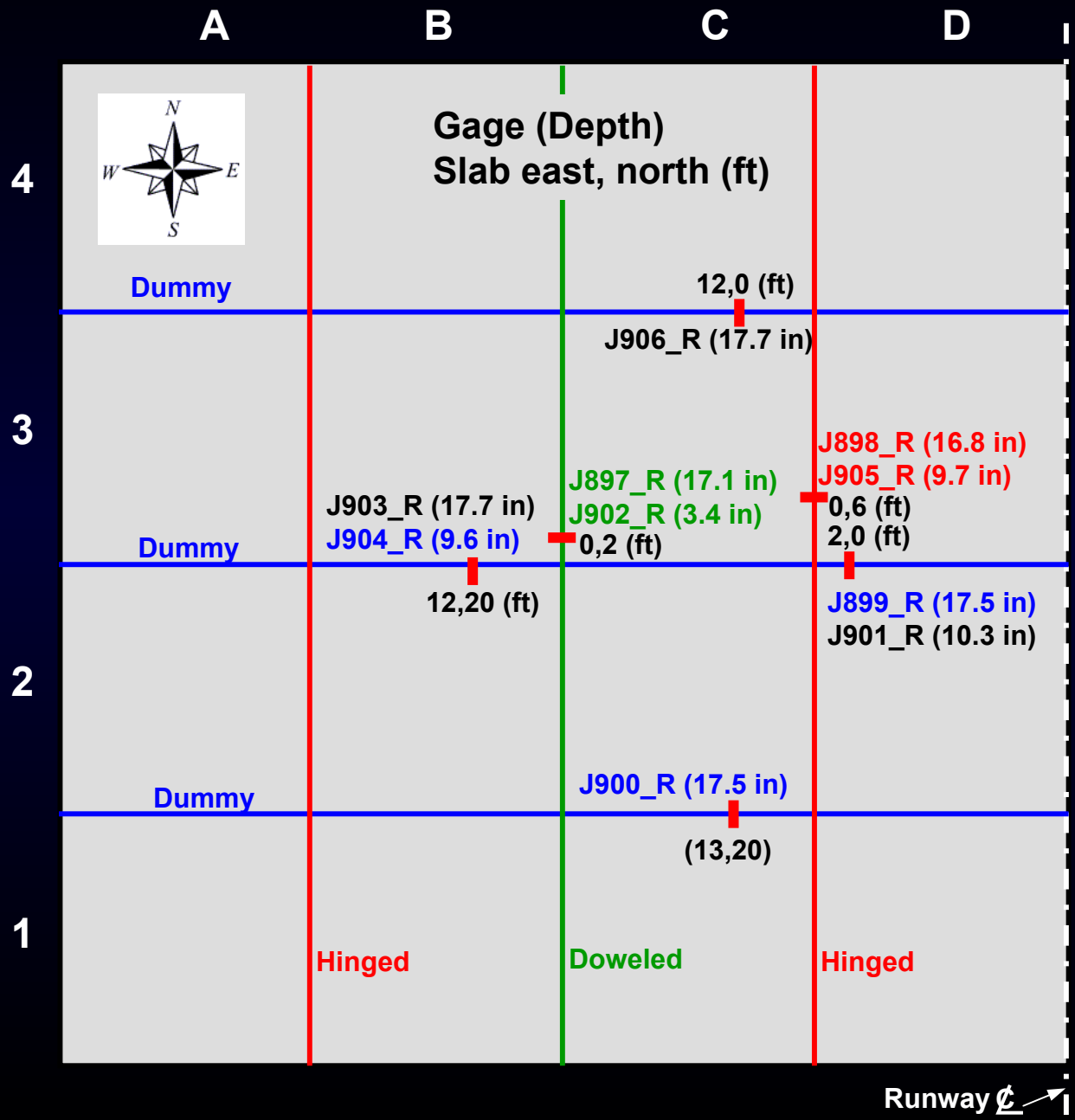
A
B
C
D
4
3
2
1
N
W
E
S
Gage (Depth)
Slab east, north (ft)
Dummy
12,0 (ft)
J906_R (17.7 in)
J898_R (16.8 in)
J905_R (9.7 in)
J897_R (17.1 in)
J902_R (3.4 in)
J903_R (17.7 in)
J904_R (9.6 in)
0,6 (ft)
2,0 (ft)
0,2 (ft)
Dummy
12,20 (ft)
J899_R (17.5 in)
J901_R (10.3 in)
J900_R (17.5 in)
Dummy
(13,20)
Hinged
Doweled
Hinged
Runway ℄

Dummy joint opening by season

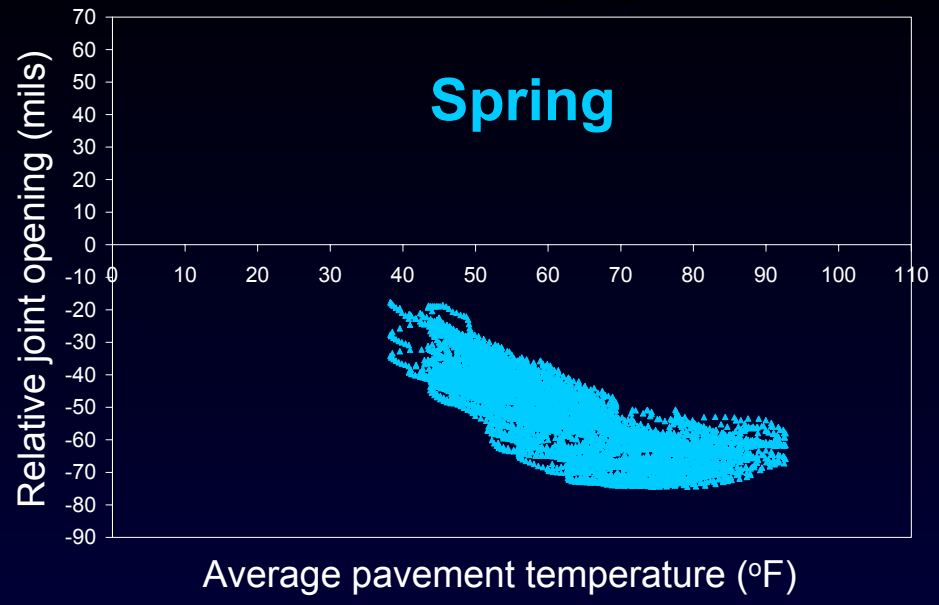

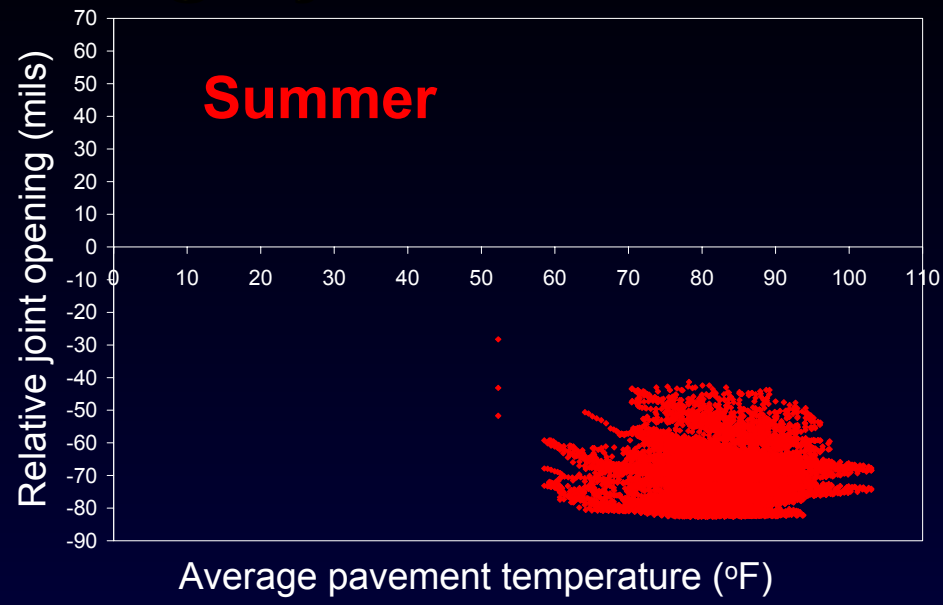

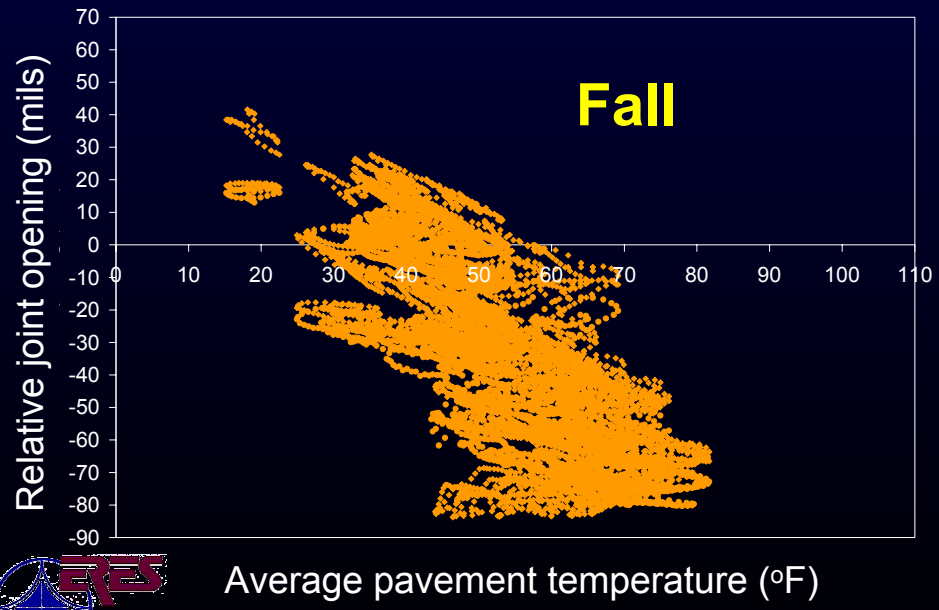

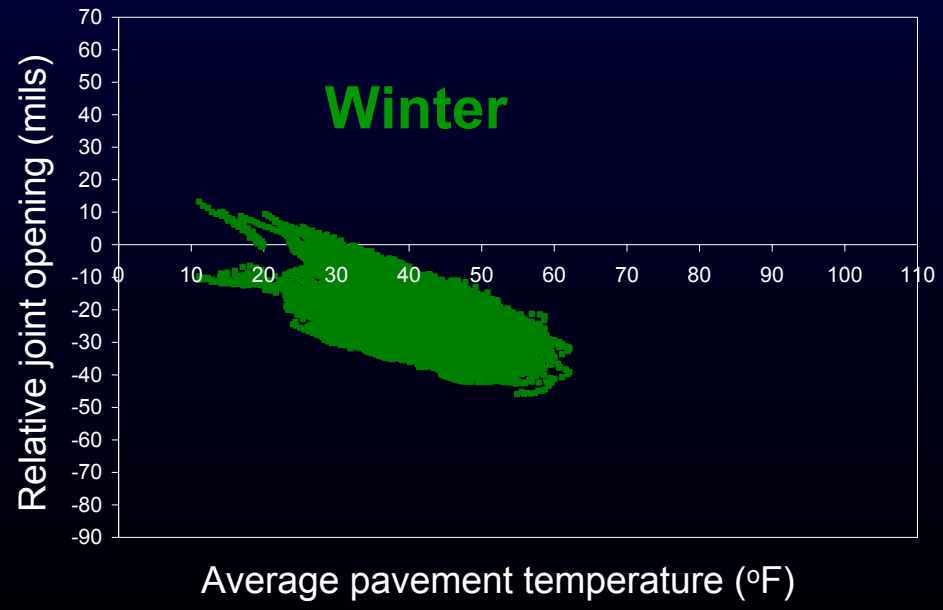

Hinged joint opening by season

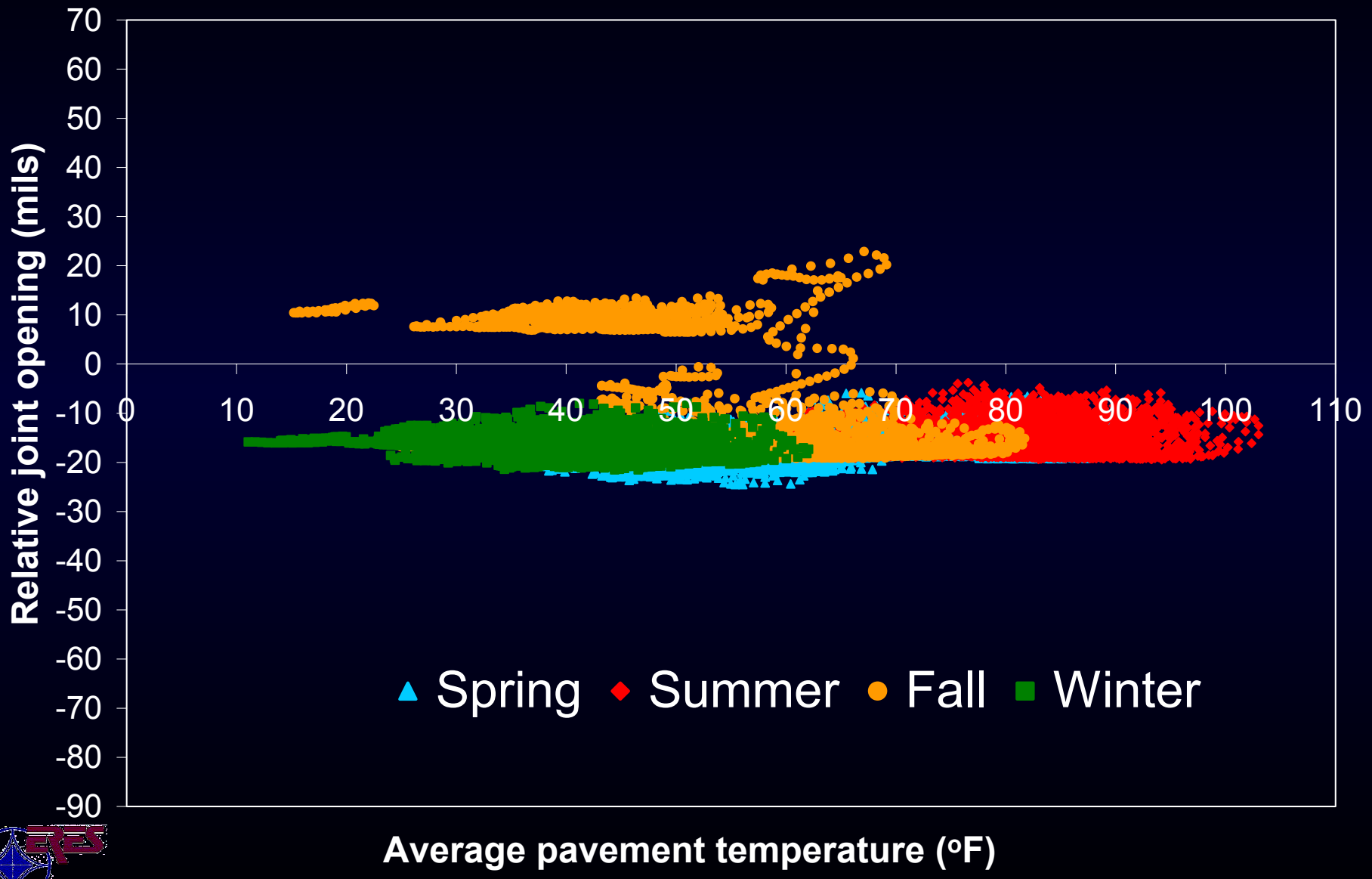

Load transfer efficiency

Date: Test #
05/03/95: 9, 32
09/16/95: 33
03/03/96: 10, 34
04/12/97: 31
08/01/97: 83

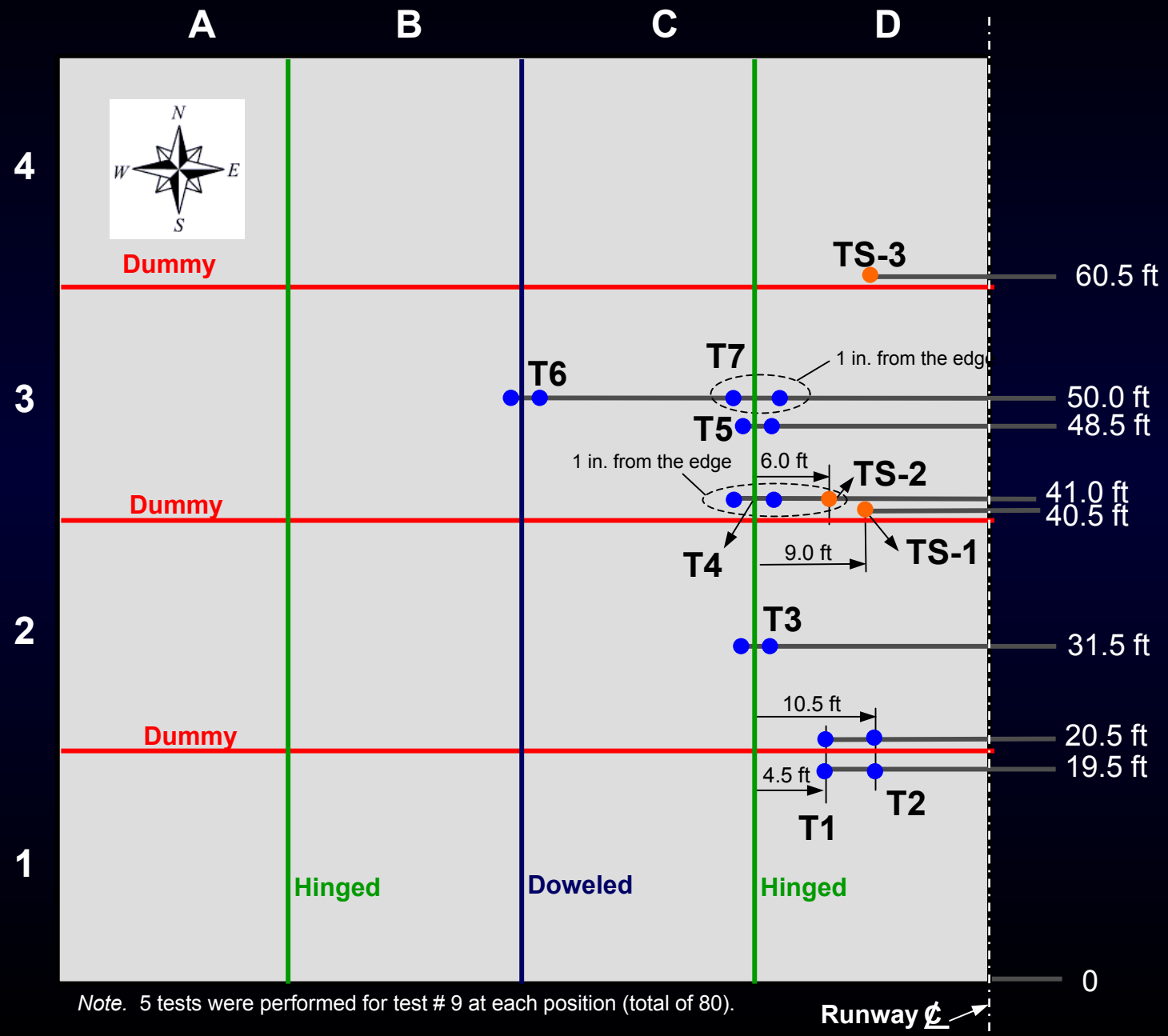

Note. 5 tests were performed for test # 9 at each position (total of 80).

LTE for doweled joints

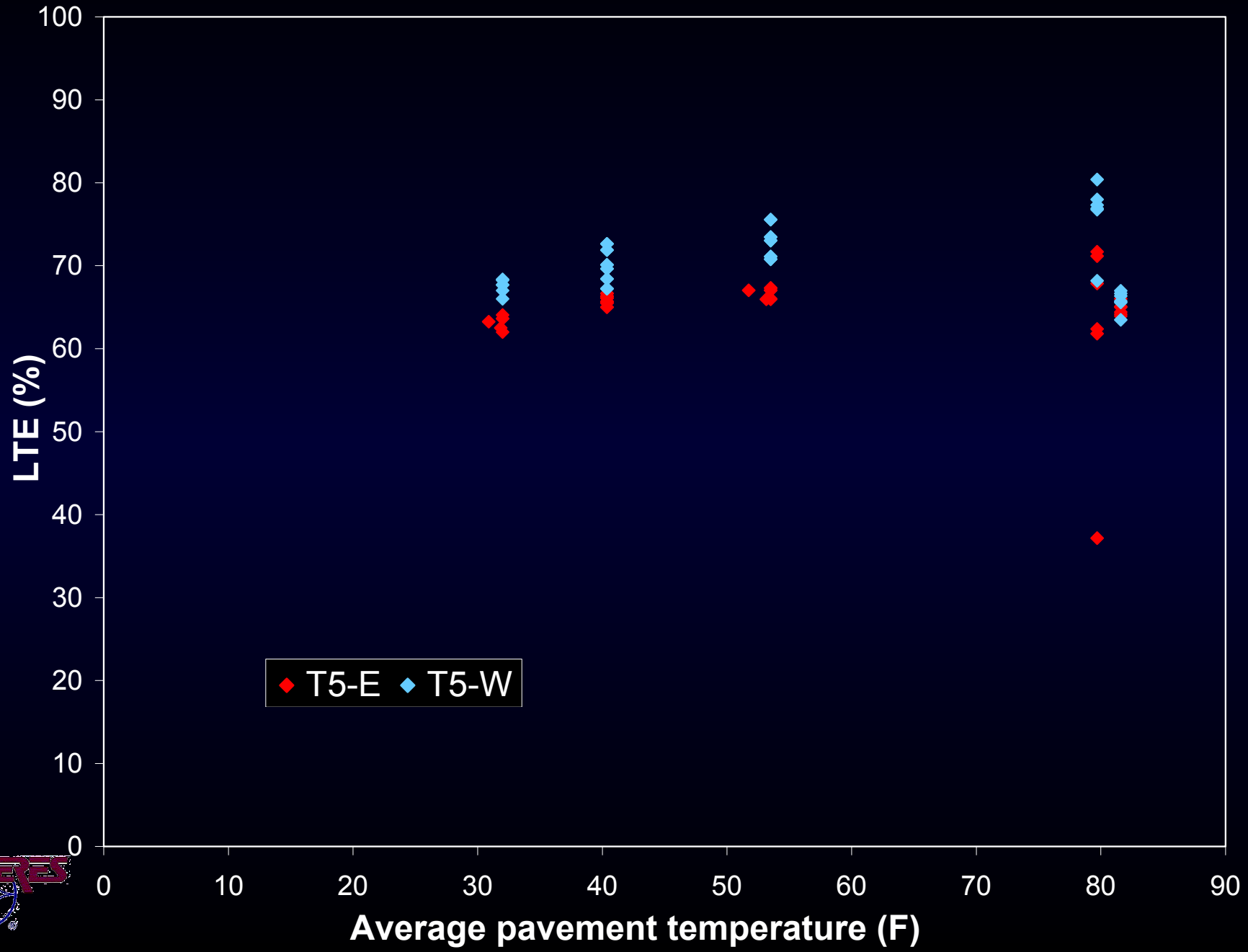

Prediction of LTE for dummy joints

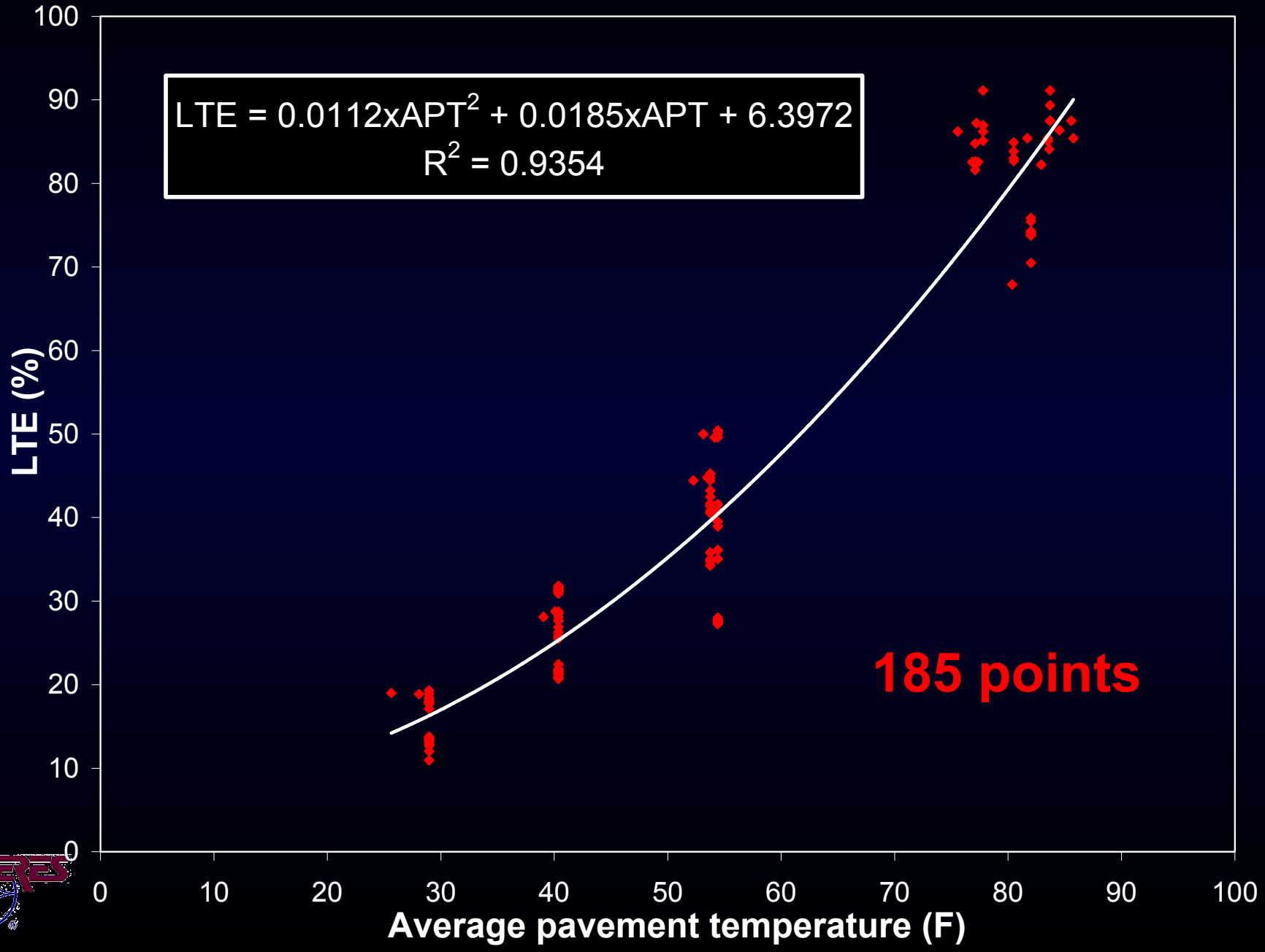

Frequency of predicted dummy joint LTE for seven years

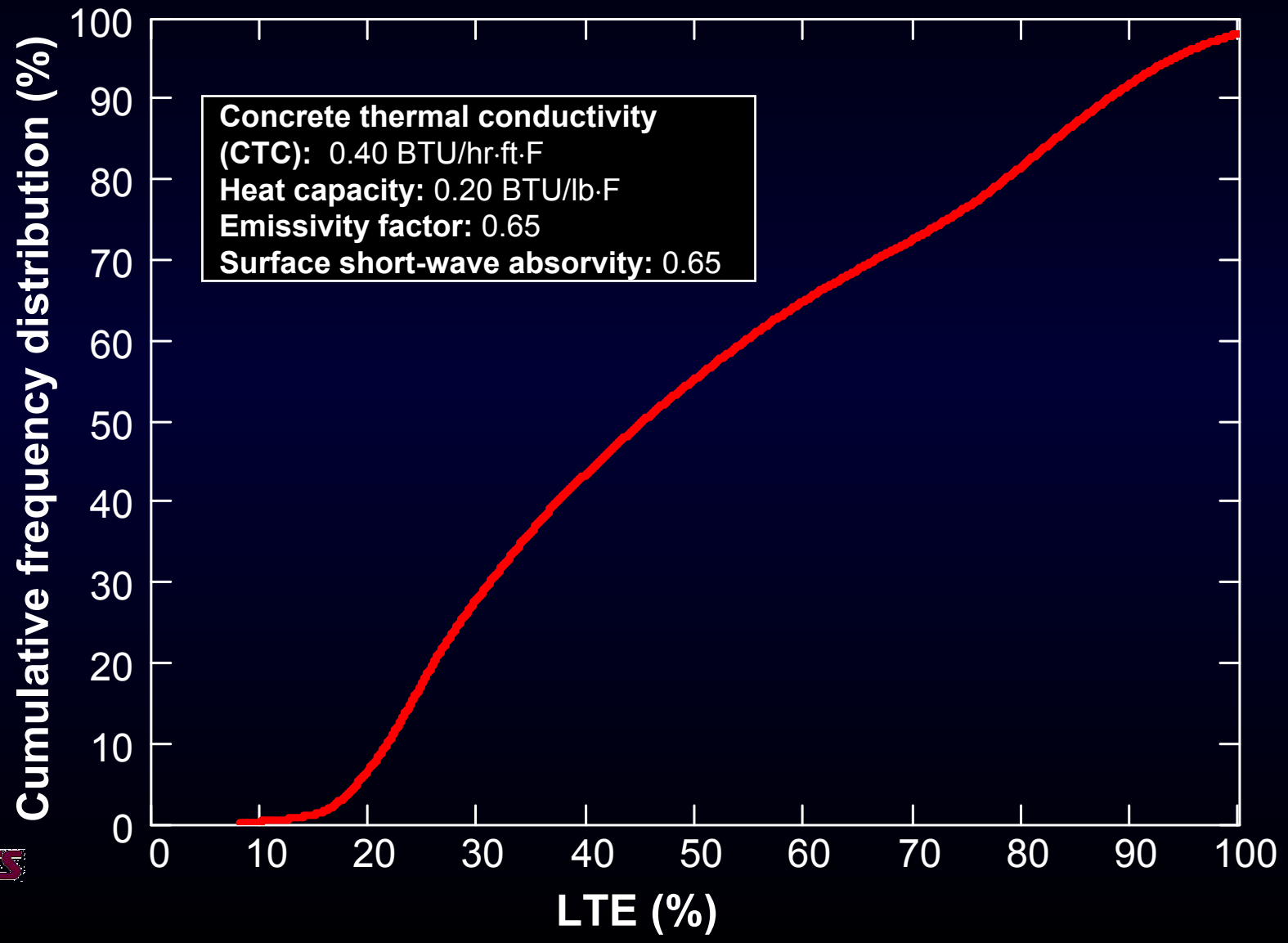

LTE for hinged joints

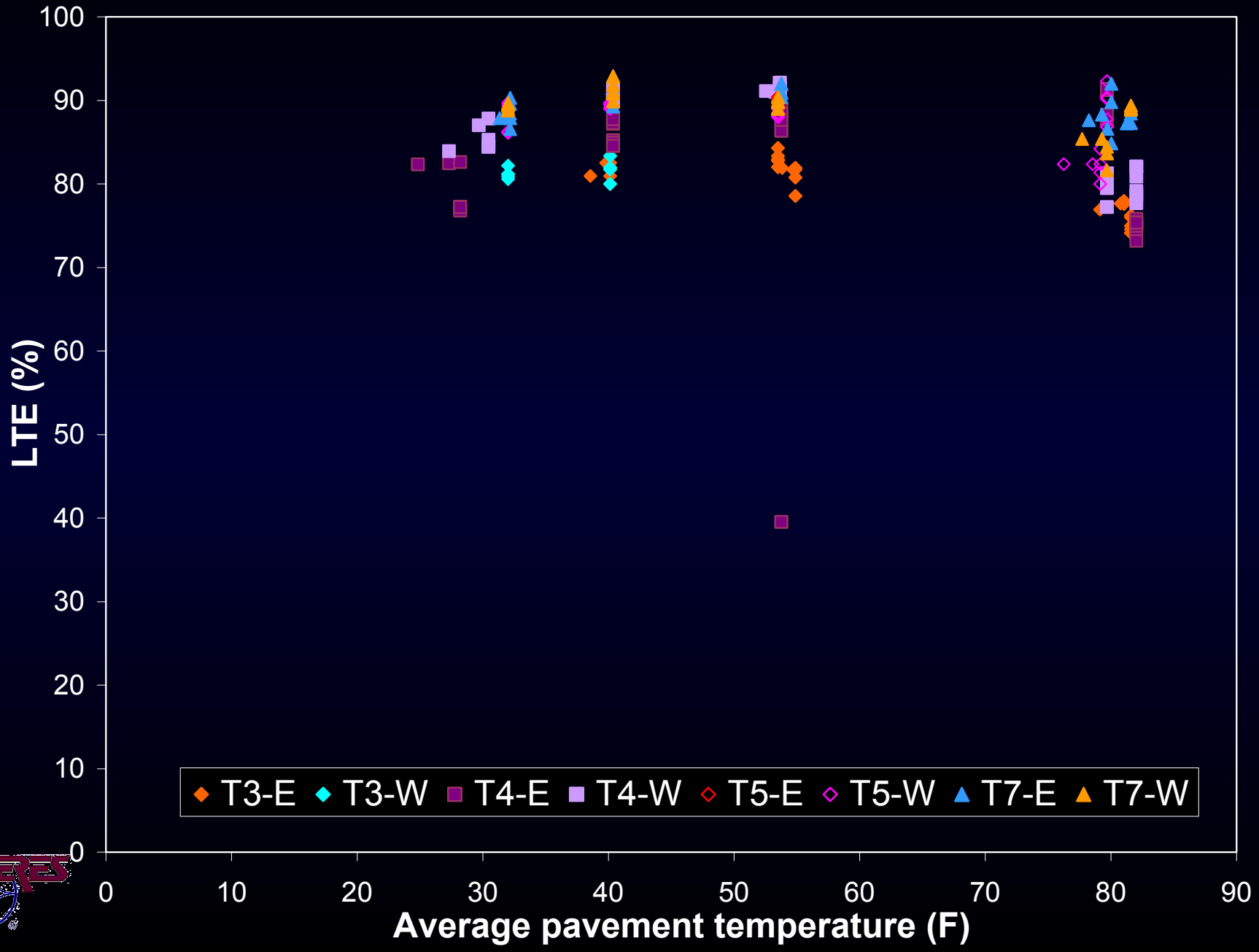

Effects of Temperature Curling on Airfield Pavement Responses

Theoretical analysis

- Load:
  - 36,000-lb single wheel
  - Size: 15-in. by 15-in.
  - Tire pressure: 160 psi
- Temperature:
  - Linear and nonlinear
  - 523 randomly selected cases

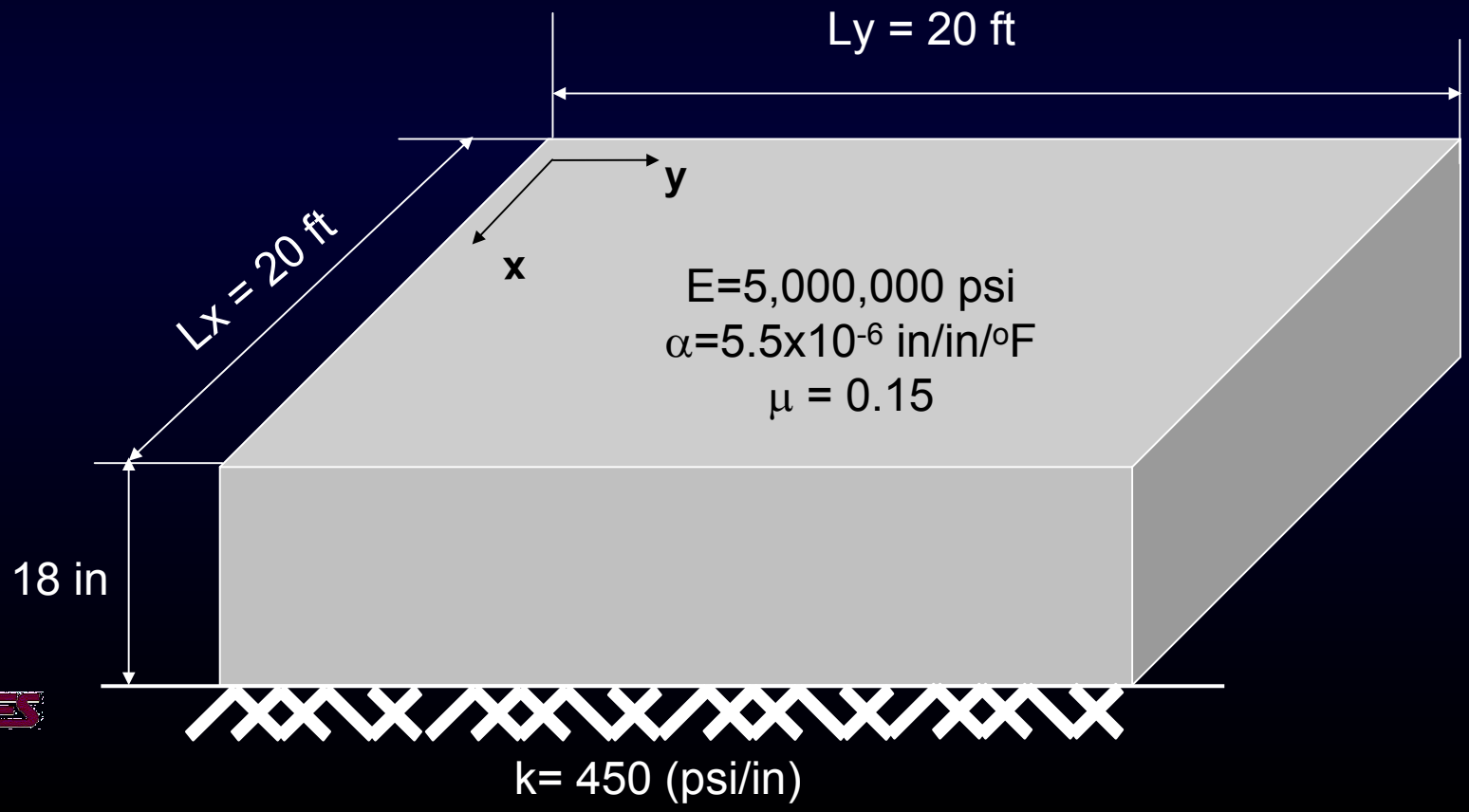

Theoretical effect on stress

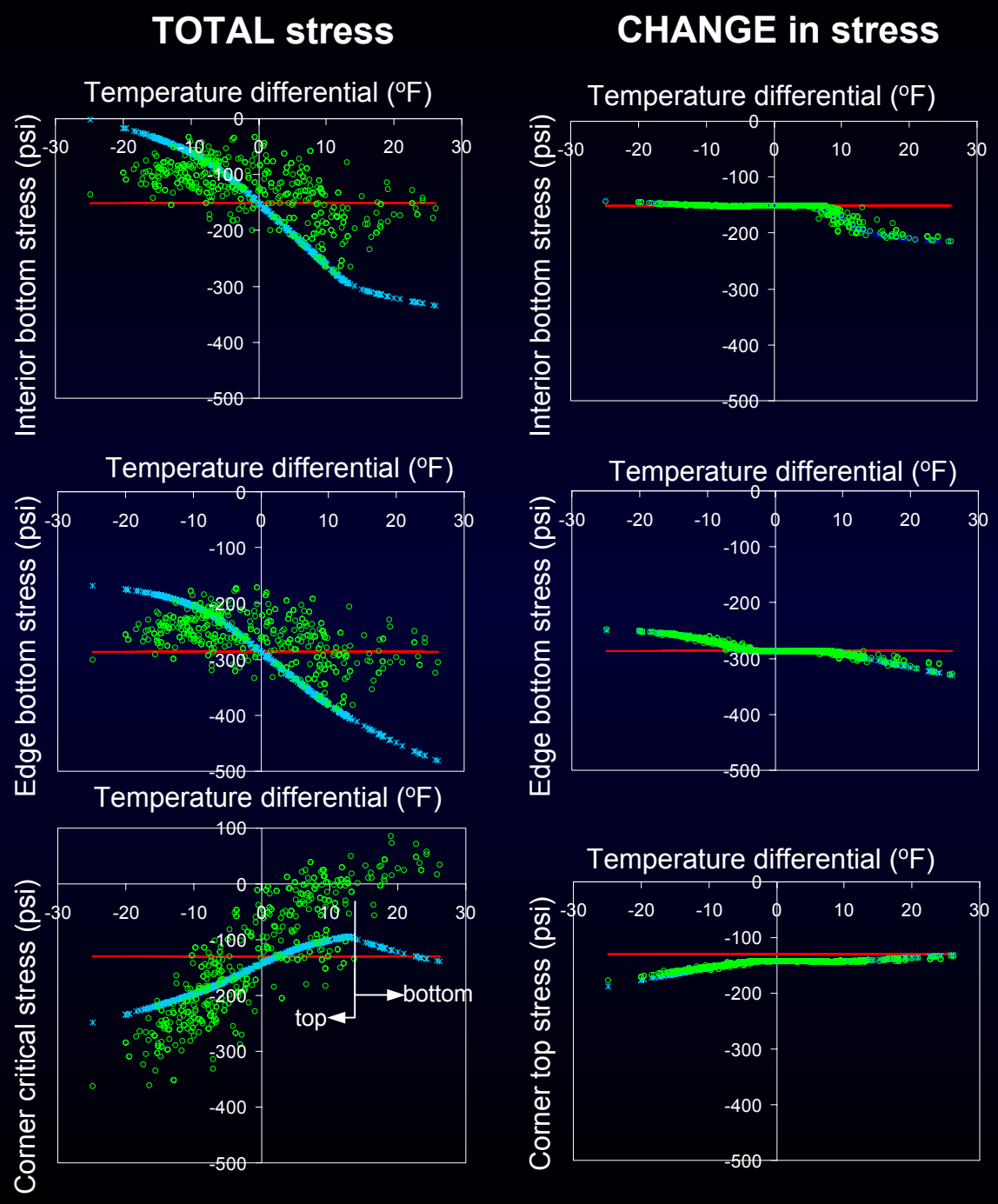

Linear
NonLinear
Only Load

Theoretical effect on deflection and stress

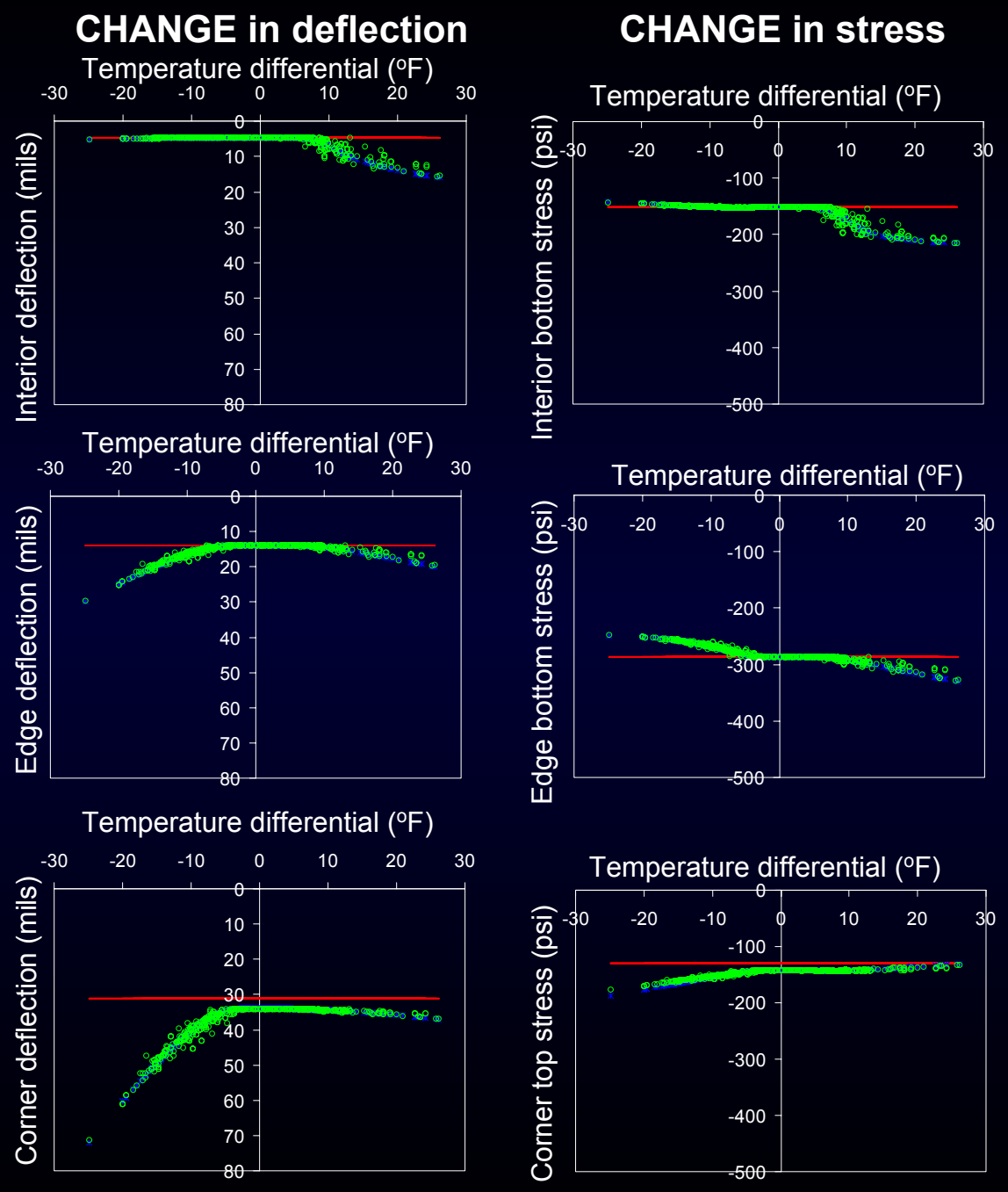

Aircraft weight used to normalize pavement response

Aircraft type	Number of events	Average total weight (kips)	Std dev total weight (kips)	Average wheel weight (kips)
B-727	523	160.5	10.9	38.1
B-737	382	109.8	9.0	26.1
B-757	132	192.3	11.6	45.7
DC-10	54	355.9	18.3	42.3

Selected LVDTs for a detailed measured deflection analysis

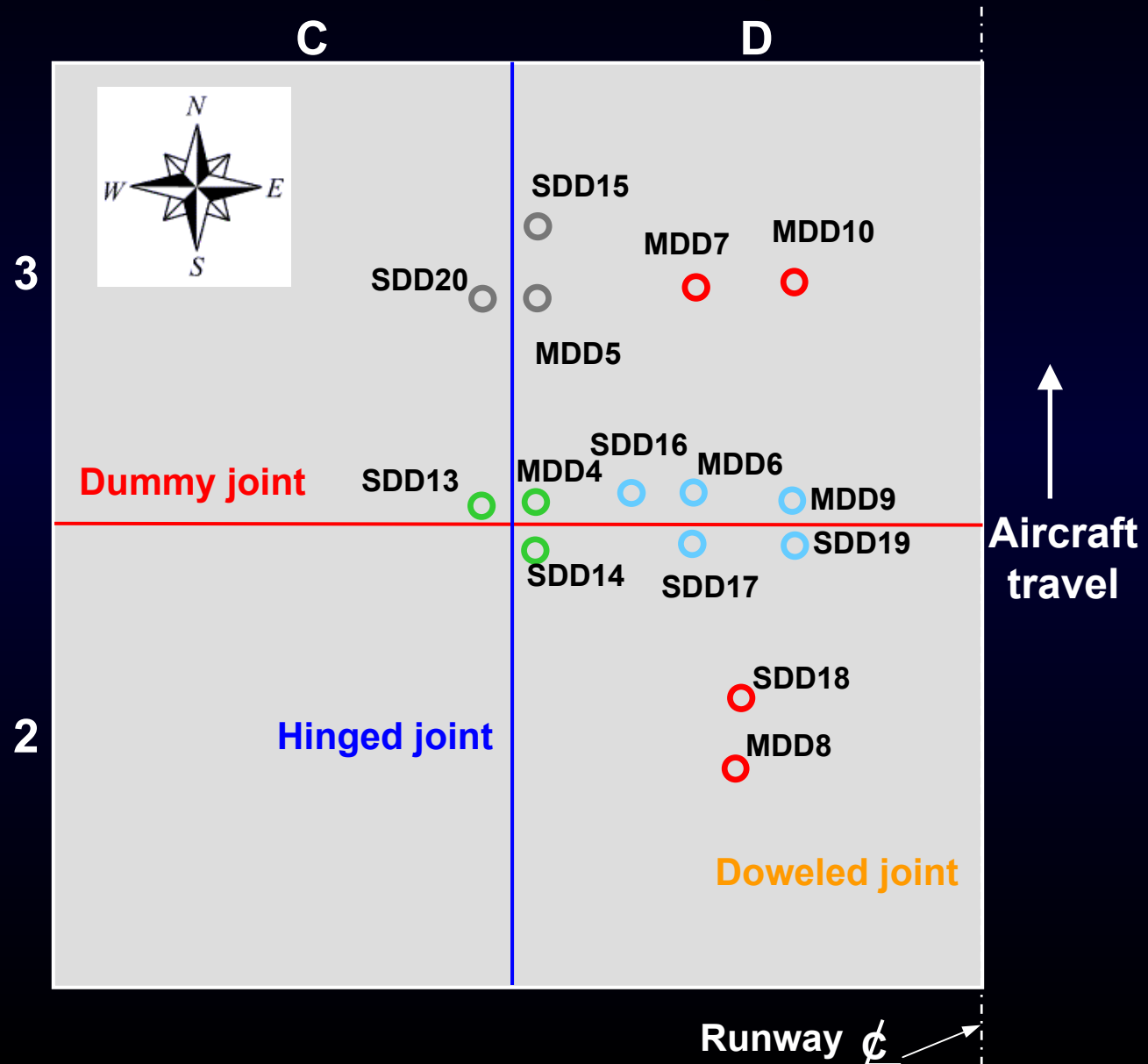

Measured B-727 interior deflection

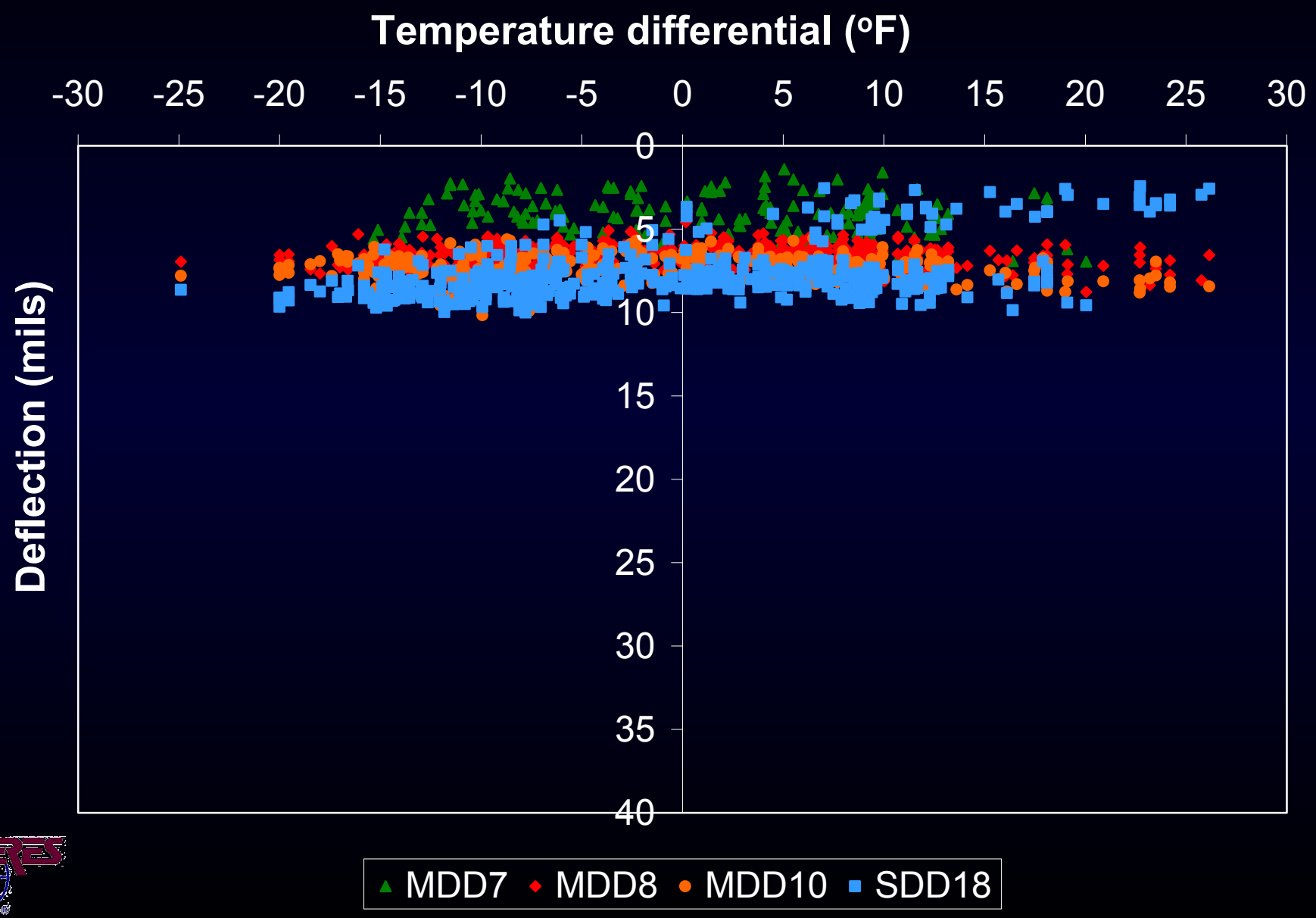

Measured B-727 dummy TJ deflection

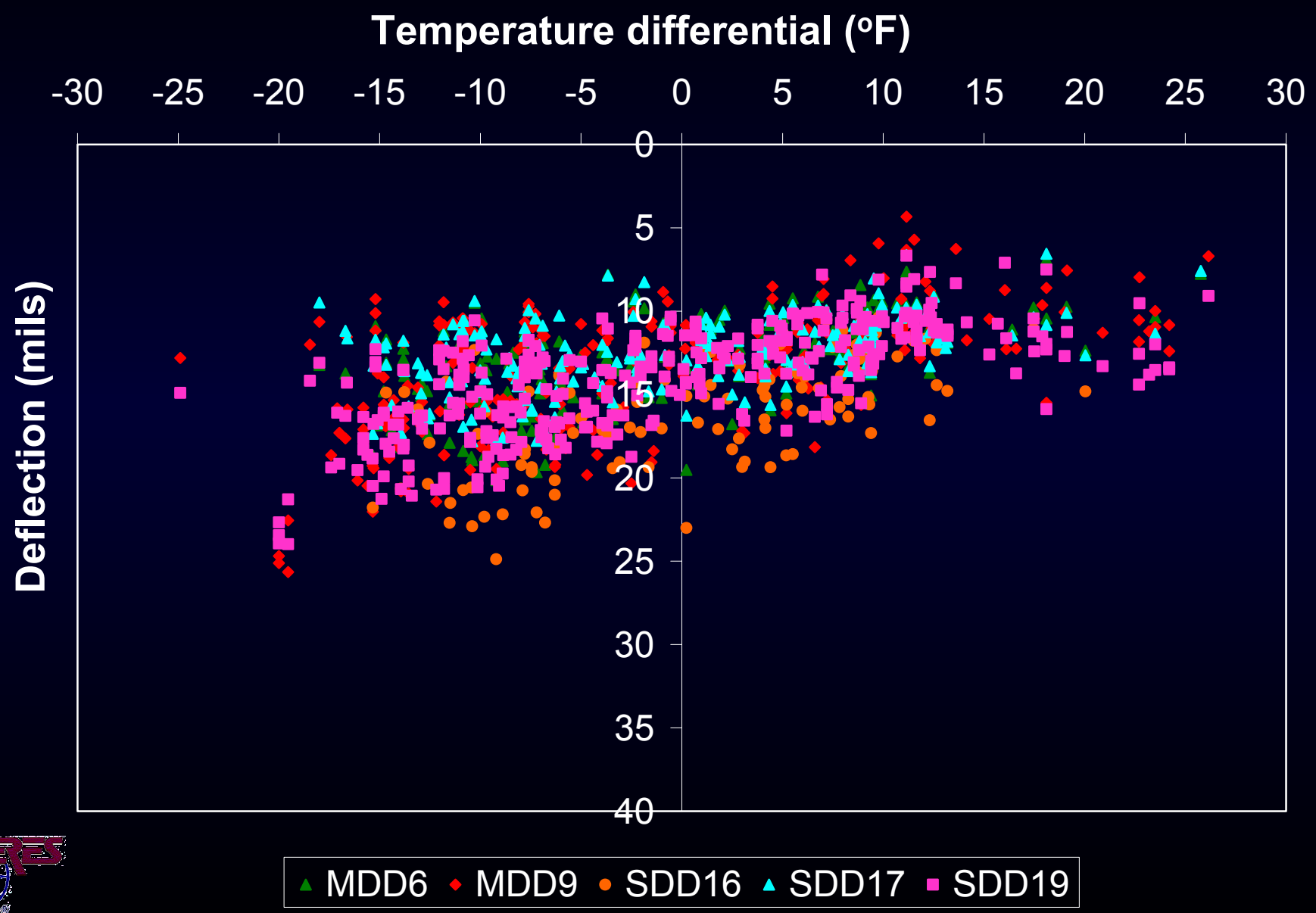

Measured B-727 hinged LJ deflection

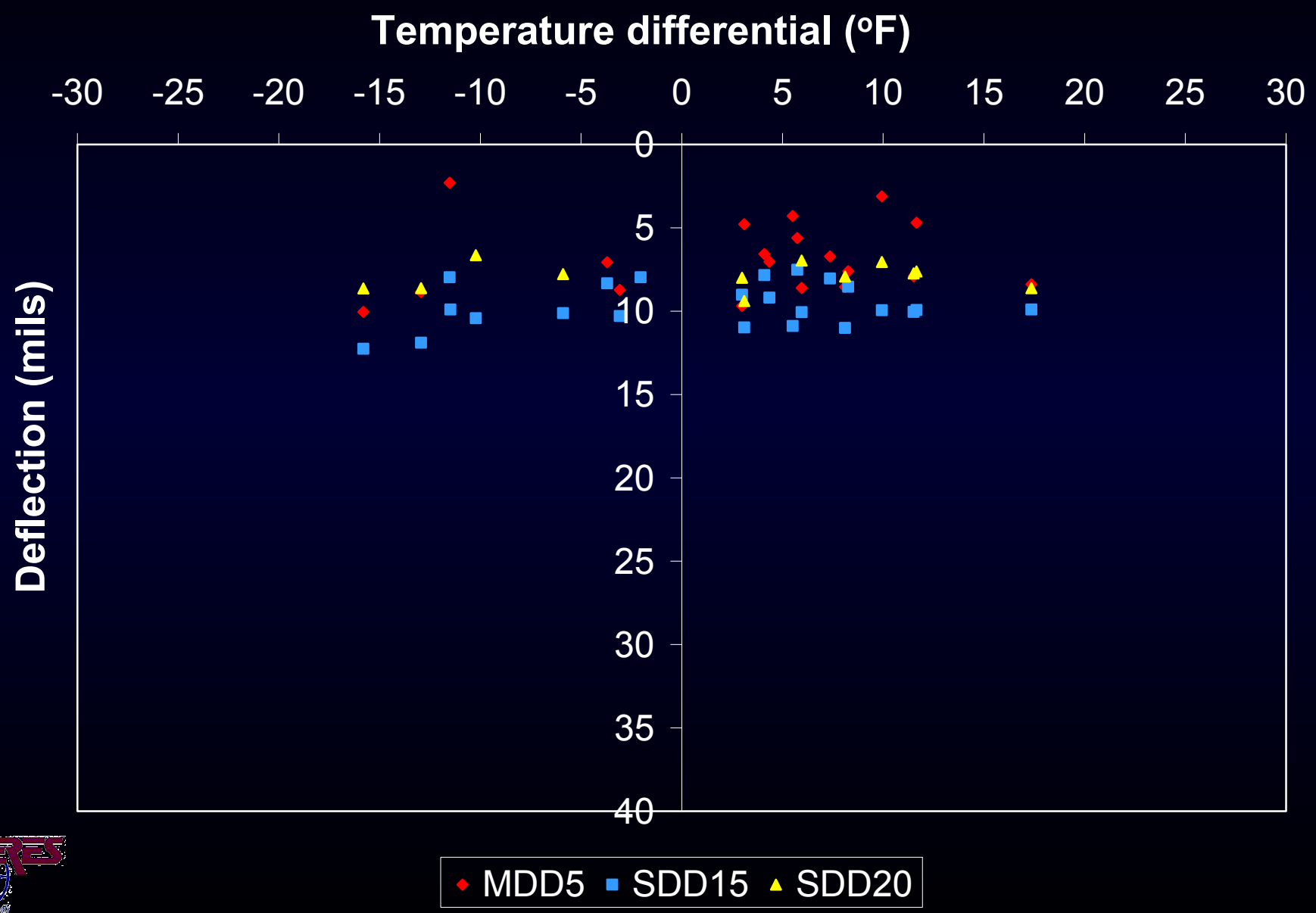

Measured B-727 corner deflection

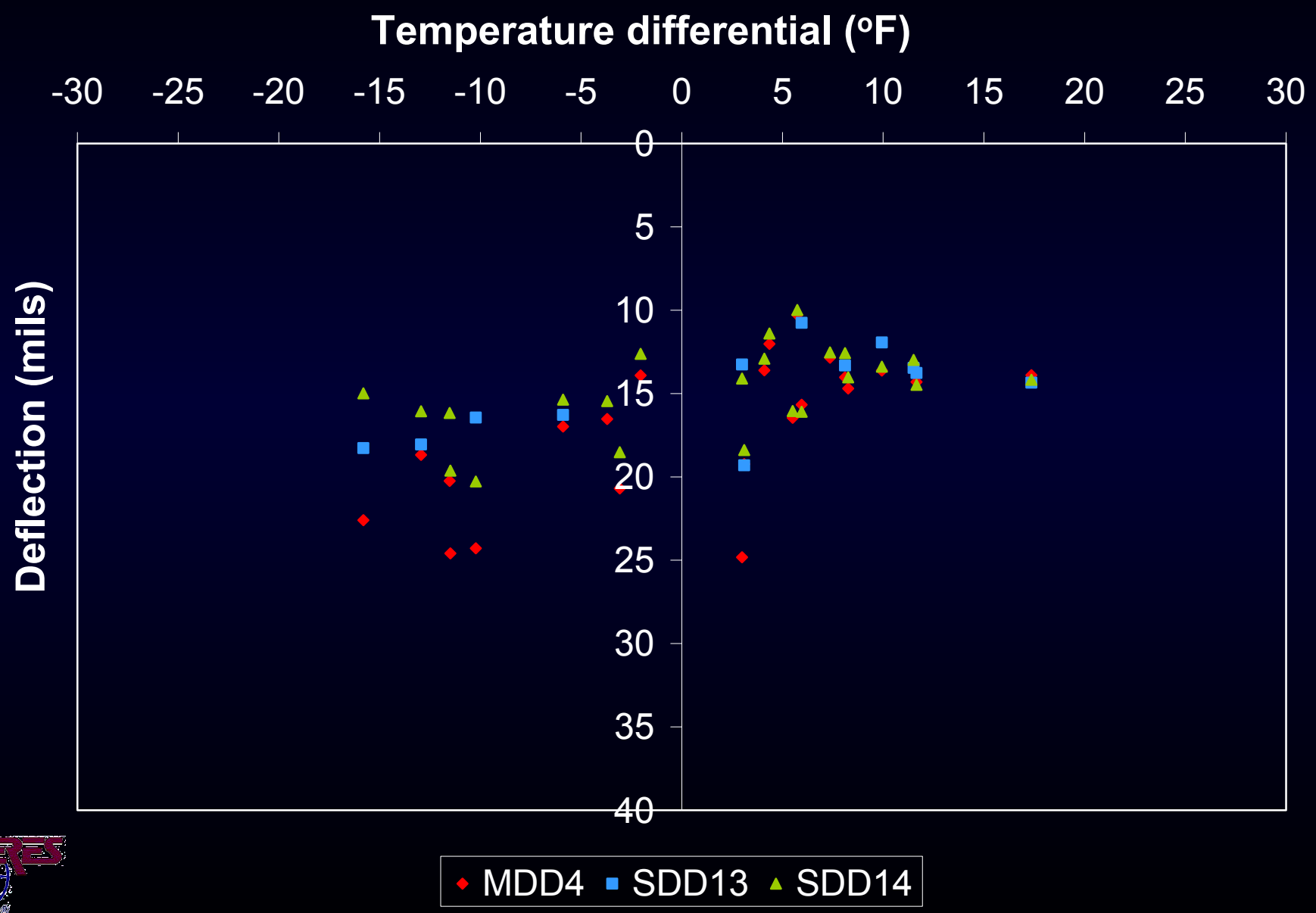

Summary of normalized mean deflections

Location or load level	Aircraft			
	B727	B737	B757	DC-10
Interior (mils)	6.9	4.9	7.1	11.3
TJ (mils)	13.6	10.8	13.7	21.5
LJ (mils)	8.3	6.6	10.3	17.3
Corner (mils)	15.7	12.5	15.5	23.9
Wheel Load (kips)	38.1	26.1	22.8	42.3
Gear Load (kips)	76.2	52.9	91.3	169.1

Selected strain gages

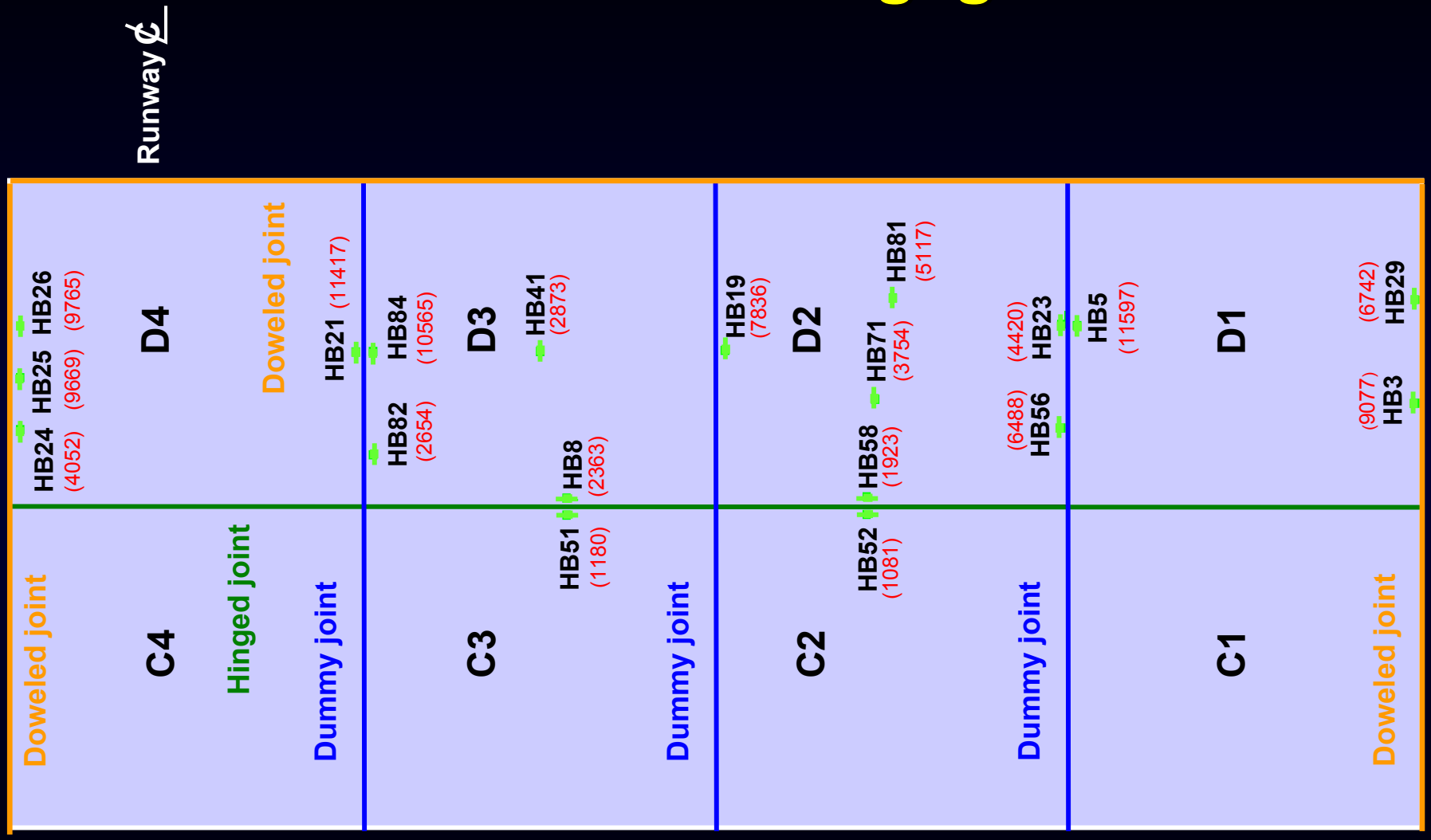

Measured B-727 interior strain

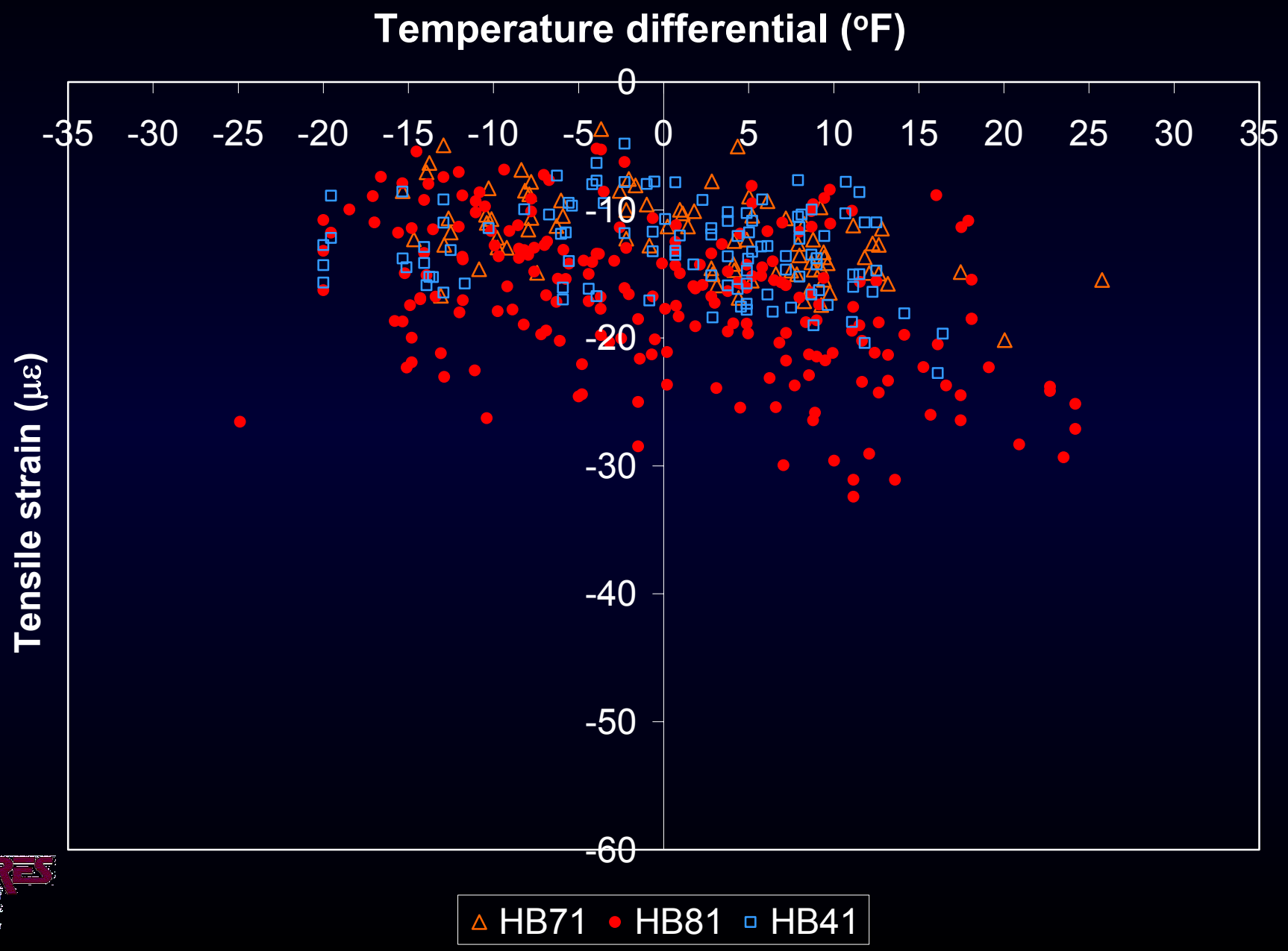

Measured B-727 TJ dummy strain

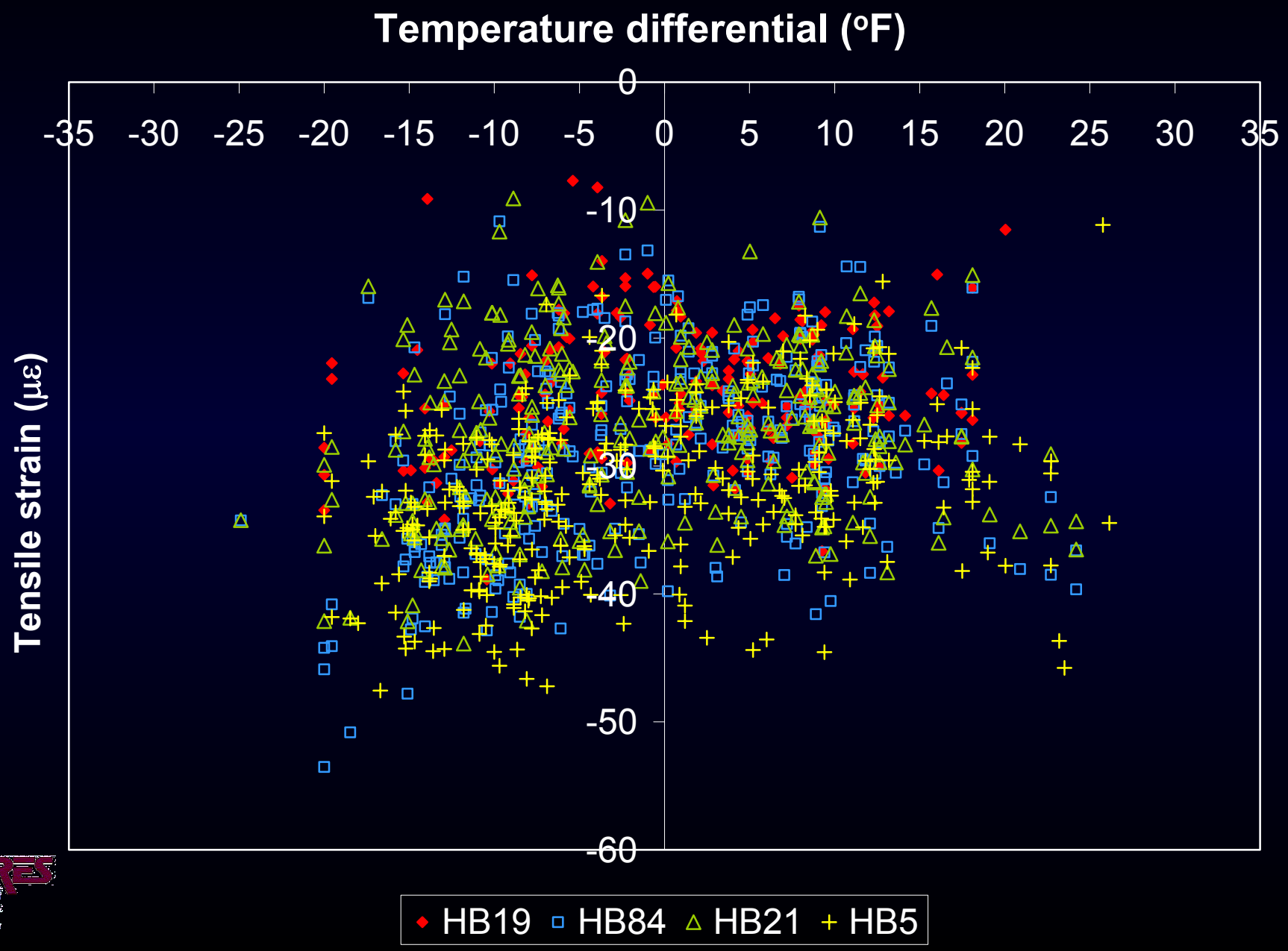

Measured B-727 doweled TJ strain

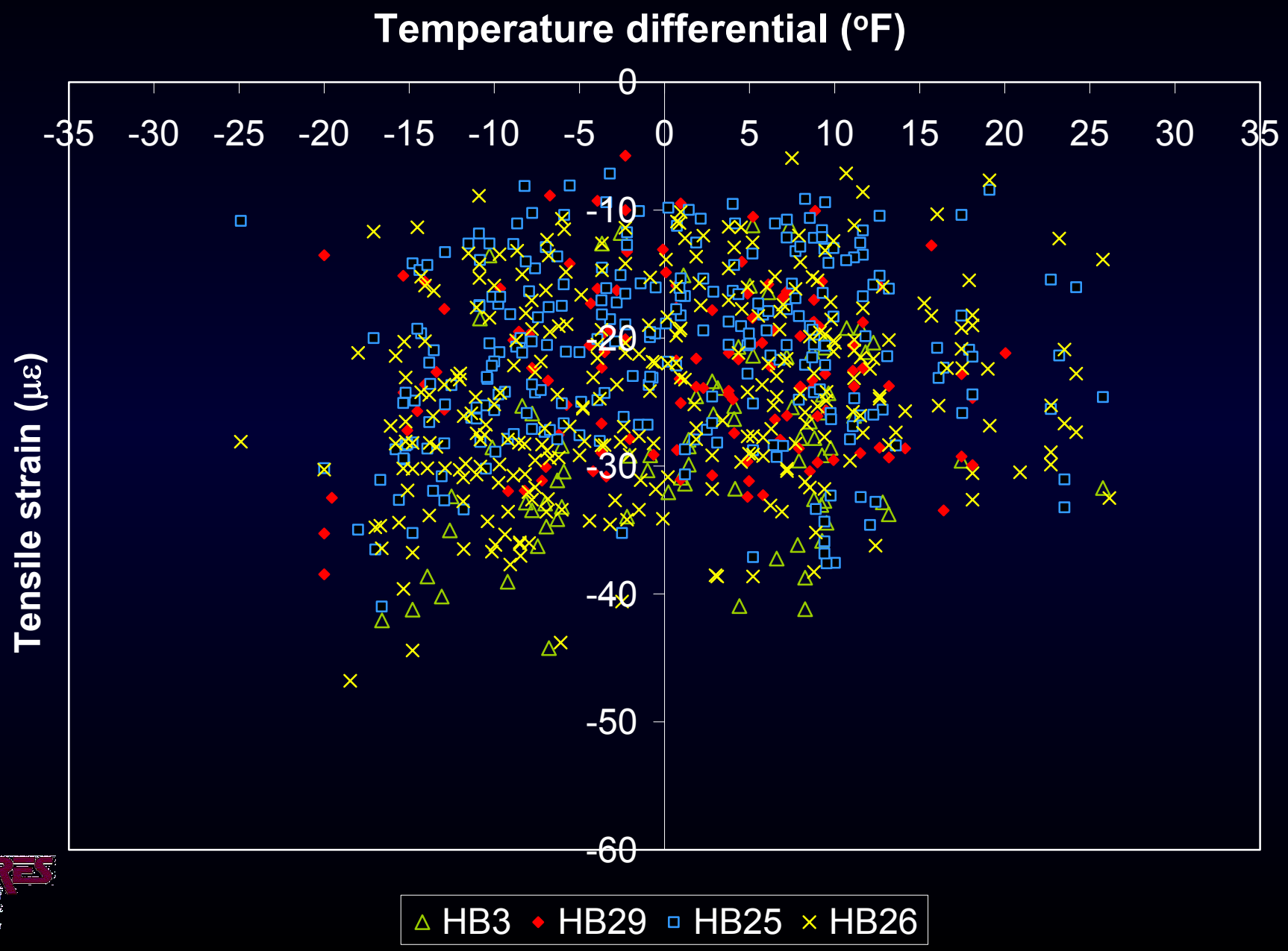

Summary of measured strains

Location	Aircraft			
	B727	B737	B757	DC10
Interior (microns)	-14.8	-9.9	-11.9	-19.3
TJ dummy (microns)	-28.2	-21.4	-25.6	-30.9
TJ doweled (microns)	-23.2	-17.2	-21.4	-29.4
LJ (microns)	-26.3	-20.4	-17.8	-21.9
Wheel Load (kips)	38.1	26.1	22.8	42.3
Gear Load (kips)	76.2	52.9	91.3	169.1

Analysis of Slab-base Interface Interaction

Sliding friction

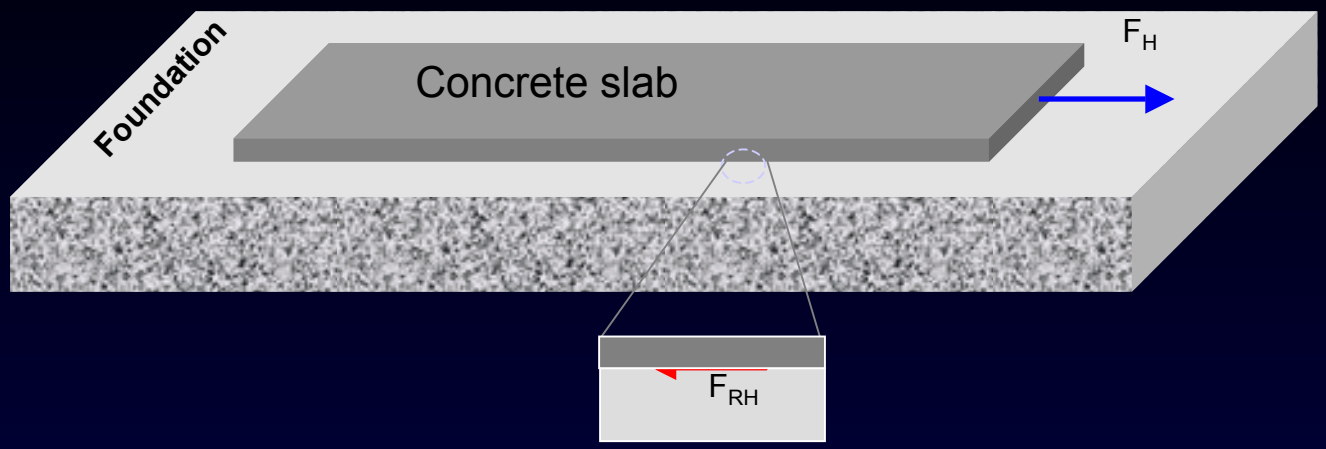

Contact friction

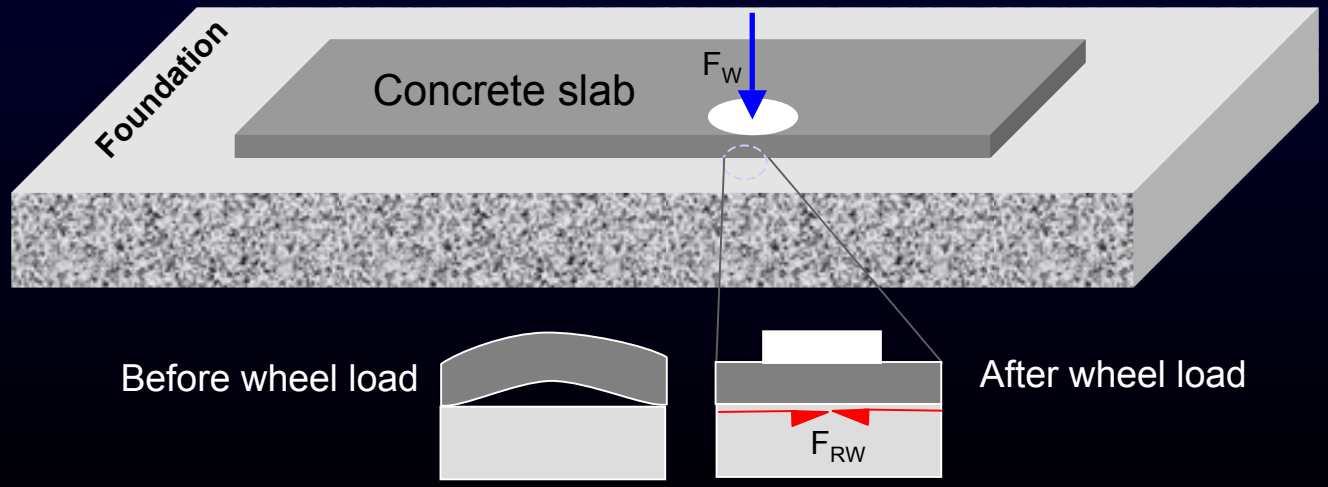

Sliding friction

- Many theoretical and experimental studies
- Traditionally long slabs
- Recently short slabs

Contact friction

- Composite plate concept
- Intermediate levels of contact friction (Rollings, 1988)
- Design of UTW
- ISLAB2000
- Limited field studies

Multi-depth LVDT sensors

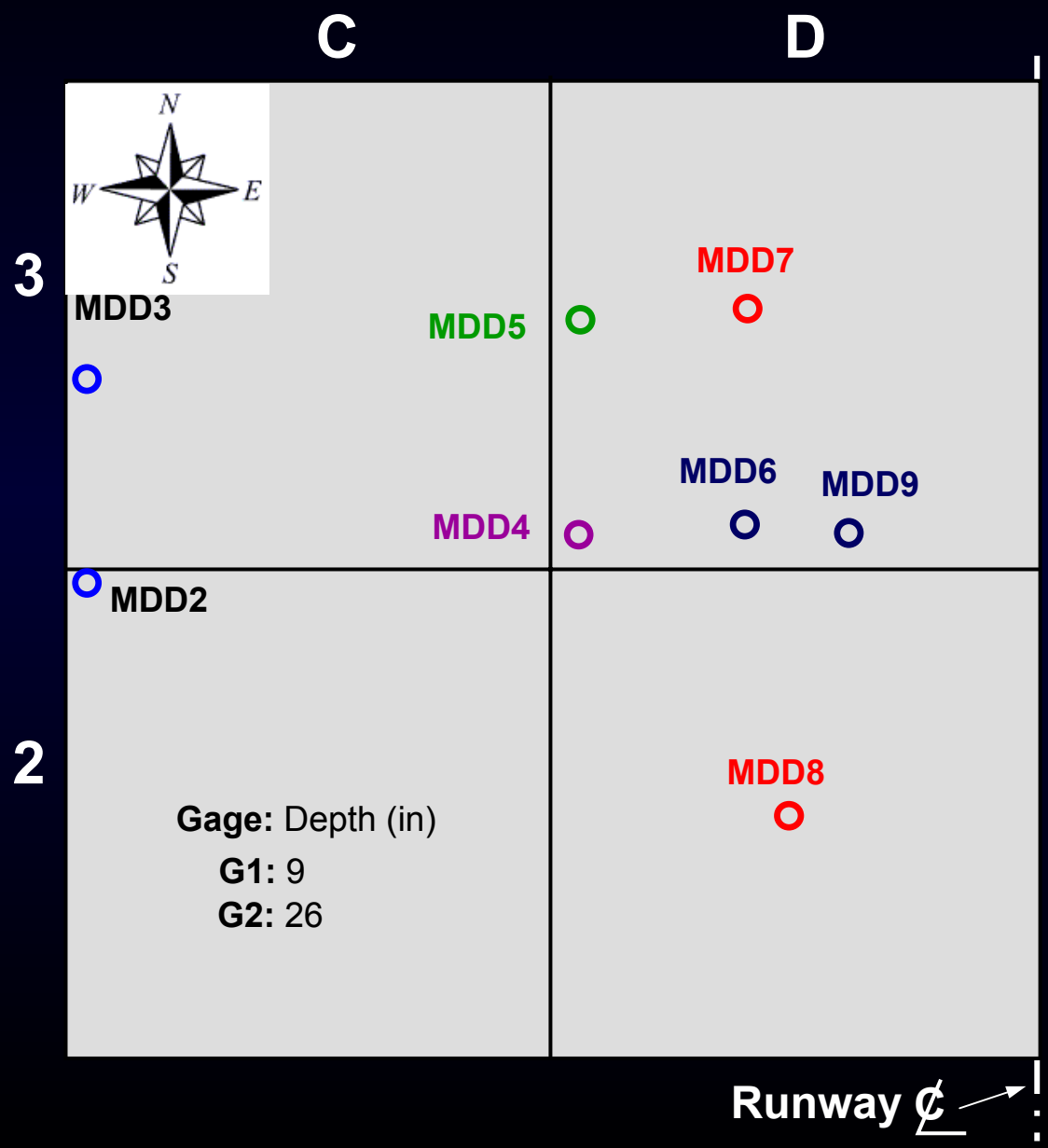

Daytime condition

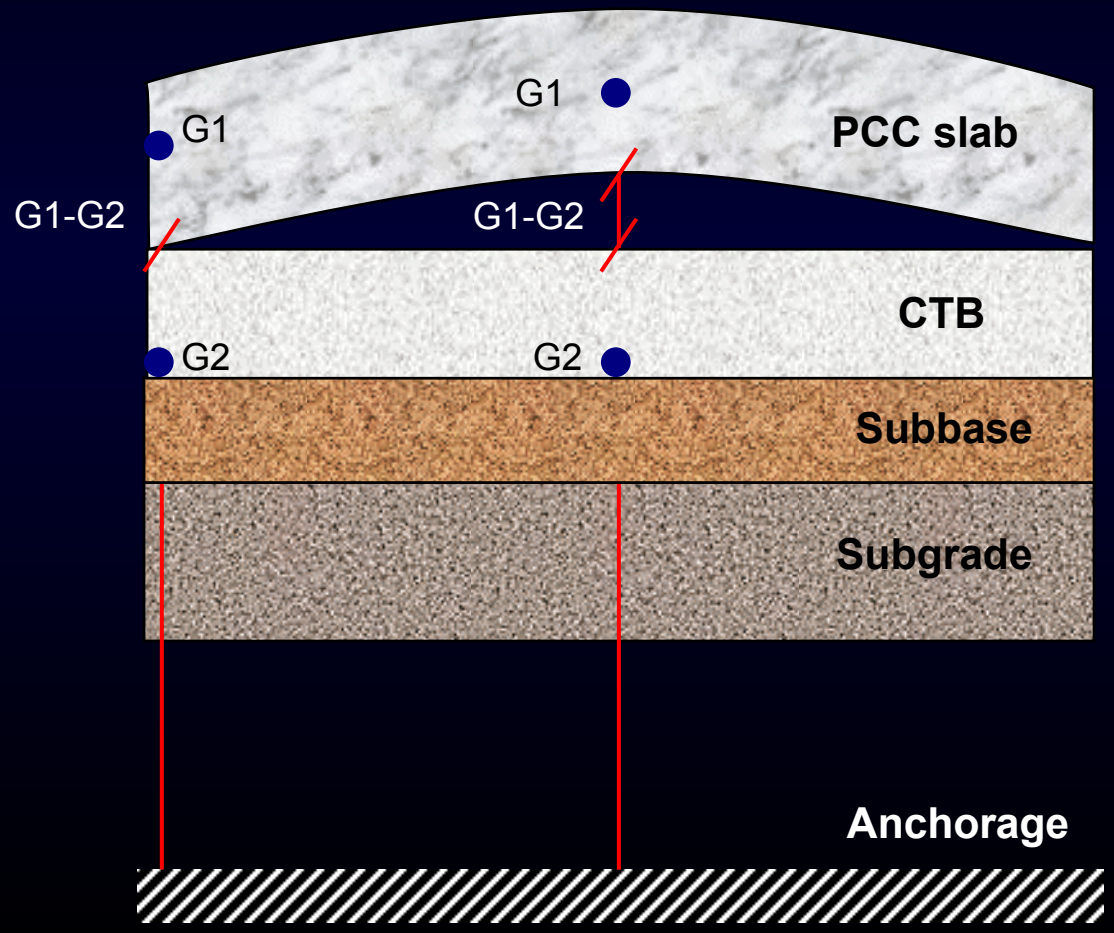

Nighttime condition

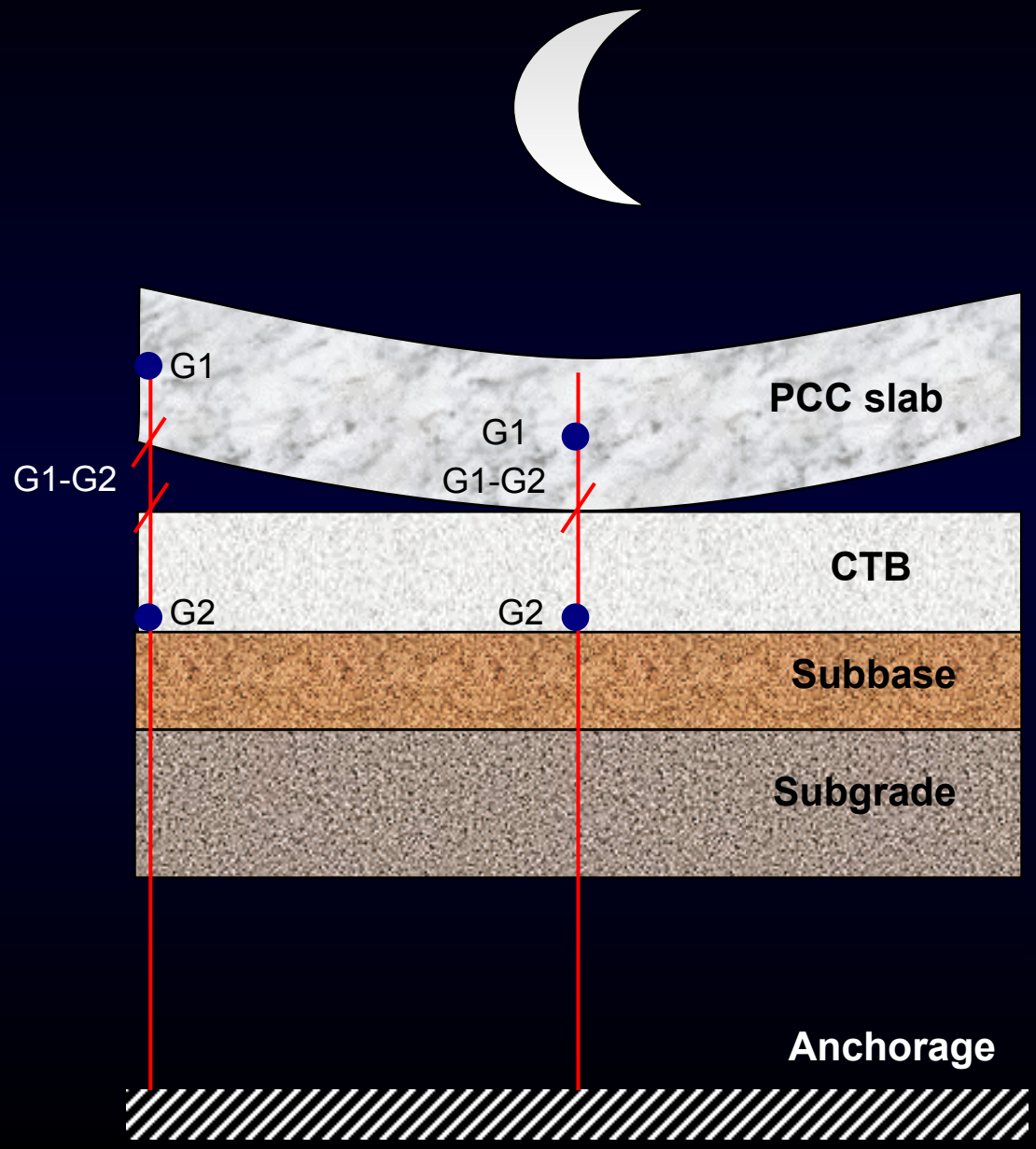

Corner deflection versus temperature differential

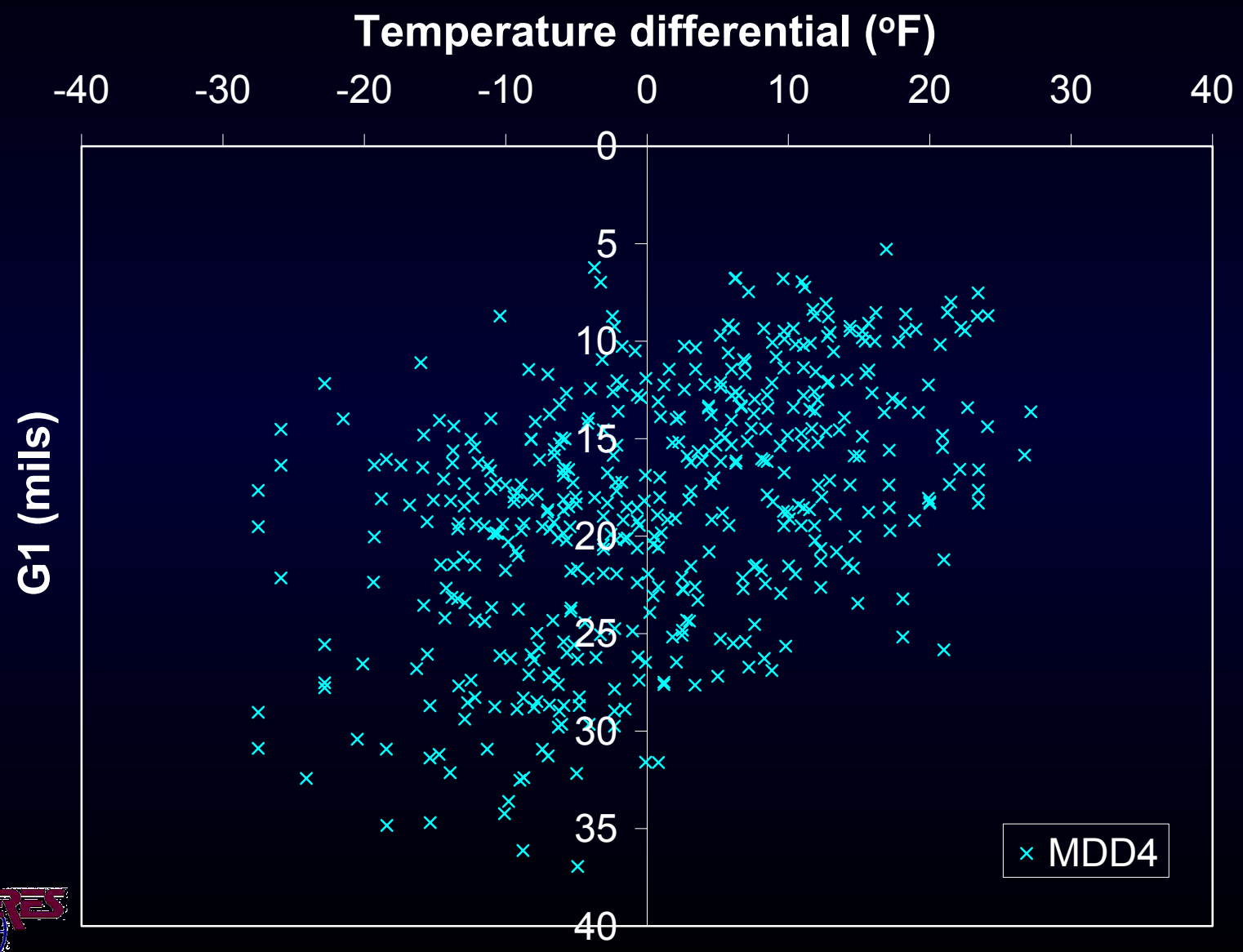

Interface corner deflection versus temperature differential

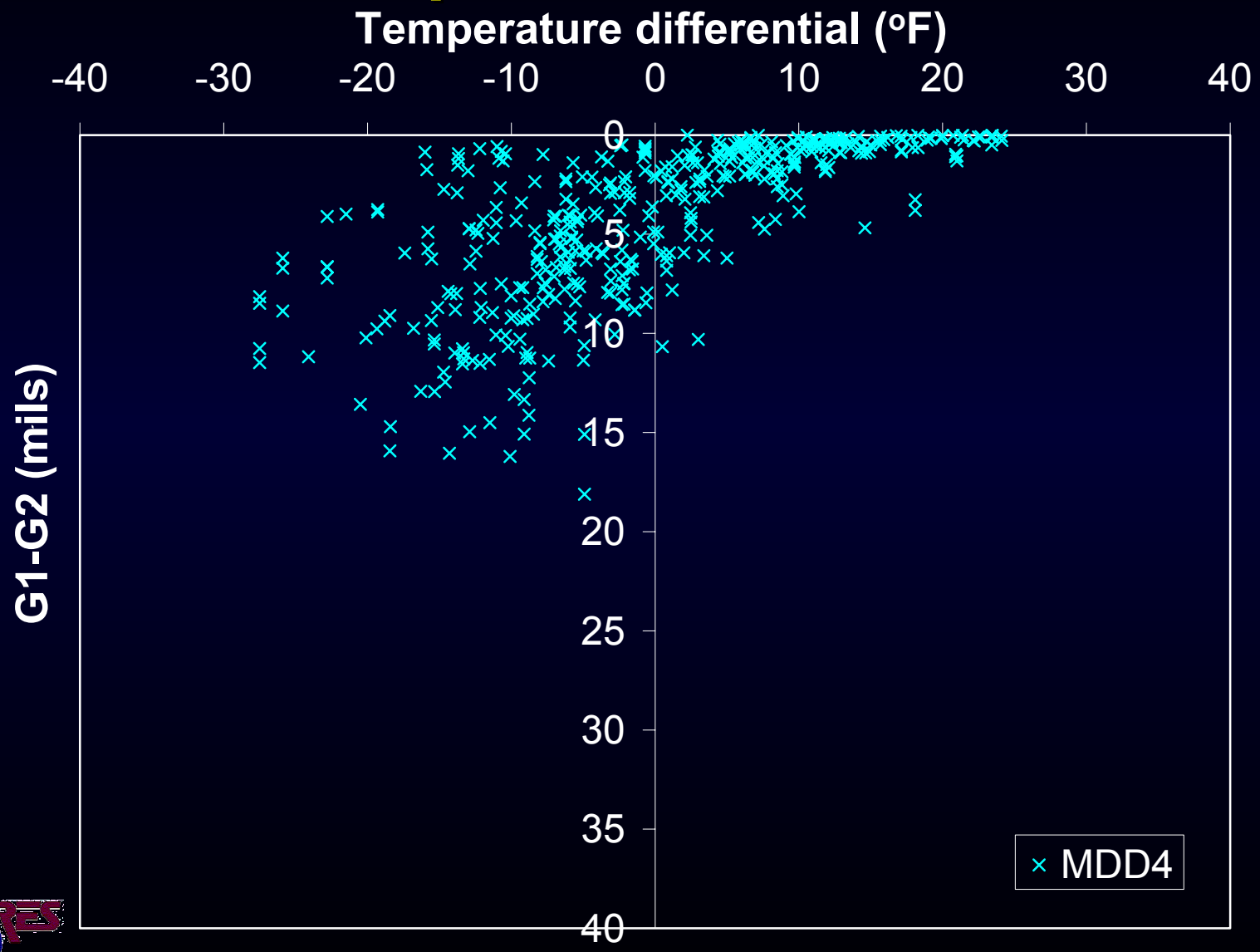

Interface TJ deflection versus temperature differential

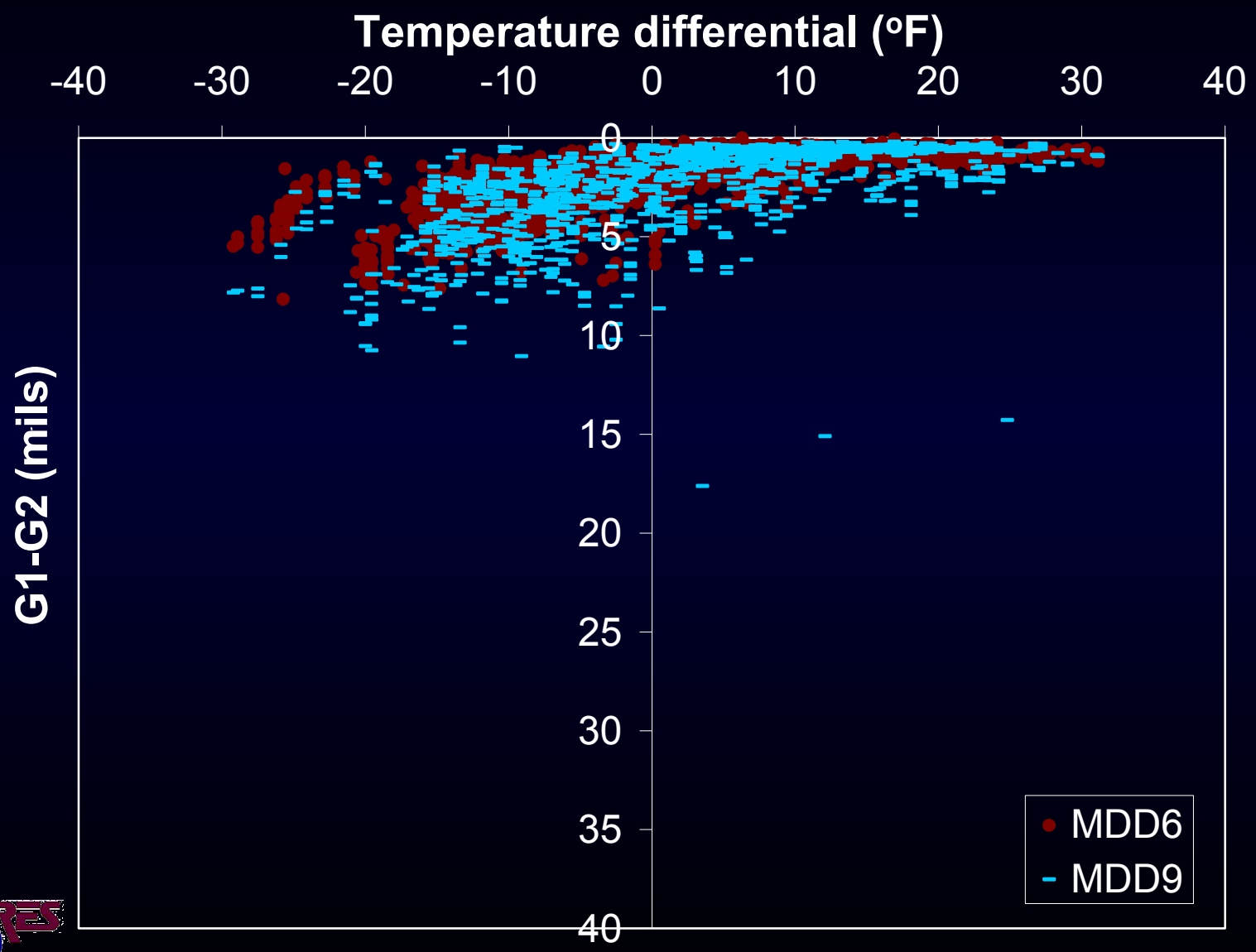

Interface LJ deflection versus temperature differential

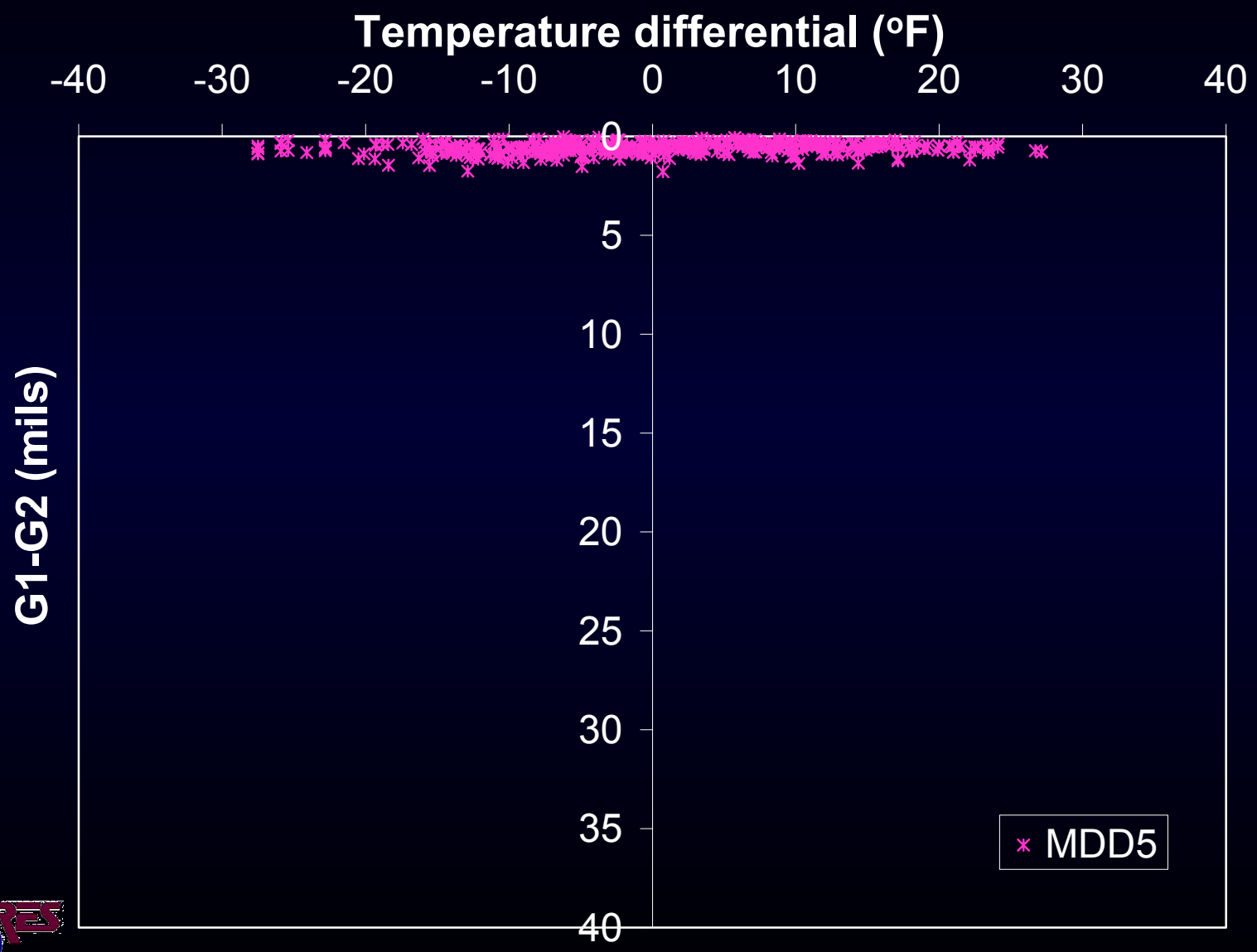

Interface interior deflection versus temperature differential

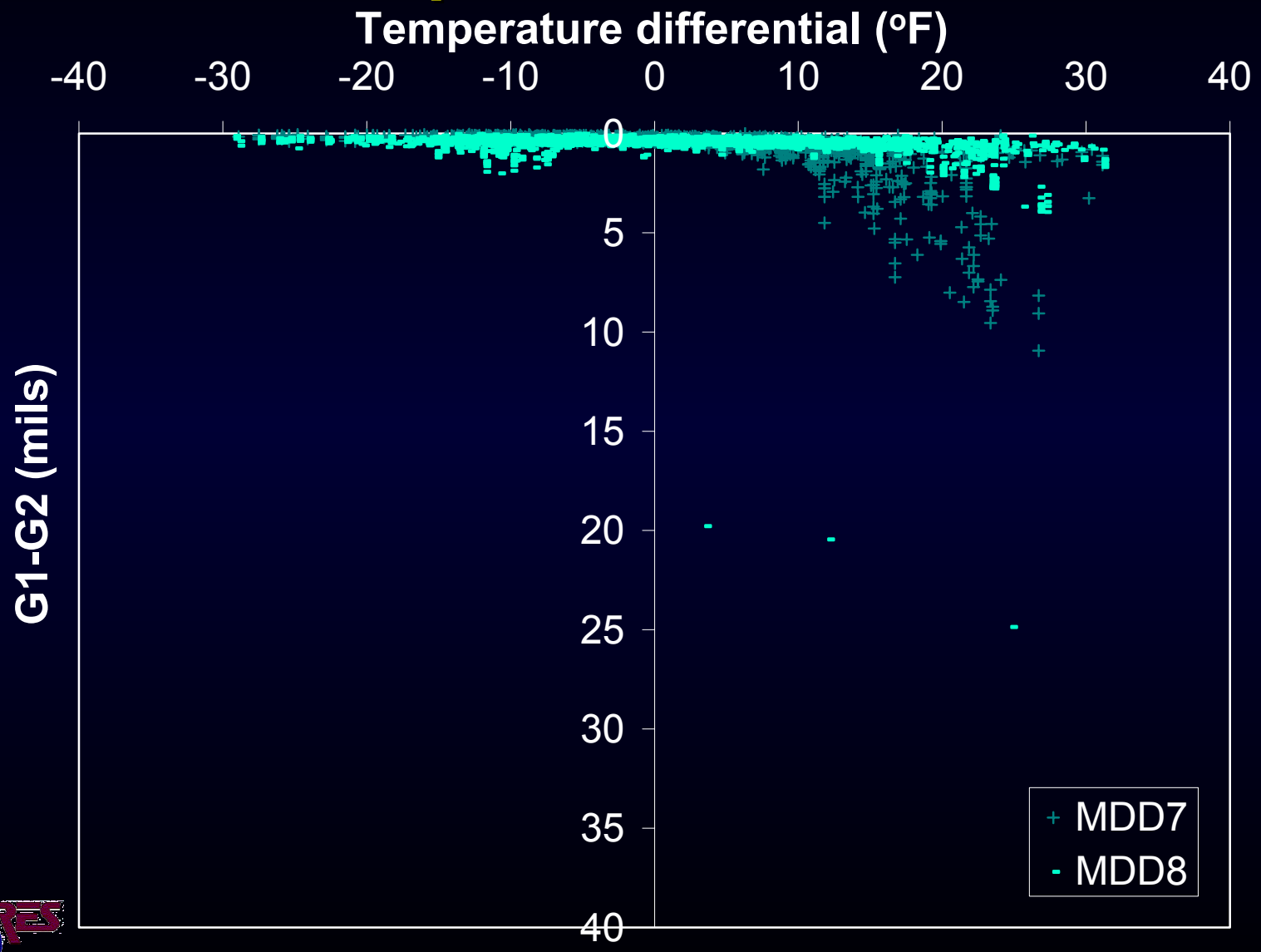

Selected paired strain gages

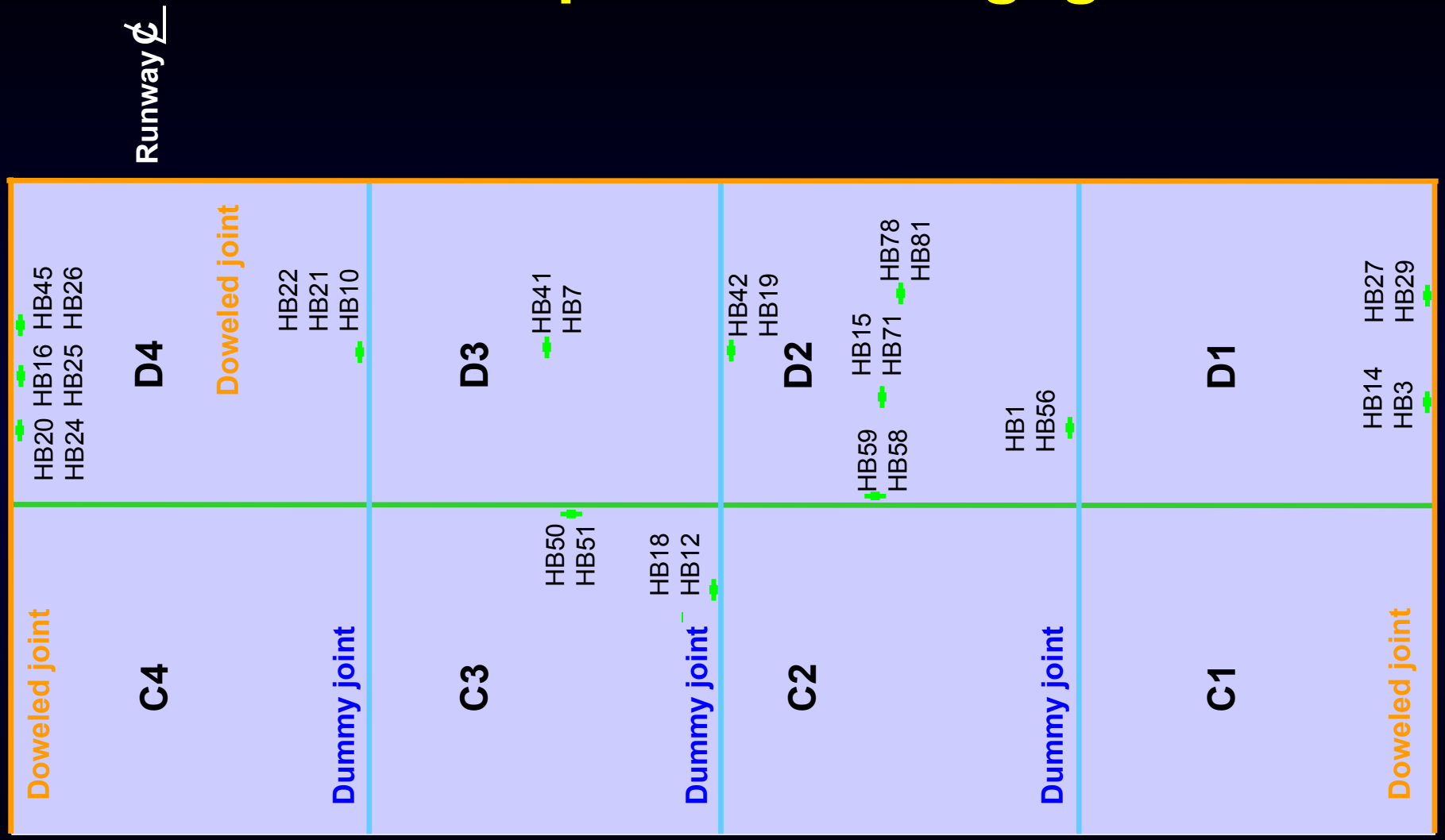

Interface condition

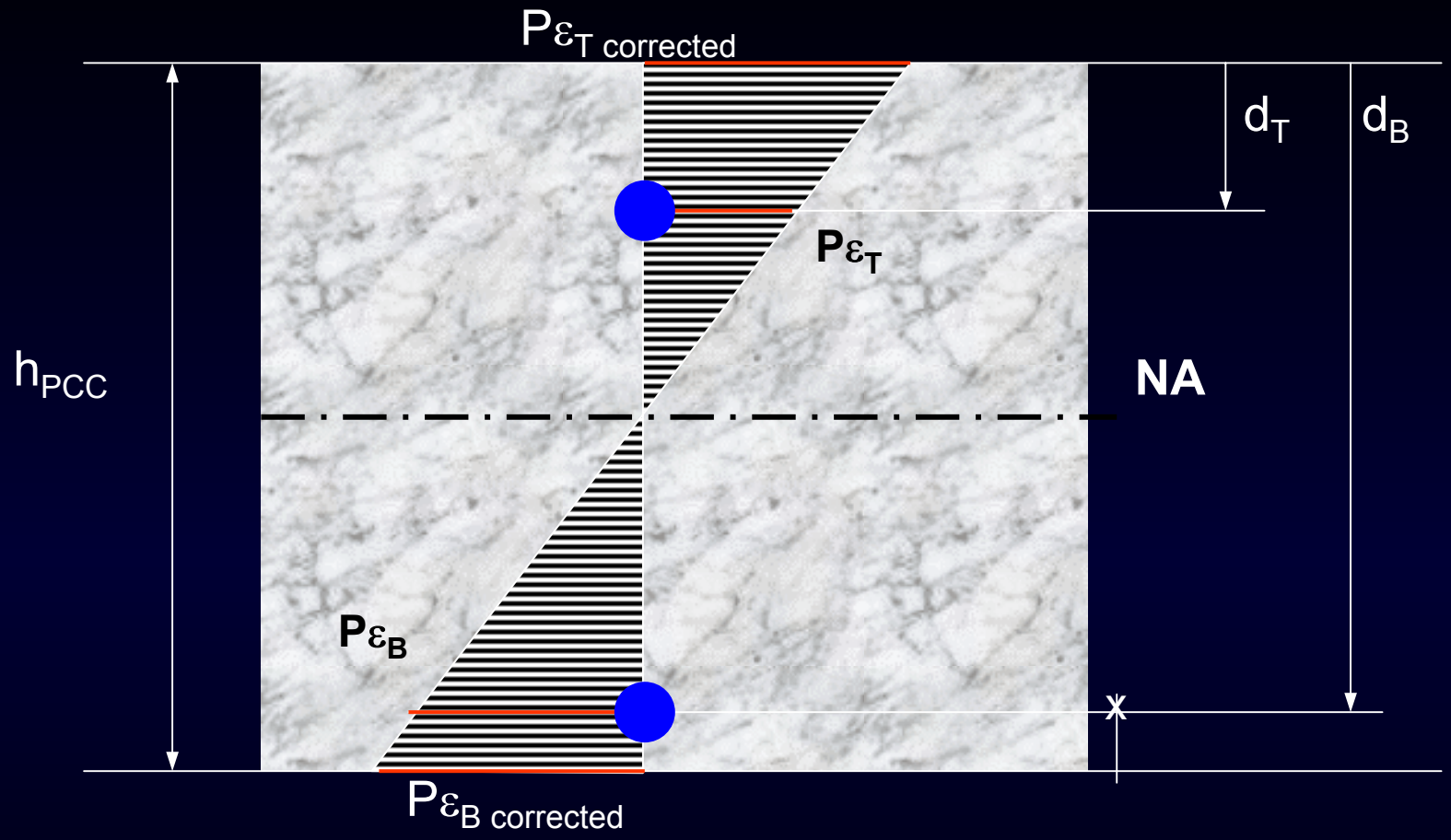

If $P\varepsilon$ <0 Then:

$$P\varepsilon_{T\,corrected} = P\varepsilon_T - (d_T) \times CSPD$$

$$P\varepsilon_{B\,corrected} = P\varepsilon_B + (x) \times CSPD$$

If $P\varepsilon$ >0 Then:

$$P\varepsilon_{T\,corrected} = P\varepsilon_T + (d_T) \times CSPD$$

$$P\varepsilon_{B\,corrected} = P\varepsilon_B + (x) \times CSPD$$

$$CSPD = \frac{|P\varepsilon_B| + |P\varepsilon_T|}{d_B - d_T}$$

Comparison between top and bottom slab at the slab interior

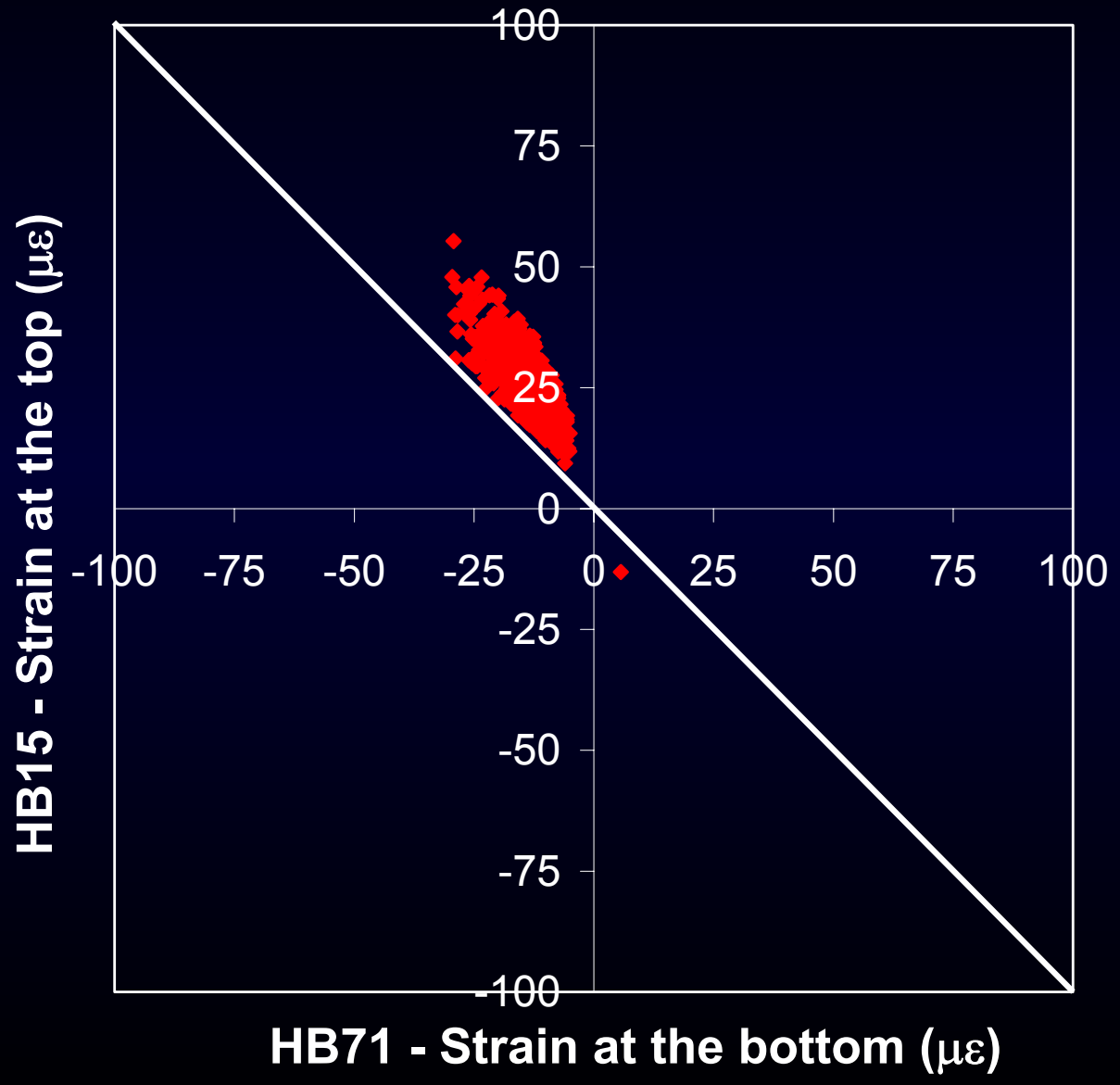

Comparison between top and bottom slab at the slab longitudinal hinged joint

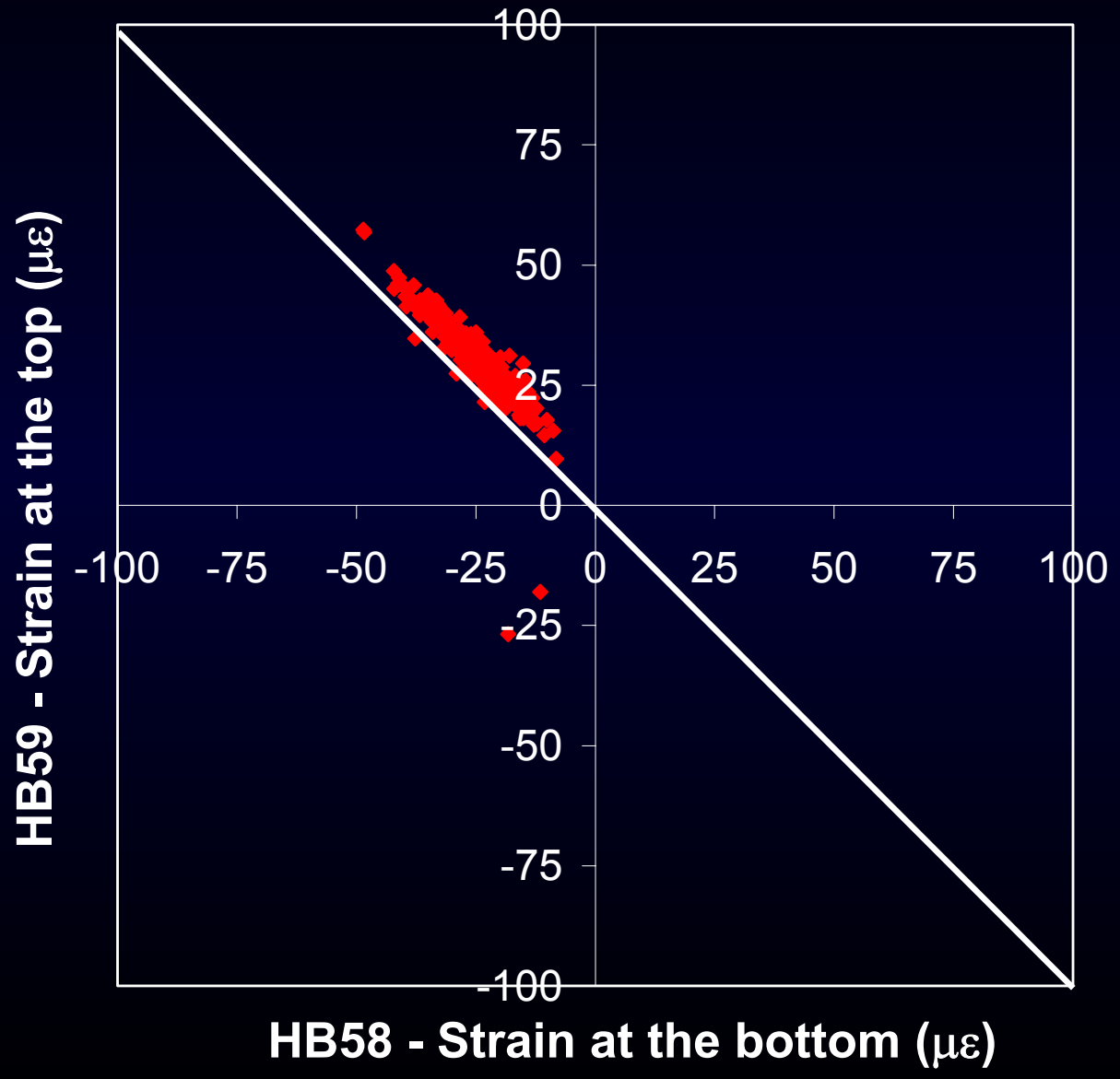

Comparison between top and bottom slab at the slab dummy transverse joint

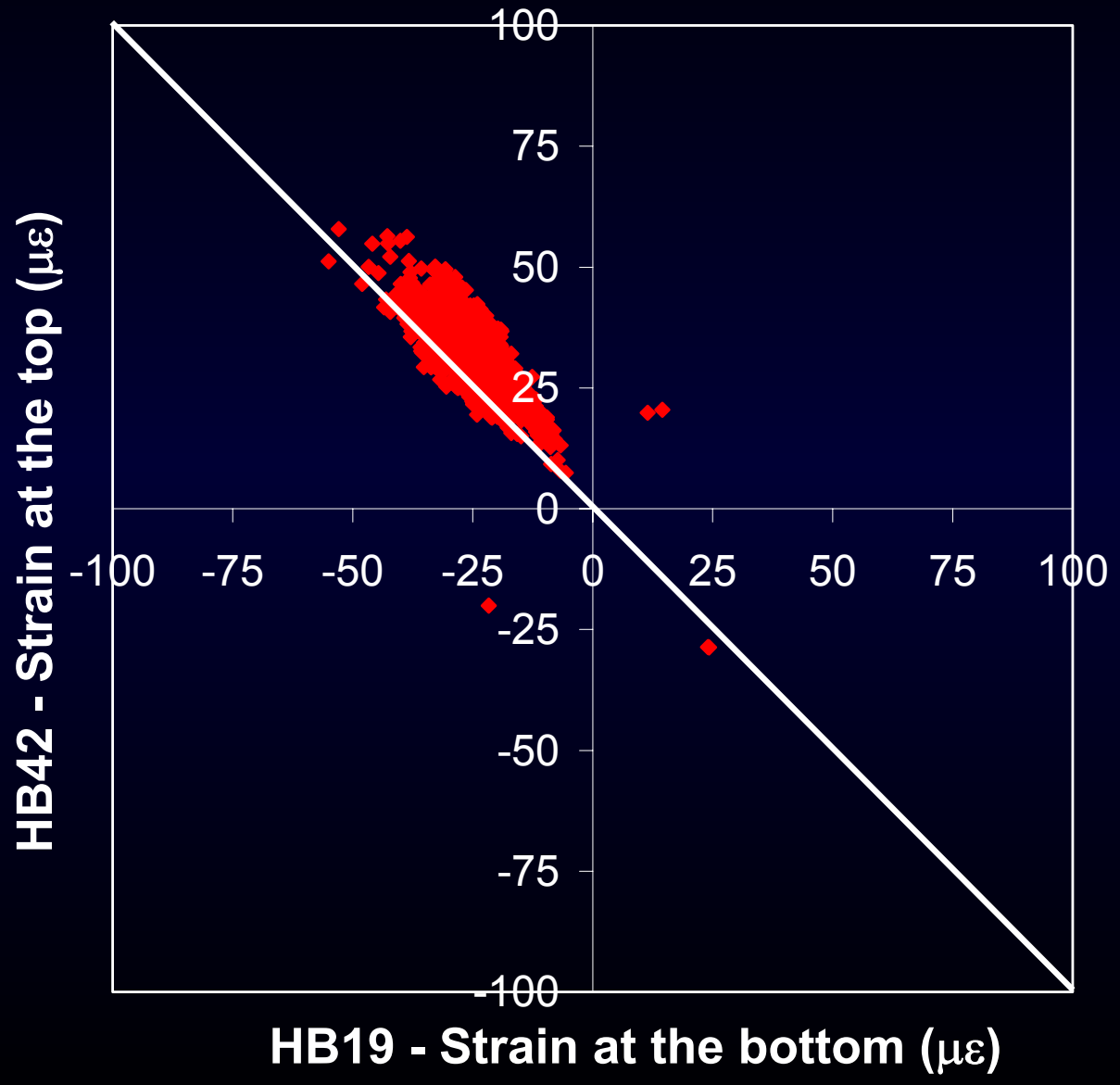

Comparison between top and bottom slab at the slab doweled transverse joint

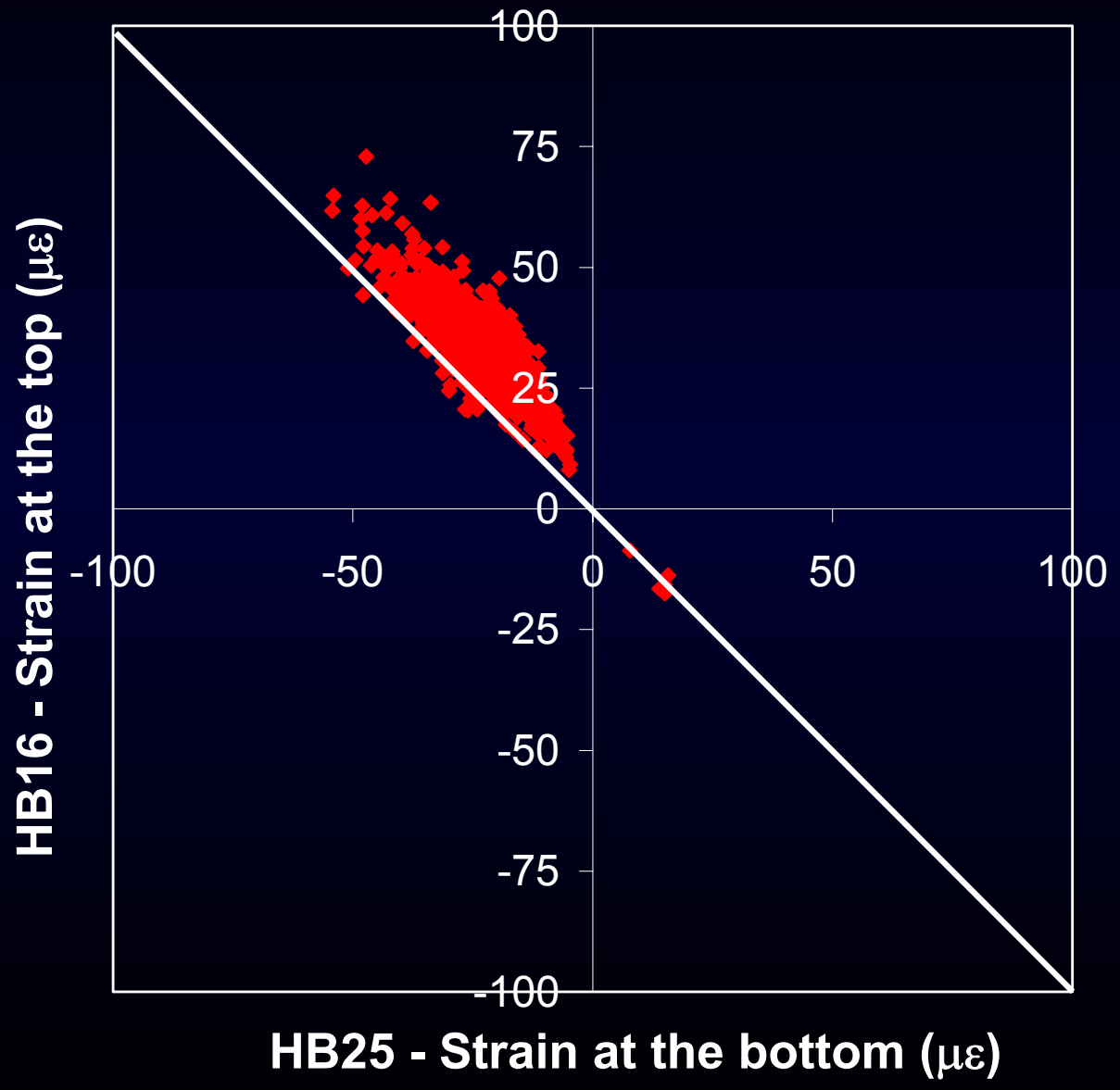

Comparison between strain at the bottom of the slab and at the top of the base

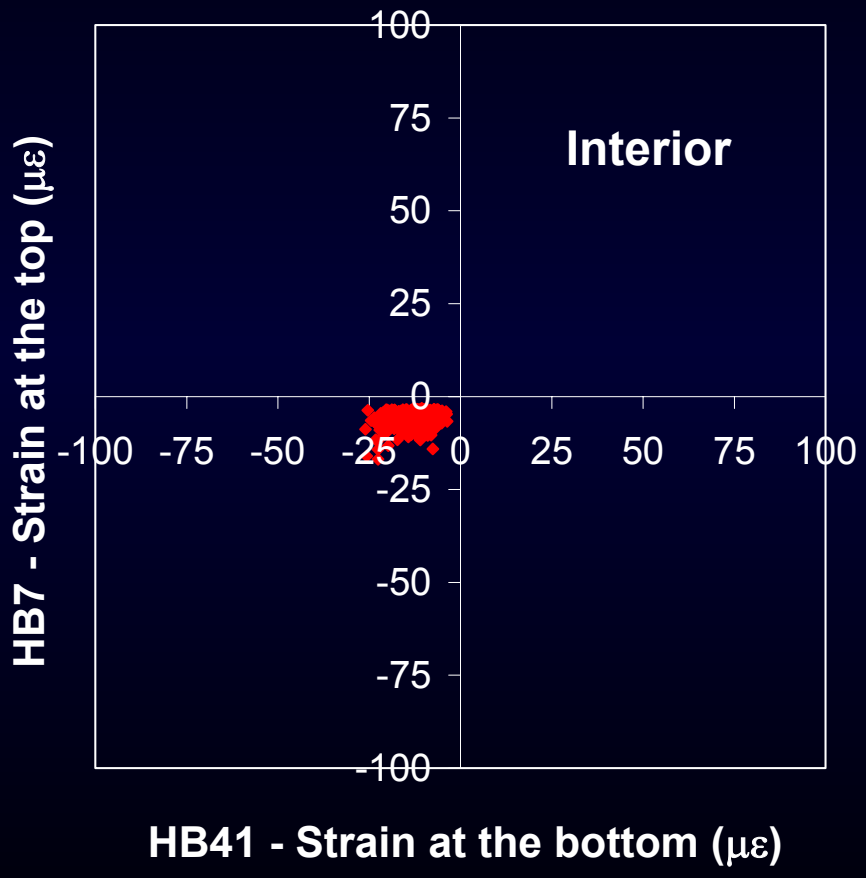

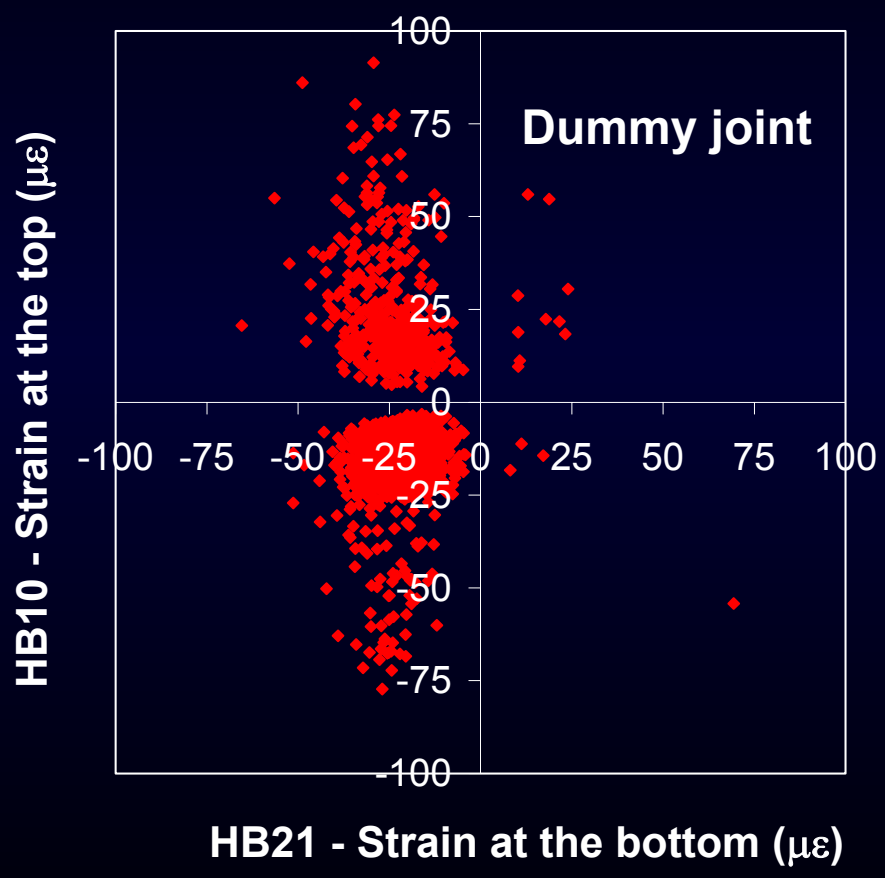

Summary of temperature differential effect on measured interface parameter

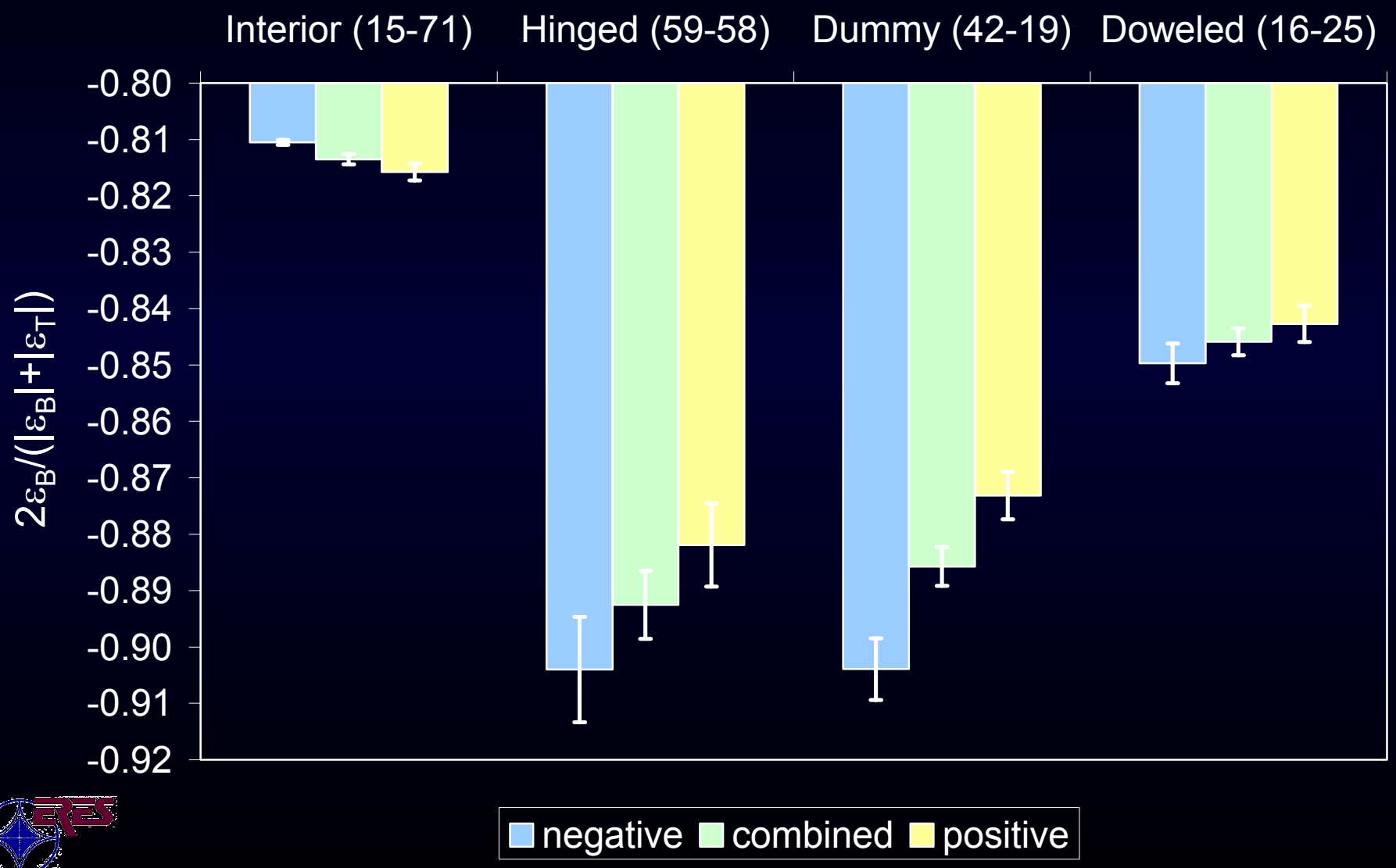

Effect of load location on measured interface parameter

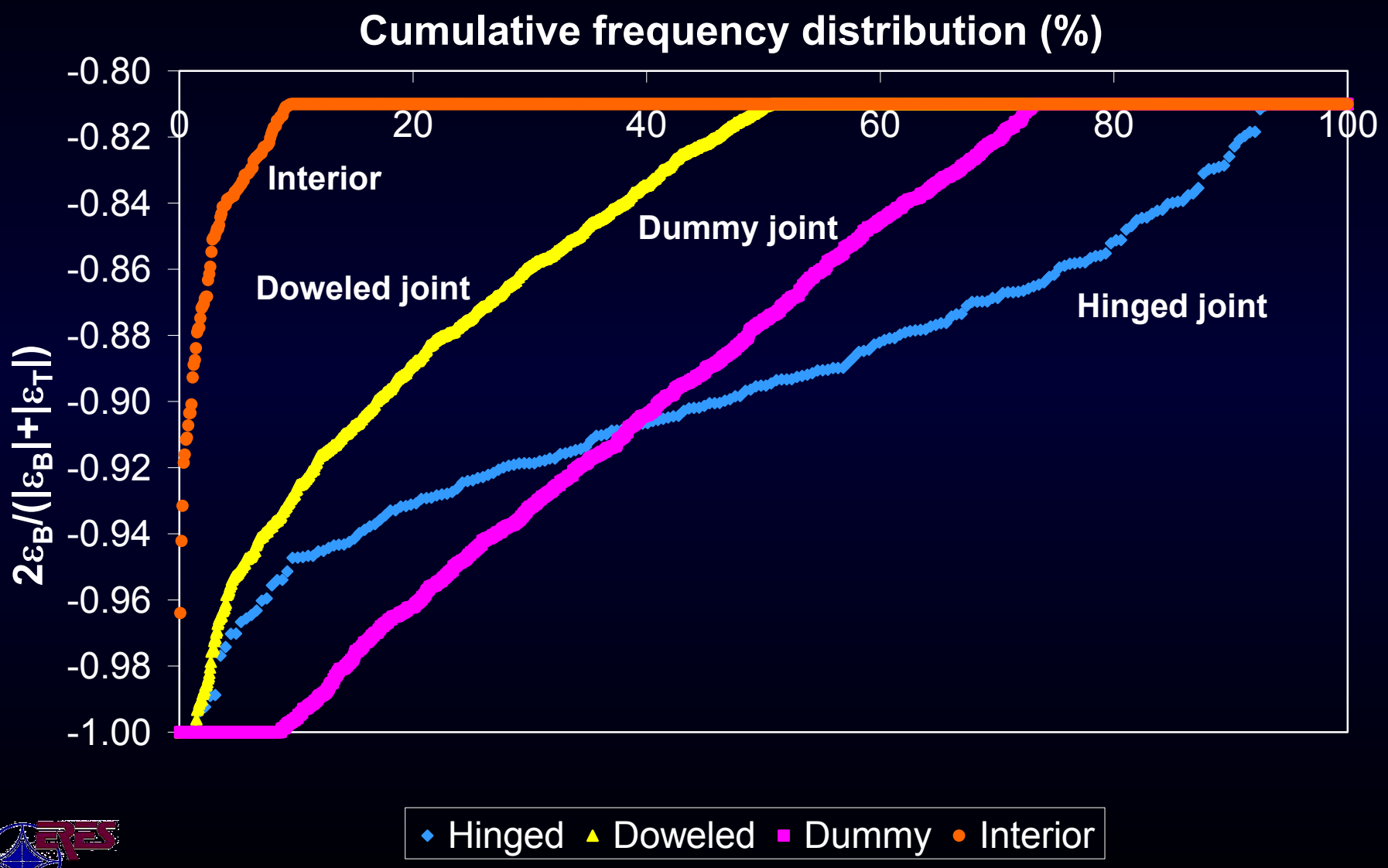

Measured versus predicted responses

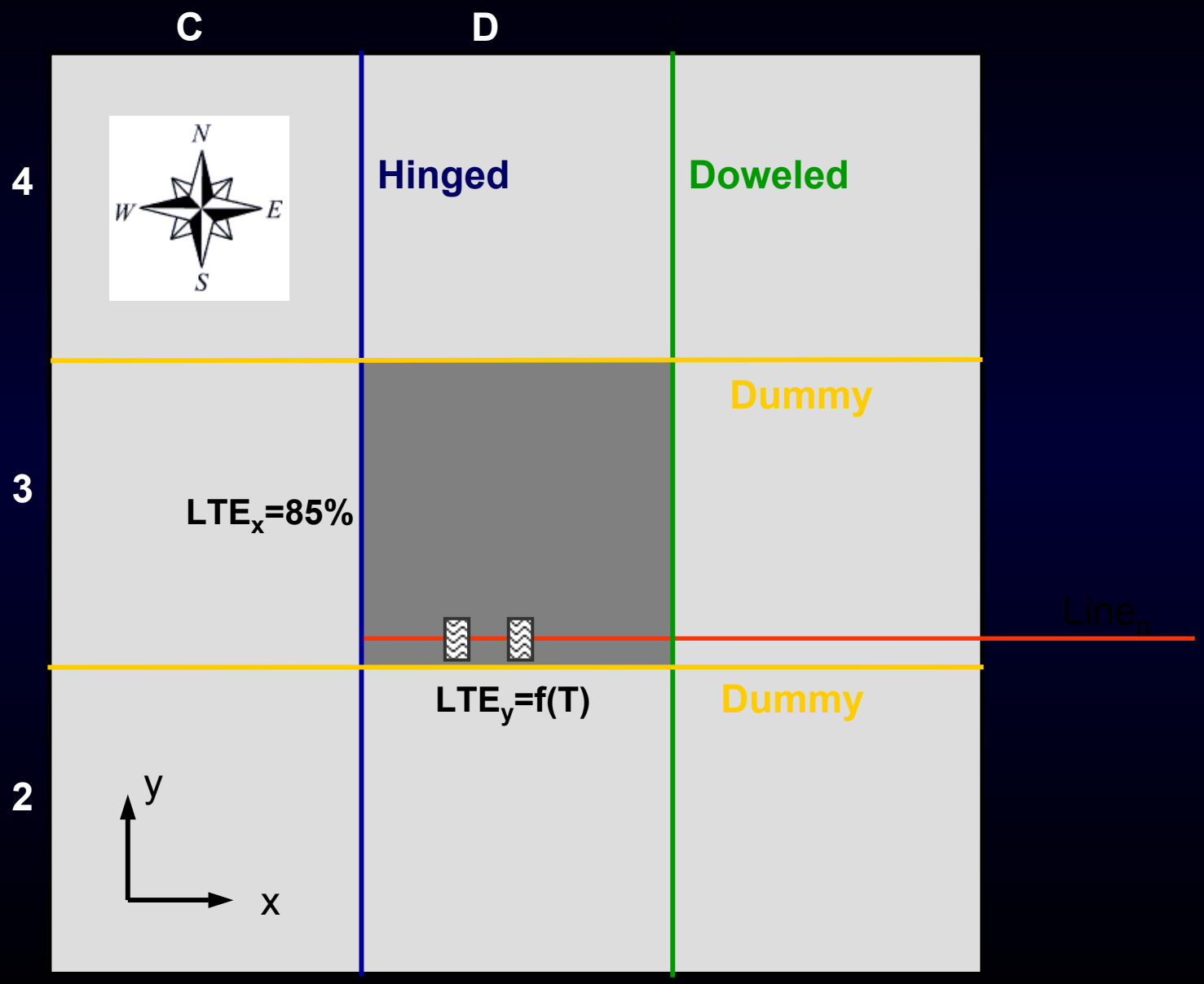

Selected gages for a detailed analysis

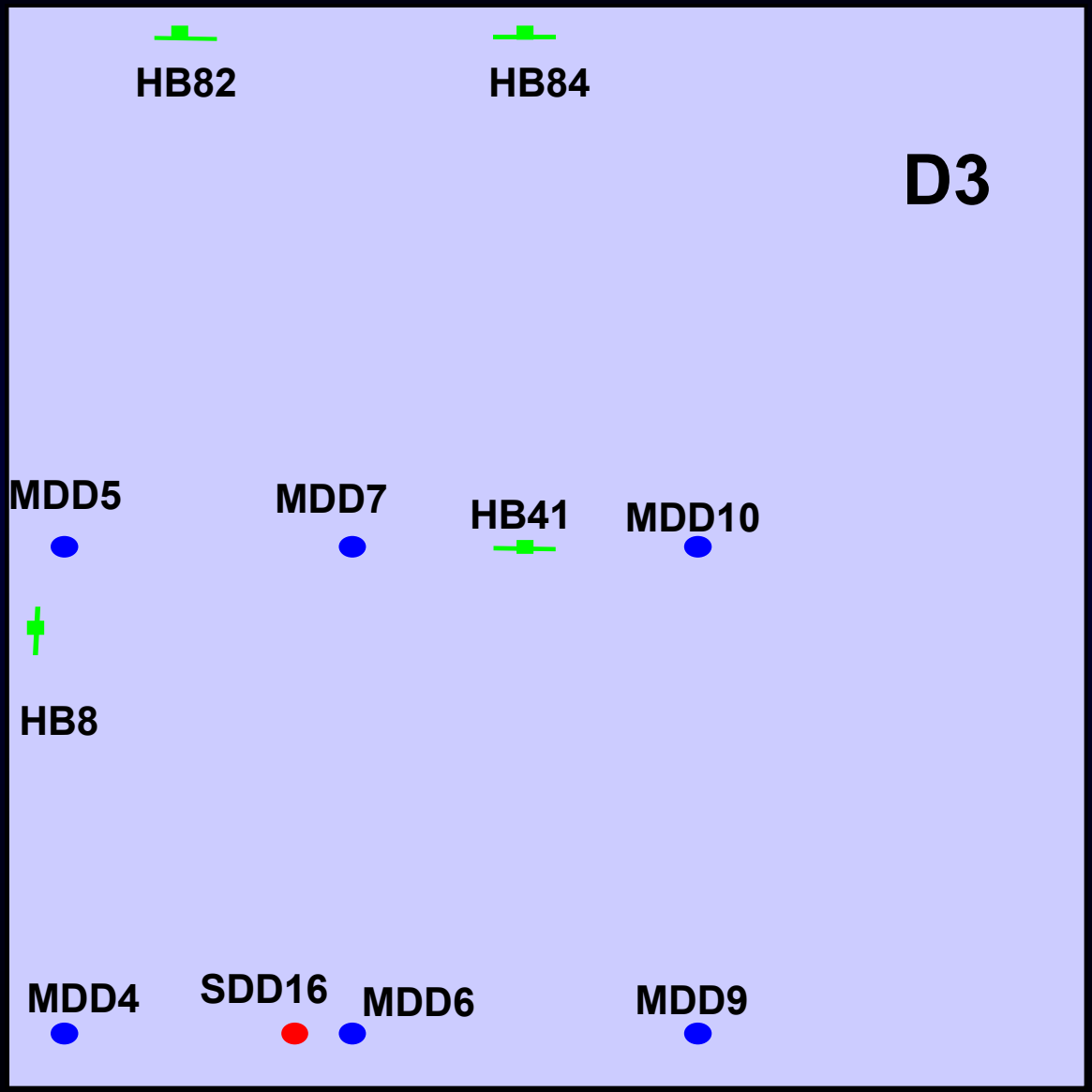

Measured and predicted B-727 interior strain (HB41)

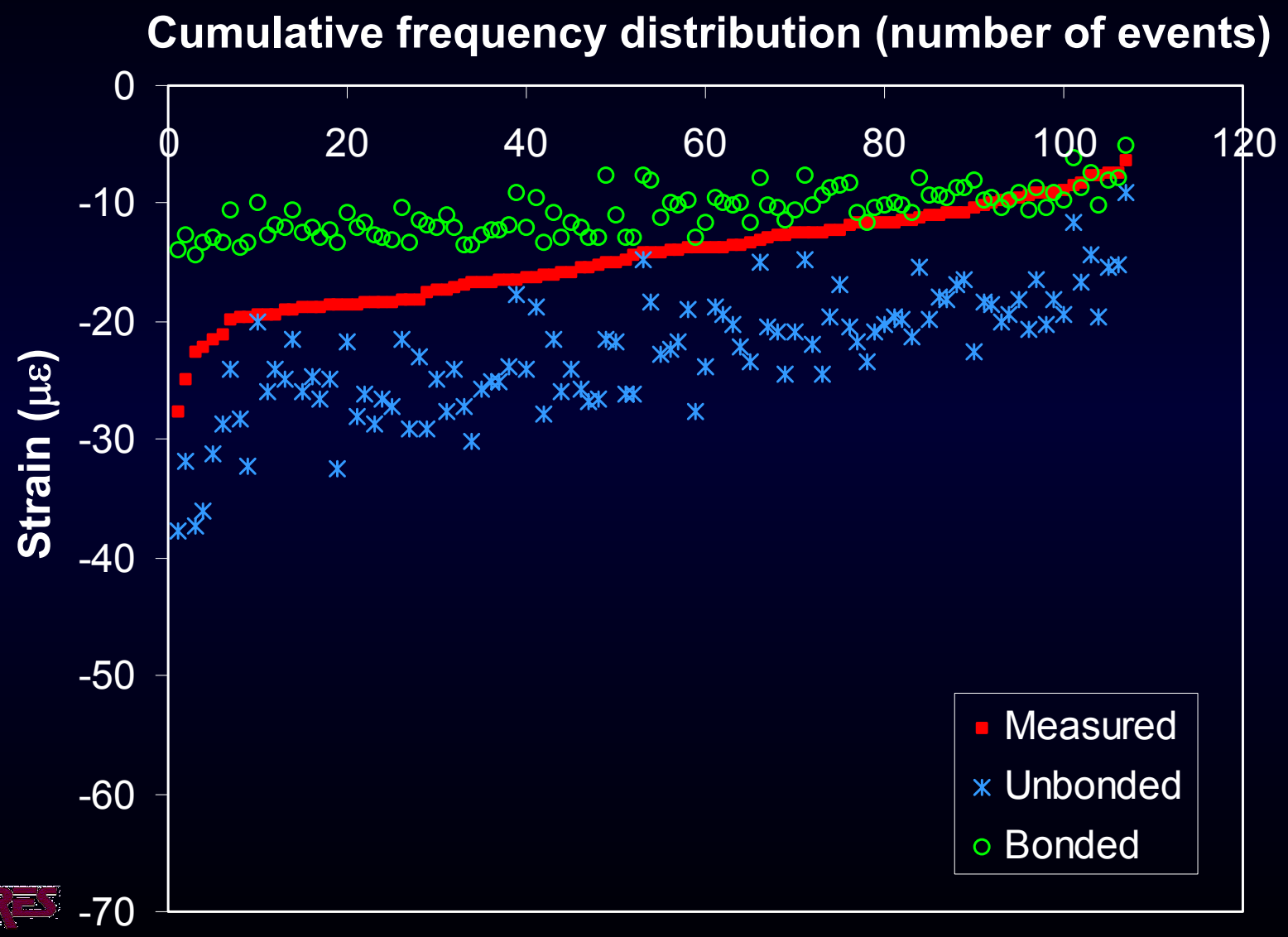

Measured and predicted B-727 transverse joint strain (HB84)

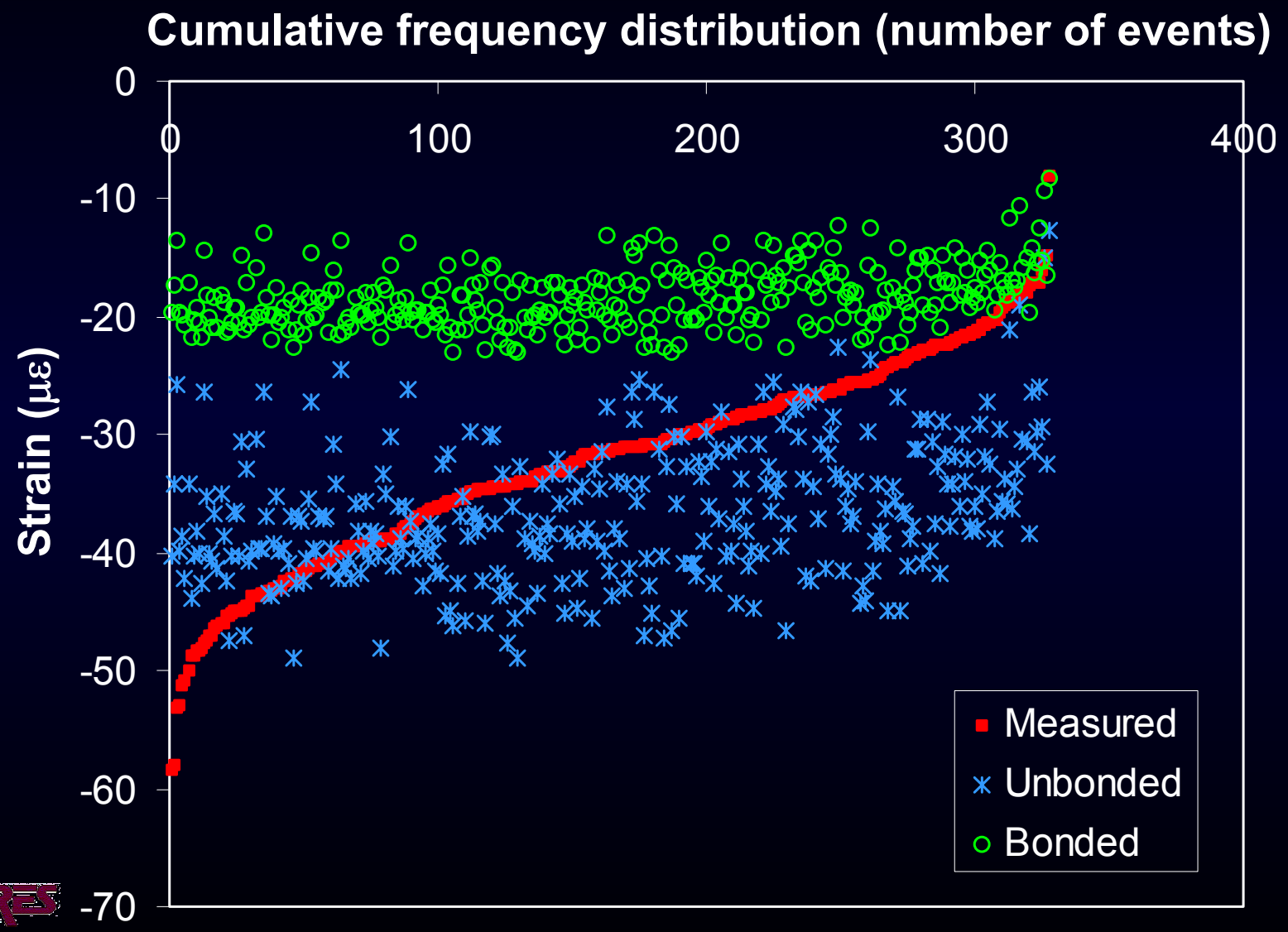

Measured and predicted DC-10 longitudinal joint strain (HB8)

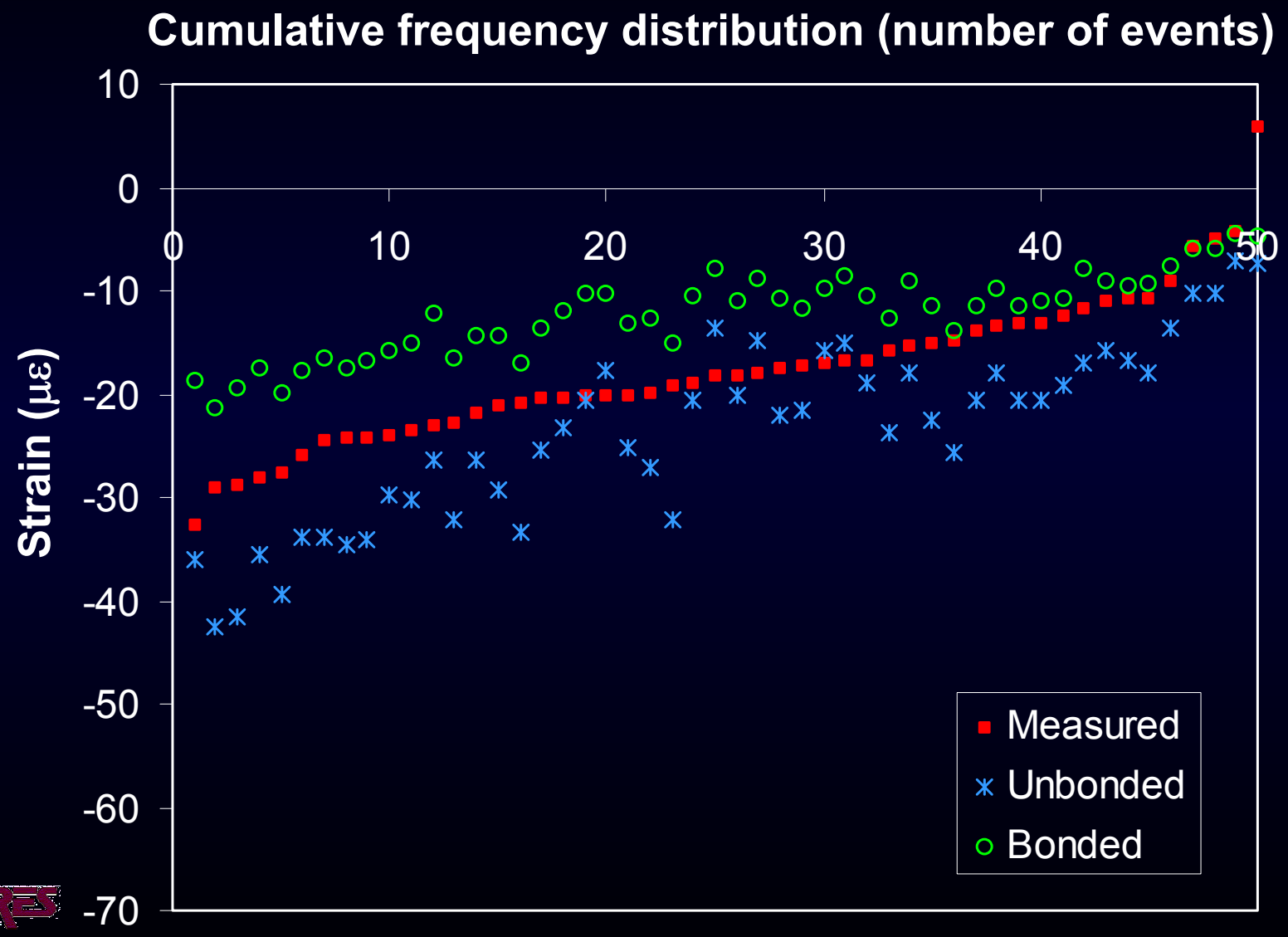

Summary of comparison between measured and predicted tensile strains (με)

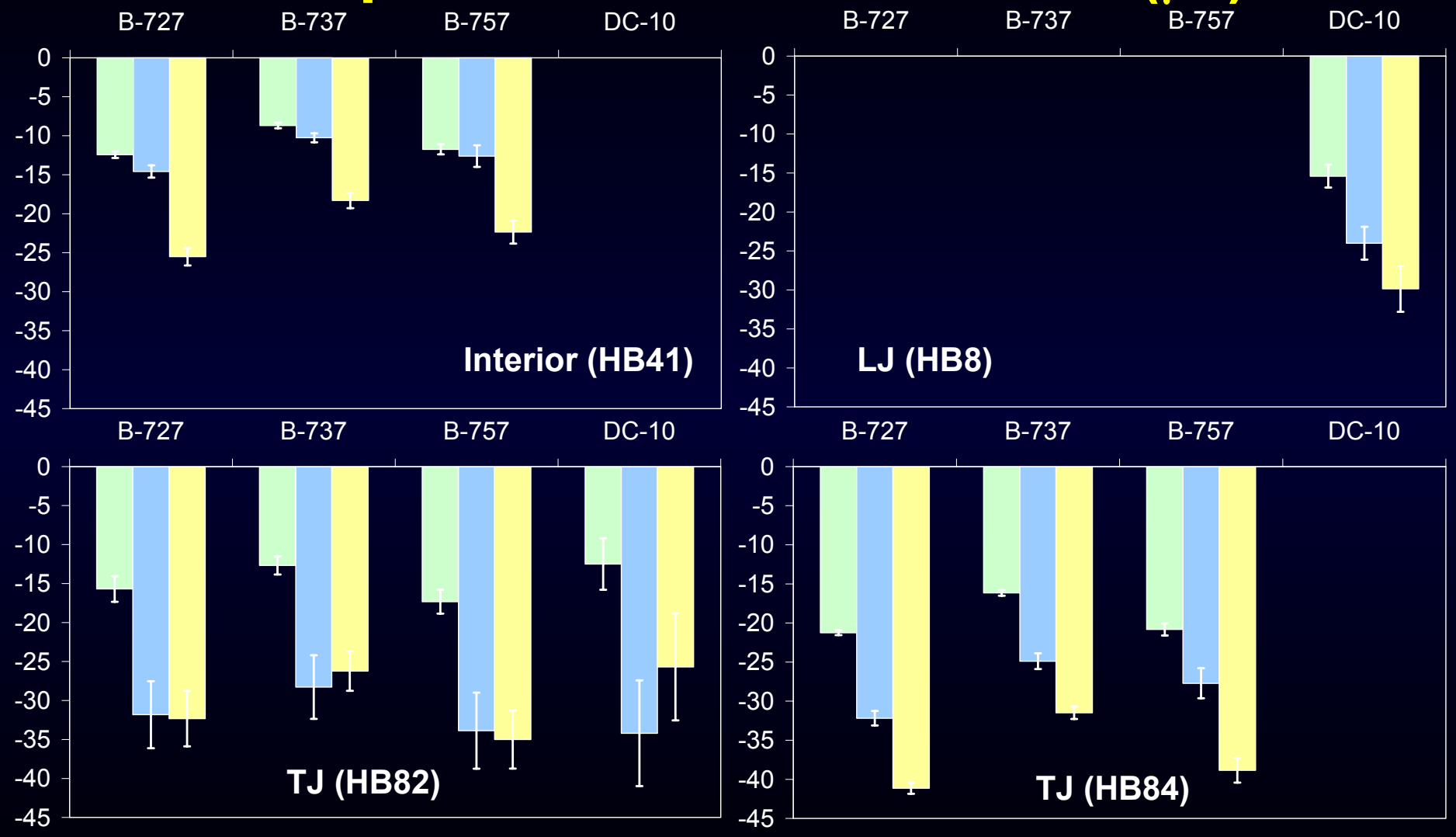

Measured and predicted B-727 interior deflection (MDD10)

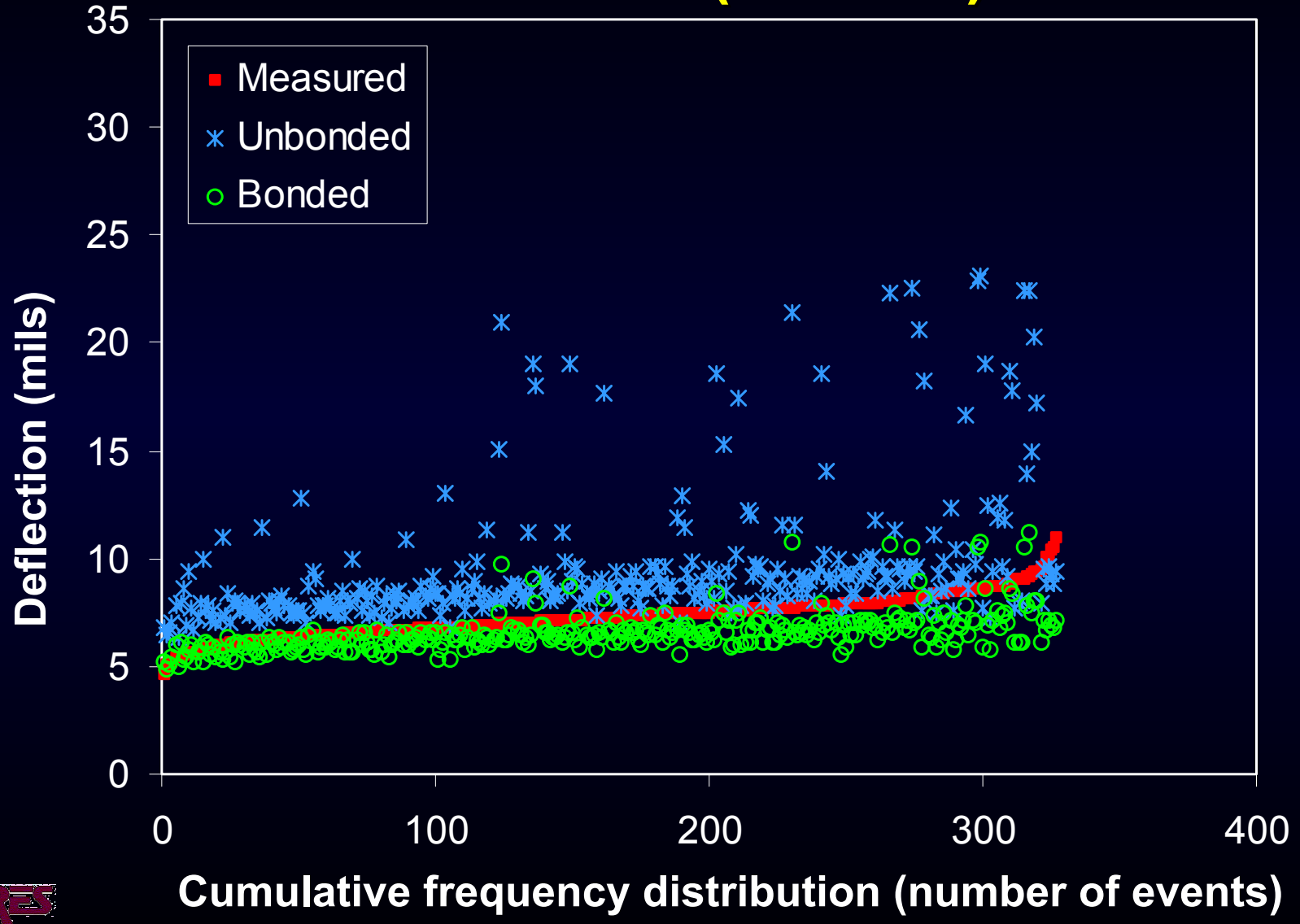

Measured and predicted B-727 TJ dummy deflection (MDD6)

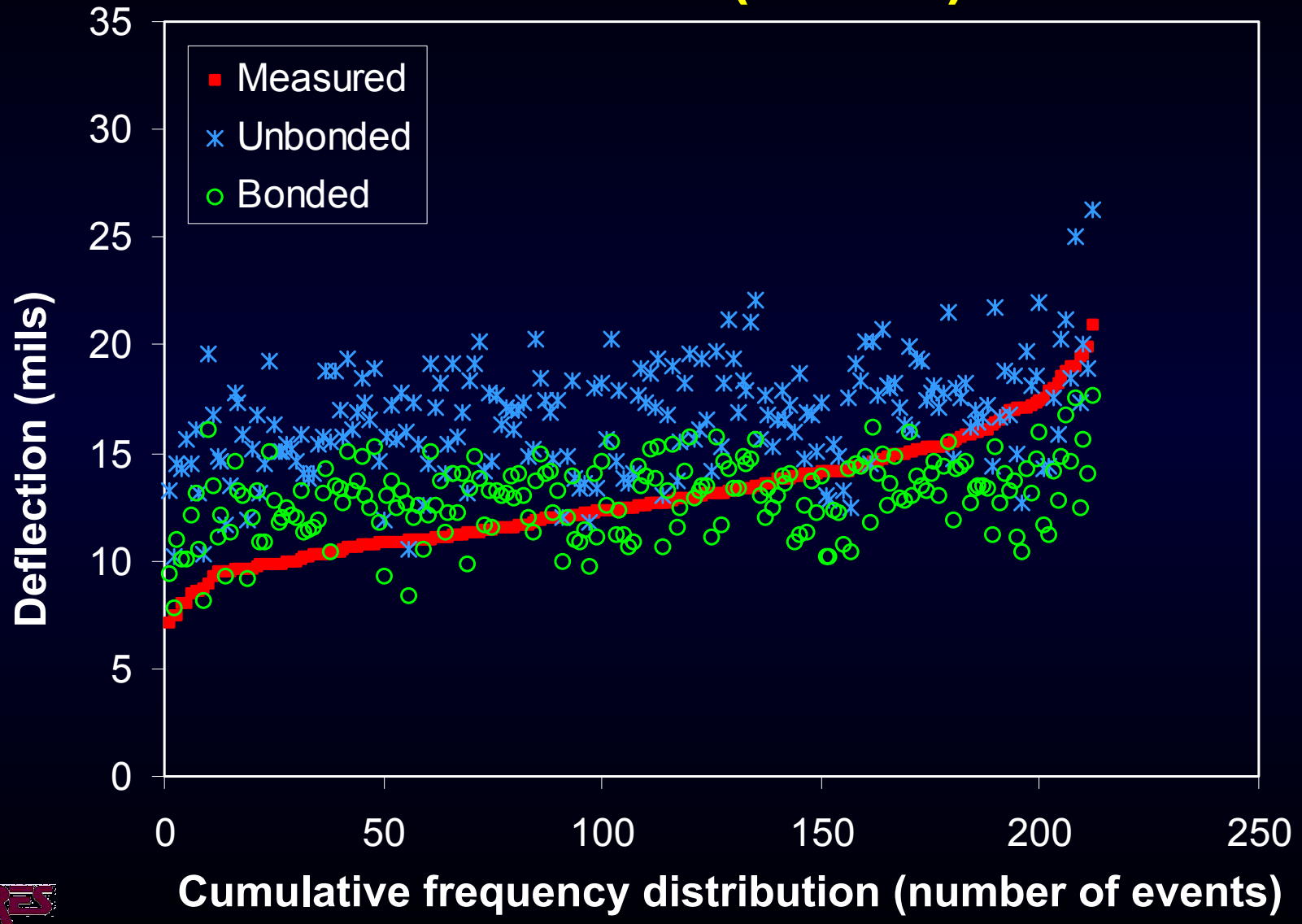

Measured and predicted DC-10 hinged LJ (MDD5)

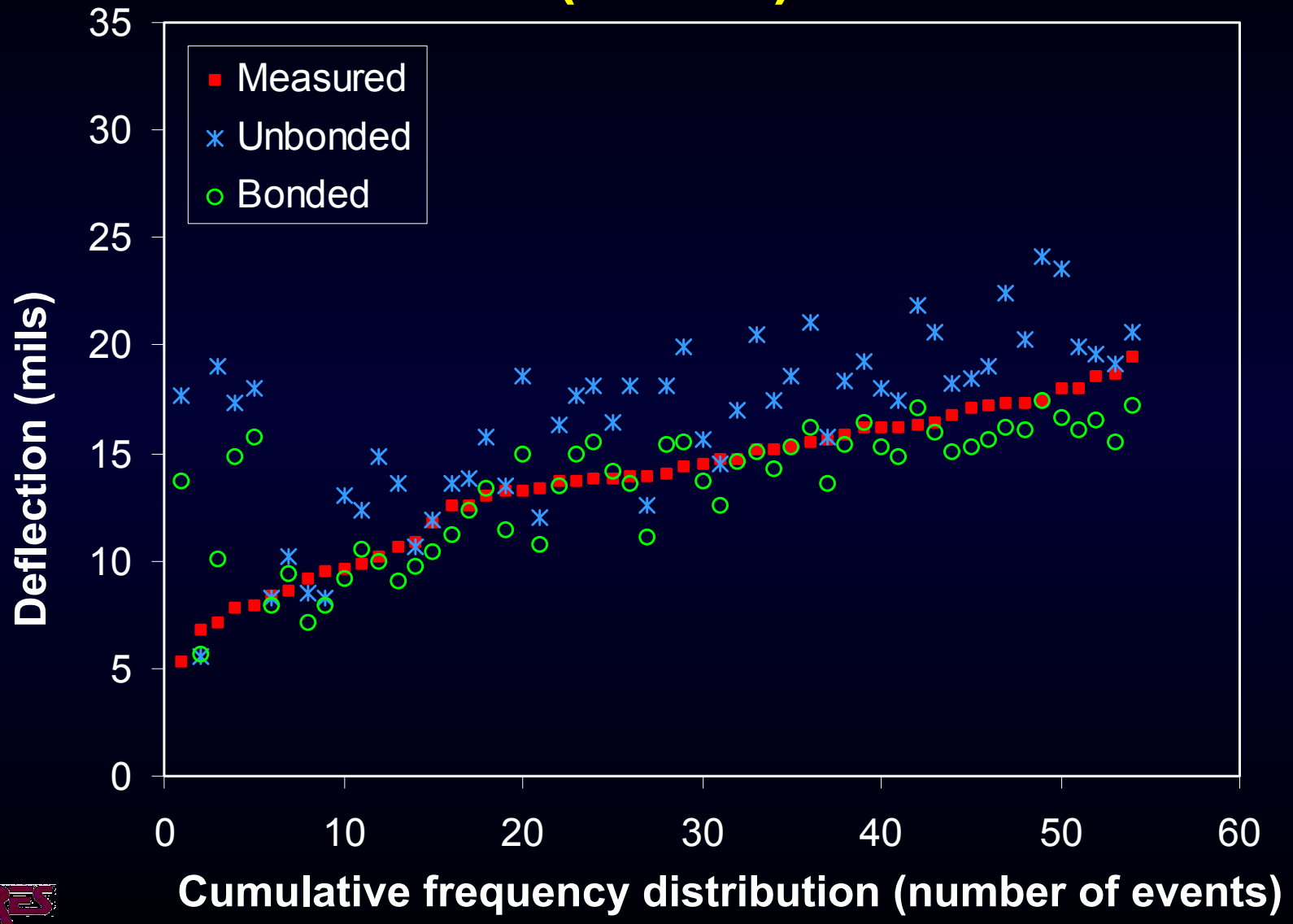

Measured and predicted DC-10 corner deflection (MDD4)

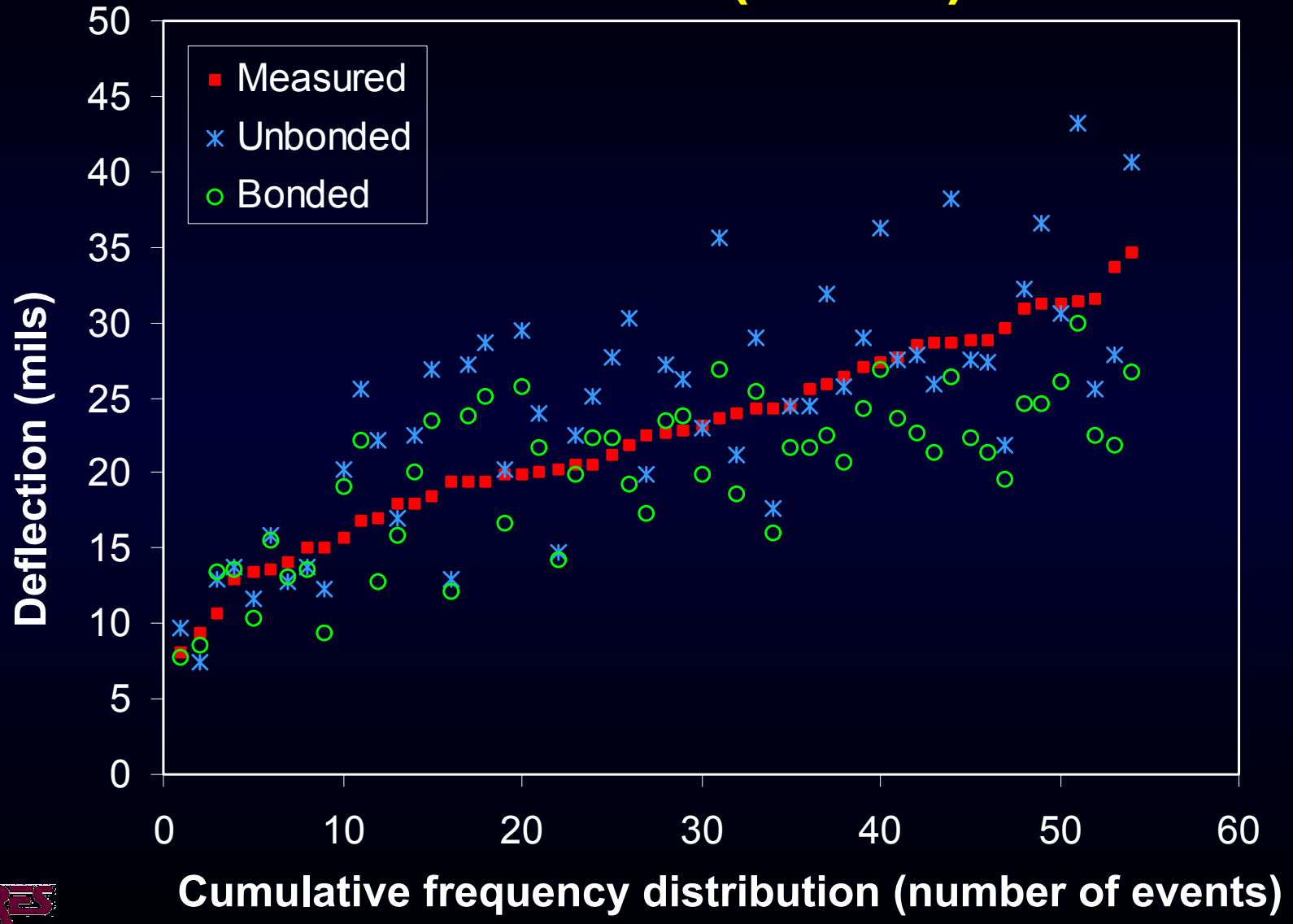

Summary of comparison between measured and predicted deflection (mils)

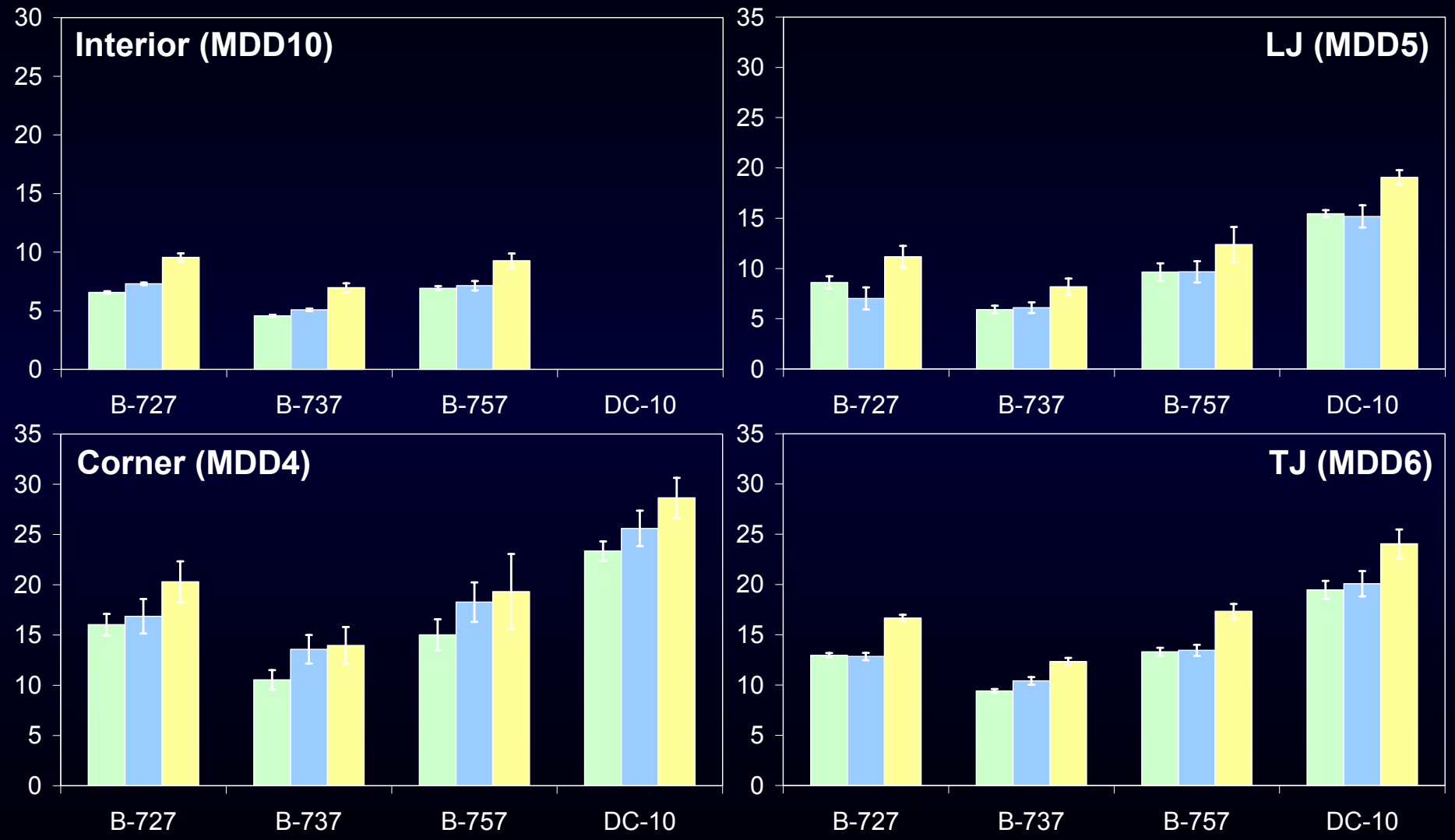

Conclusions

Wander Analysis

- Normal distribution
- B-777 and DC-10 had similar distributions
- Gear path distribution
- Interaction between gear type and joint location

Backcalculation

- Adequate properties

Pavement Temperature

- ICM evaluation
- Joint opening
- LTE

Temperature versus pavement response

- Theoretical analysis
  - Effect of temperature distribution and type of response
- Analysis of measured responses
  - Change in strain
    - Interior (strong correlation)
    - TJ dummy joint (strong correlation)
    - TJ doweled joint (some correlation)
    - LJ hinged joint (no correlation)
  - Deflection
    - Interior (some correlation)
    - TJ dummy joint (strong correlation)
    - LJ hinged joint (no correlation)
    - Corner (some correlation)
  - Effect of load magnitude
- Design implications
  - Total or stress range?
  - Which stress component causes failure?

Interface condition

- Gap analysis
  - Temperature differential and location
  - EBITD
- Paired strain analysis
  - Location: interior, TJ and LJ
  - Interface parameter and slab-base contact
- Measured versus predicted responses
  - Strain
    - Interior (bonded)
    - TJ dummy joint (partial)
    - LJ hinged joint (unbonded)
  - Deflection
    - Interior (bonded)
    - TJ dummy joint (bonded)
    - LJ hinged joint (bonded)
    - Corner (partial)

Acknowledgments

- Iowa State University
- Center for Transportation Research and Education
- Midwest Transportation Consortium
- David Plazak
- Federal Aviation Administration, Airport Technology R&D Branch, at the FAA William J. Hughes Technical Center.